

TU DELFT

Geological characterization of Hardeggen reservoirs

in the West Netherlands Basin

Bram ter Meulen – Tim Lottman

10/31/2016

Contents

Abstract	4
Introduction	5
Geological Framework	6
Permian	6
Tectonics and Paleogeography	6
Rotliegend	8
Zechstein	9
Triassic.....	10
Buntsandstein	10
Muschelkalk	14
Keuper Formation	14
Jurassic, Cretaceous and Cenozoic times and the Alpine orogeny	15
Jurassic until Early Cretaceous	15
Late Cretaceous and the Alpine orogeny.....	15
Data and Methods	17
NLog	17
Core description.....	18
Core plug measurements.....	18
Well operator reports	18
Gamma ray log	18
Field description.....	19
Results.....	20
Core section description	20
P11-02	20
P15-14 and P18-02.....	21
Distance from the basin margin.....	21
Silt and Clay Deposits.....	22
Well operator reports	23
Core plug measurements.....	24
Field description.....	25
Interpretation	27

Core plug measurement interpretation.....	27
Continuous core plug measurement plot	27
P11-02	27
P15-14	29
P18-02	31
RDK-01.....	33
MSG-01	35
RTD-01.....	37
RZB-01.....	39
OBLZ-01.....	41
GAG-03.....	43
Well operator interpretations.....	45
P11-02	45
MSG-01	45
OBLZ-01.....	45
RDK-01.....	46
Gamma ray log interpretation	48
P11-02	48
Integration	49
Influence of clay content on reservoir properties	49
Influence of geographic orientation on homogeneity of Hardegsen reservoirs	50
Influence of diagenesis on reservoir quality.....	52
Chemical diagenesis.....	52
Physical processes.....	53
Influence of depositional environment on reservoir quality	55
Permeability to porosity, depth model.....	57
Discussion and recommendations	59
Conclusion.....	61
Acknowledgements.....	62
References	63
Appendix	65
Appendix A – Core section description	65

Appendix B – Off shore core plug measurements 72
Appendix C – On shore core plug measurements 75
Appendix D – Composite well logs..... 81
Appendix E – Field description.....**Fout! Bladwijzer niet gedefinieerd.**
Appendix F – Inversion of reservoir quality F and L quadrants, summary. 109

Abstract

Geothermal energy is strongly dependent on the geothermal gradient; this means that with increasing depth an increase in temperature is found. The targeted formation of our research is the Hardeggen which reaches depths of around three kilometers in the West Netherlands Basin. At three kilometers depth the temperature is around 90 C° which is interesting for geothermal exploitation. However, rock at increasing depth generally shows a decrease in reservoir properties.

This study investigates whether the reservoir properties of the Hardeggen formation at a depth of three kilometers are still interesting for geothermal exploitation. This is done by determining to what extent the Hardeggen has been influenced by depositional history, diagenetic processes and inversion.

Determining the reservoir properties is done by studying a data set that consists of core descriptions, core plug measurements, gamma ray logs, microscopy analysis, literature studies and a field study. From the core plug measurements a simple model was created describing how porosity and permeability of the Hardeggen behave with increasing depth.

The Hardeggen succession in the West Netherlands Basin consists mainly out of (cross-bedded) arkosic fine to medium grained sandstones intercalated by 0.2-1 meter thick laterally consistent shales and shaly/silty very fine sands. High minus-porosities (up to 45 %) are reported which could have played an important role in the preservation of the reservoir properties. Core plug measurements show that the Hardeggen has good prospects for a potential reservoir with porosities ranging from 10-20% and permeability's ranging from 50-1000 mD.

The presence of the laterally consistent shale and sandy/silty very fine sand layers is heavily dependent on the location in the reservoir. This research shows absence of these layers in wells that are located closer to the basin margin. Since these layers decrease vertical flow drastically, further investigation of the extent of these layers is needed to give a better prediction of the quality of the reservoir as a whole.

Introduction

Geothermal energy is a renewable energy source that shows large potential for the future. To exploit geothermal energy there must be a reservoir rock in the subsurface nearby. The target of the Delft Aardwarmte Project (DAP) are reservoirs of the Lower Cretaceous Delft Sandstone located in the West Netherlands Basin. This report investigates the properties of the Lower Triassic Buntsandstein, in particular Hardegsen, reservoirs in the West Netherlands Basin for their reservoir potential.

This research is set to investigate a deeper located potential reservoir rock in the subsurface of the West Netherlands Basin called the Buntsandstein, more particularly the Hardegsen formation. In the past the Hardegsen formation proved to be a potentially good reservoir rock and has a rich history in hydrocarbon exploration. We are interested in potential reservoir rock at a depth of 3 kilometers because of high temperatures due to the geothermal gradient. Since the Hardegsen formation reaches this depth in large parts of the West Netherlands Basin the formation meets the criteria for further study.

The goal of this research is to determine whether the Hardegsen formation around 3 kilometers depth is a potential reservoir for geothermal exploitation, and if so, to describe what factors influence its reservoir quality throughout the West Netherlands Basin.

During this research a dataset that consists of borehole cores, gamma ray logs, microscopy analysis, XRF analysis, thin section analysis and core plug permeability and porosity measurements of multiple wells in the West Netherlands Basin penetrating the Hardegsen formation were studied. Also a field study on the Buntsandstein in Thüringen, Germany, was performed. These data have been studied to obtain a general view on the Hardegsen formation in the West Netherlands Basin at a depth around 3 kilometers. The study reveals what influences depth, location, diagenesis and depositional environment have on the reservoir quality of the Hardegsen.

In the end a general description on reservoir quality of the Hardegsen throughout the West Netherlands Basin gives an indication whether the Hardegsen has potential as a reservoir and thus is interesting for further exploration for geothermal exploitation.

Geological Framework

Permian

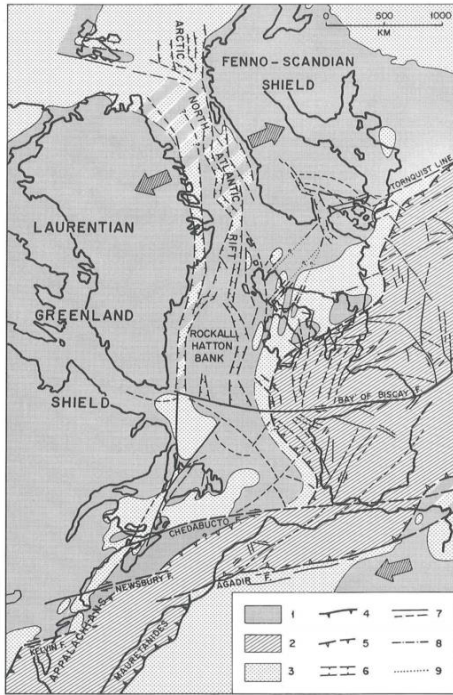
Tectonics and Paleogeography

The study area of the project is the West Netherlands Basin. The tectonic setting of the study area before deposition of the Buntsandstein has been influenced by two major events (Geluk 2005). At first the North-South collision of Gondwana and Laurussia during the Late Carboniferous causing the formation of the supercontinent Pangea. This started with the subduction of the Proto-Tethys Ocean during the Carboniferous (Autran and Cogné 1980). The spreading of the Buntsandstein has strongly been influenced by this Late Carboniferous Variscan Orogeny. Secondly the disintegration of Pangea (figure 1). In the Late Permian/Early Triassic, the supercontinent Pangea started to break up. This rifting caused basins to form all over the European continent of today.

The Triassic fluvial systems filled up these basins of up to eight kilometers thick (McKie and Williams 2009). The disintegration started during the Late

Permian and followed through during Triassic, Jurassic, Cretaceous and Early Cenozoic times, causing extensional tectonics in the West Netherlands Basin (Ziegler 1982, Rohling 1991, Kockel 1995). It is evident that the breaking up of the Pangea supercontinent in the North-Atlantic and Tethys domain predominantly follows the sutures that were formed in pre-Triassic times (Ziegler 1982). This caused large subsidence around the complex rift patterns on the plate boundaries (Ziegler 1982). These two events formed, combined with the already anisotropic and thickened crust of the Variscan fold belt, a complex system of basins and rifts in NW Europe (figure 2) (Geluk 2005).

The formation of Pangea during the Late Carboniferous and Early Permian was accompanied by a Northward drift of Western and Central Europe, off the equator. This caused



1. Continental cratons and intrabasin highs; 2. Hercynian fold belts; 3. Carboniferous basins in Hercynian foreland; 4. Alleghenian deformation front; 5. Asturian deformation front; 6. Grabens, rifts; 7. Wrench faults; 8. Dyke swarms; 9. Alignments.

Figure 1. Permo-Carboniferous tectonic framework of the Arctic-North Atlantic area. (Ziegler 1982)

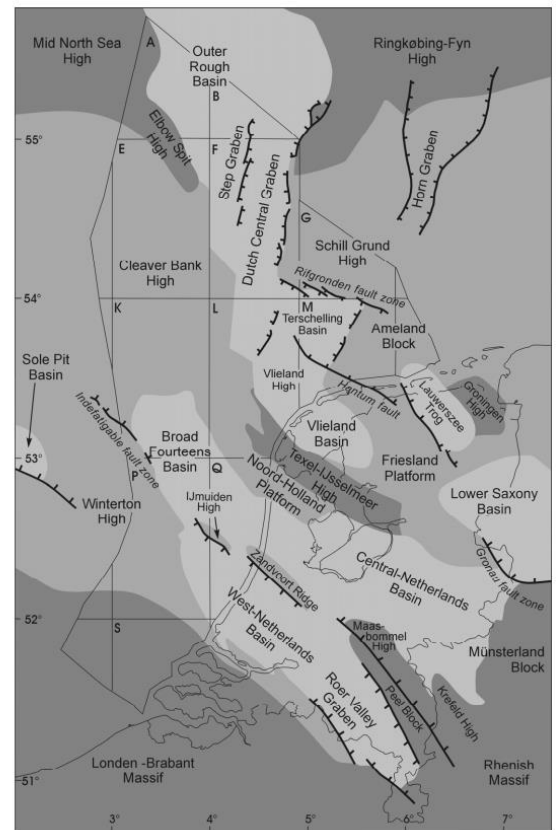


Figure 2. Basins and highs of the South-Eastern North Sea and the Netherlands during the Permian and Triassic. (Geluk 2005)

the climate to change from a tropical rainforest climate into an arid, warmer, intra-continental climate that characterizes the Permian (evaporites and sand deposits) and most of Triassic's climate in the Western and Central European area (Ziegler 1982, Habicht 1979). The Permo-Triassic environment in the Netherlands was semi-arid to arid, due to the southern Variscan mountains and the paleolatitude of ca. 10 degrees North. Southern winds prevailed and prevented humid air to reach the basins and flats (Glennie 1998, Geluk 2005). The sedimentation in the Southern Permian Basin started in the Early Permian in the Eastern part (Poland) and advanced slowly westward. The large amounts of sedimentation started in the Netherlands during the start of the Early Permian. In the Early and Middle Permian, we can find volcanic activity in the Netherlands. Although minor volcanic activity happened during the Early Permian, the higher activity followed with wrenching during the Middle Permian (figure 3)(Plein 1995, Geluk 2005).

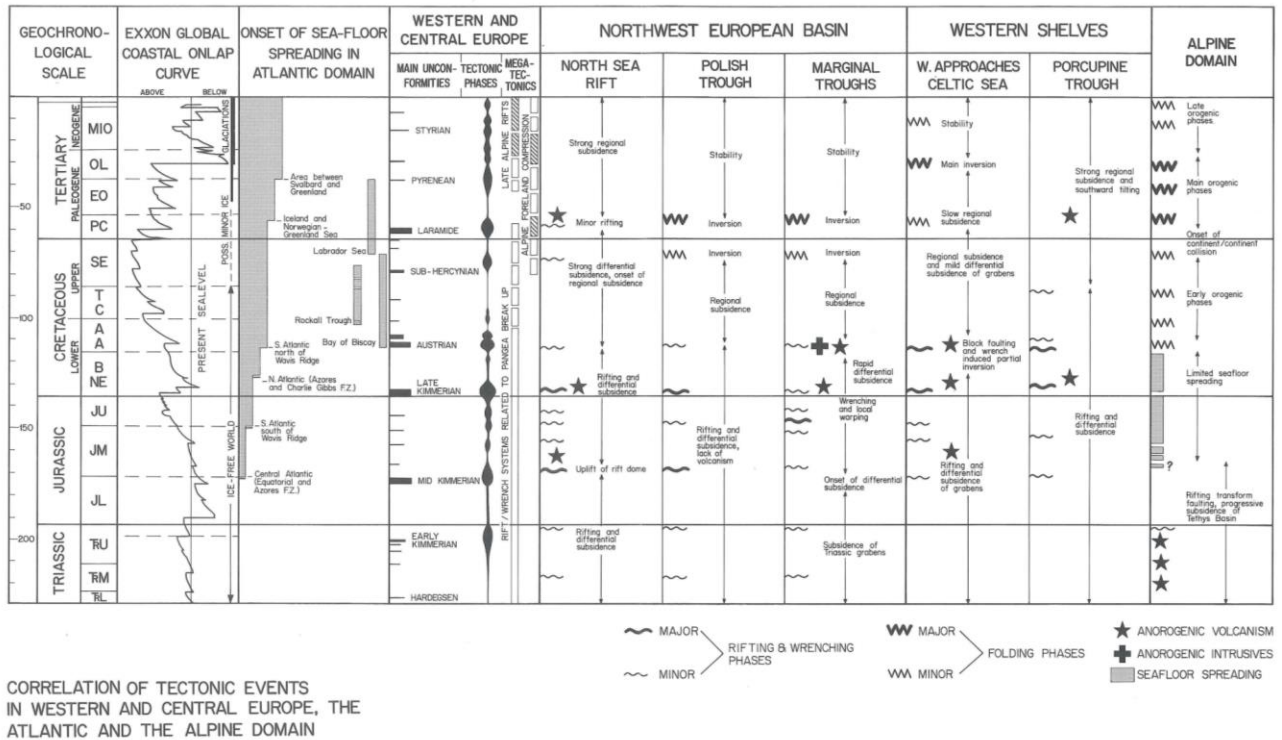


Figure 3. Tectonic timescale of North-Western Europe. (Ziegler 1982)

Rotliegend

The Rotliegend has been deposited during the Early Permian. Uplift and Erosion of the Variscan fold belt caused large amounts of clastic sediments to be deposited in the intramontane basins. The aridity of the climate during the deposition of the Rotliegend increased especially during the Autunian. Erosion of the uplifting Variscan fold belt progressively fed ephemeral streams from the mountains to the Variscan foreland (Ziegler 1982). Two large basins that were situated on this foreland, the Northern Permian Basin and Southern Permian Basin, started to subside. In these basins, Rotliegend red sandstones and halite depositions accumulated. Since the climate was semi-arid to arid, these depositions are mainly formed under desert and desert lake depositional environment. The Netherlands was situated on the southern margin of the Southern Permian Basin. The Southern part of the Netherlands was not part of the basin. From the center of the Netherlands, the clastics from the Variscan mountains were deposited, grading down north, from coarse sediments on the alluvial fans, sand and silty shales on the desert plains and shales and halite towards the center of the basin (figure 4). Easterly and north easterly winds distributed the sand from the fans all along the southern margin of the basin. The end of the deposition of the Rotliegend was inclined by subsidence rates that exceeded sedimentation rates. These depressions eventually became lain well below sea level (Ziegler 1982).

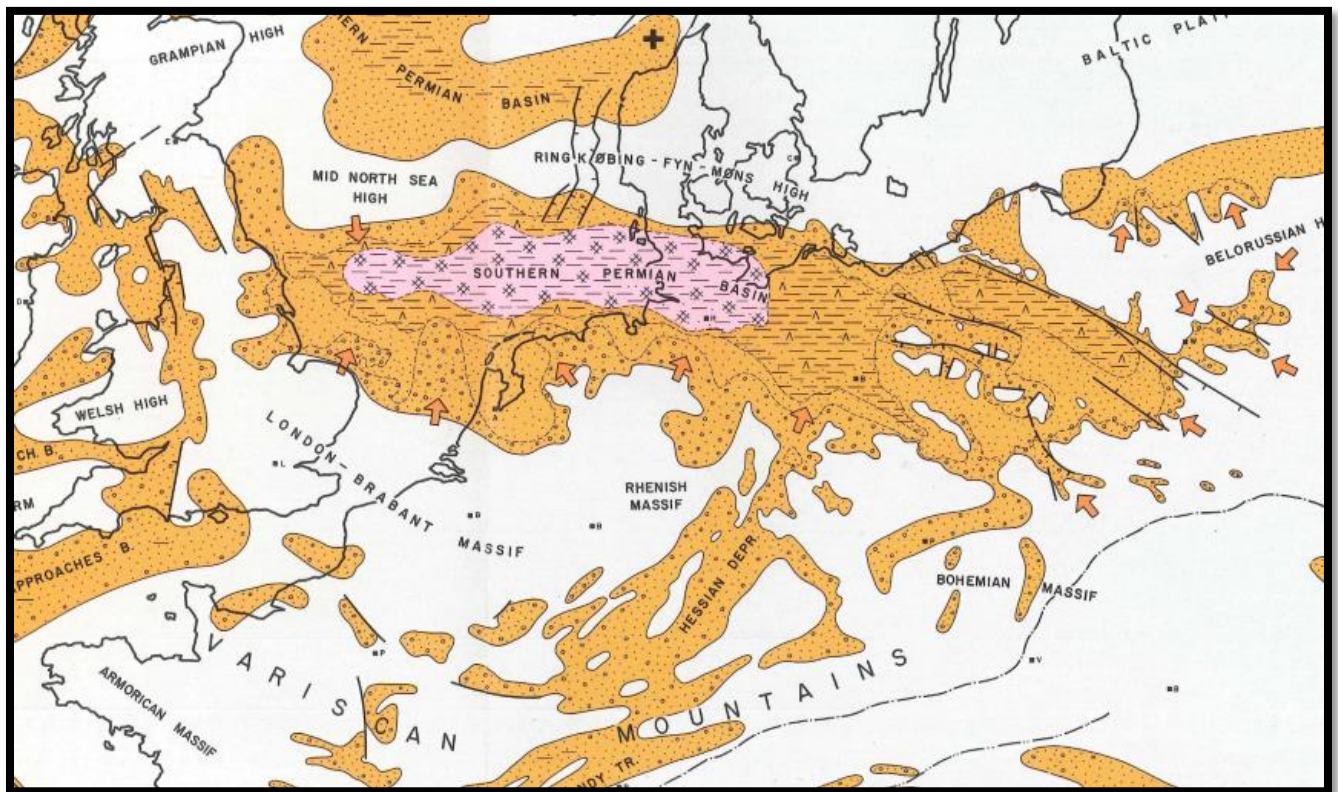


Figure 4. Paleogeography of NorthWestern Europe during the deposition of the Rotliegend formation. (detail from Ziegler 1982)

Zechstein

Deposition of sediments was absent in the Early Permian in the southern Netherlands. The deposition started during the Middle Permian and increased since that time. The increasing deposition was caused by the inclusion of the southern Netherlands with the Southern Permian Basin, that stretched from the United Kingdom to Poland (figure 5) (Ziegler 1982, Geluk 2005). The sediments were from aeolian, fluvial, lacustrine and marine environments. The Permian succession in the Netherlands stretches from 50 meter thickness in the northern part of the Netherlands up to 2000 meter thickness in the Roer Valley Graben and West Netherlands Basin. The sediments are mainly from Variscan origin (South) and from a minor extent from the Northern highs (Geluk 2005). The Zechstein group consists of 5 main evaporite cycles which have been formed during the Late Permian and form the bed on which the Buntsandstein lies (Van Adrichem Boogaert & Kouwe 1994, Geluk 2005). These cycles have been caused by restrictions of influx of seawater from different origin into the Southern Permian Basin (Ziegler 1982). With open connections to the sea, carbonate deposition prevailed. When the influx of seawater became restricted, sulphates and halites were deposited. All cycles show different characteristics and thickness caused by minor changes in the environment (Ziegler 1982).

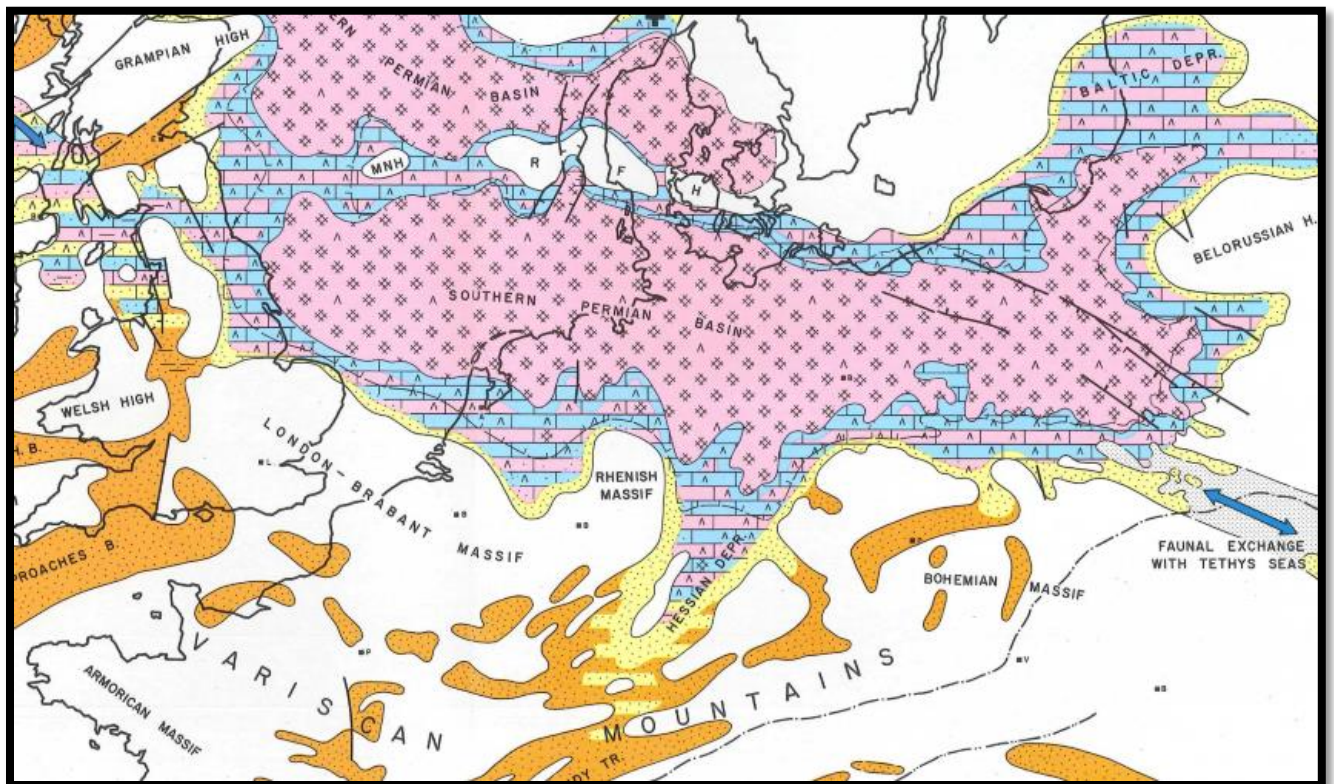


Figure 5. Paleogeography of NorthWestern Europe during the deposition of the Zechstein formation. (detail from Ziegler 1982)

Triassic

Buntsandstein

In Western Europe, the start of the Triassic can be recognized by the return to an arid continental to shallow-marine environment and the regression of the Arctic seas (figure 6) (Ziegler 1982). The periodic marine influences were caused by incursions of the Tethys ocean through the rapidly subsiding Polish Trough (Peryth 197, Fuglewicz 1980). Influx of fine and coarse clastic sediments from the Variscan mountains around the West Netherlands Basin happened through fluvial deposition all along the margins of the basin. In the deeper part of the Basin, reddish mudstones occur. Due to cyclical change of water level from tectonic as well as eustatic sea level change in the basin, silt- and sandstone intercalations are found all throughout the mud deposits (Ziegler 1982). The periods of relative high water level caused shallow, brackish lakes to form. In lakes, mud deposits as well as oolitic beds were formed while at the borders of the lakes, fluvial sediment was deposited. During periods with less influx of water, large fluvial (reddish) sand beds were formed. In some parts of the large basin, (aeolian) sand beds occur, although there is still discussion about the origin (Ziegler 1982). The constant alternations of water level in the basin caused the depositional environment to change place constantly. In combination with slower subsidence of some parts of the basin, erosional surfaces occurred at some places in the basin.

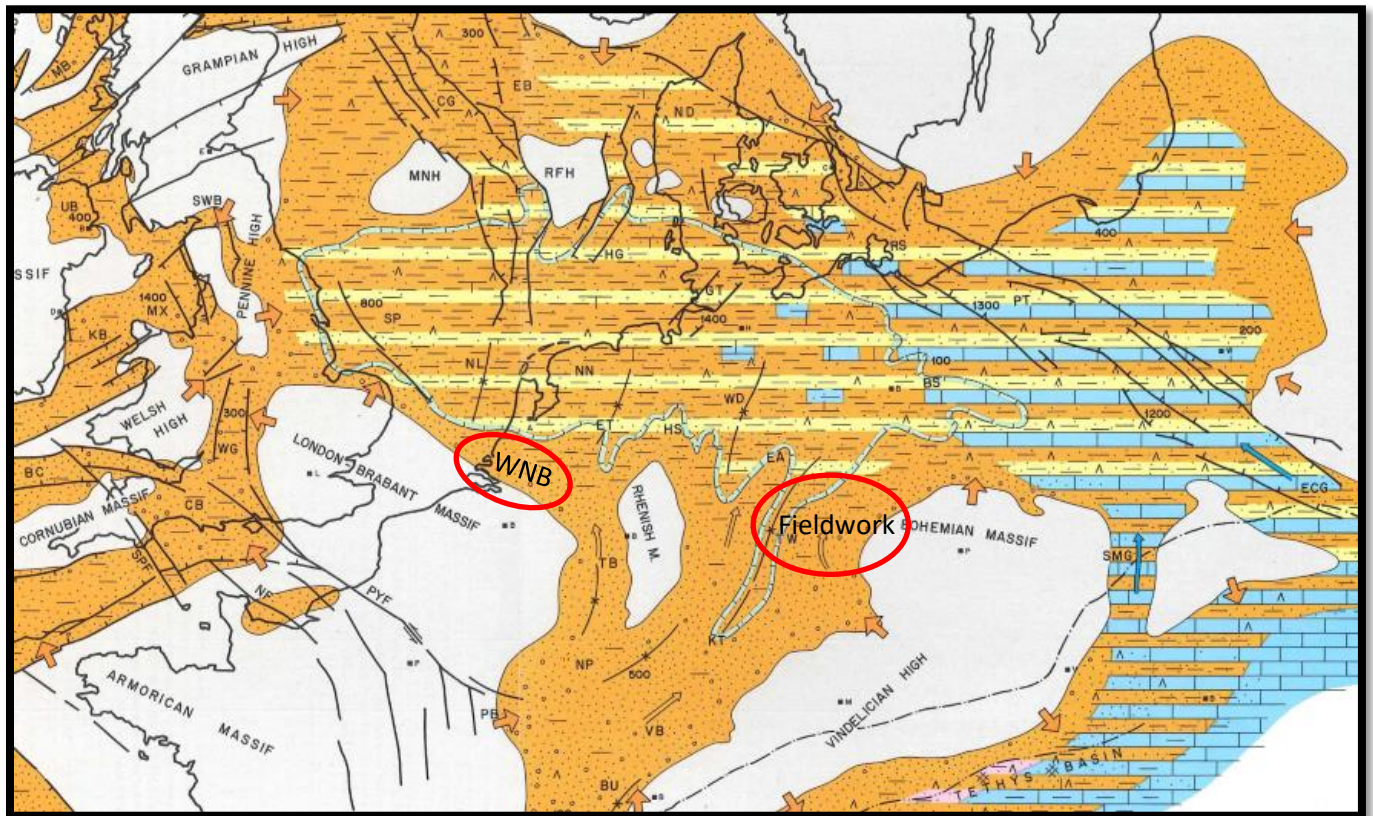


Figure 6. Paleogeography of NorthWestern Europe during the deposition of the Buntsandstein formation. (detail from Ziegler 1982)

Two of these main unconformities, the Solling and Hardegsen unconformities (Ziegler 1982), are of main interest for our study. In the end of the Late Scythian the Tethys sea started to transgress causing influx through the southeastern part of the basin. This event caused the depositional environment of especially the eastern and northern part of the basin to change into a more marine influenced basin, although water levels did not manage to reach levels that could overflow the axial high in the center of the basin. Therefore large halite, carbonate and sulfate depositions are restricted to the Poland through and northern Germany (Ziegler 1982).

The Buntsandstein formation does not form one stratigraphic entity. It consist out of up to seven different “unconformity-bounded tectono-stratigraphic sequences (Geluk & Röhling 1999).” Geluk & Röhling demonstrate that the Buntsandstein is not one stratigraphic unit, but form a complex hierarchy of high resolution cycles of different origin (figure 7). Therefore, the thickness of the Buntsandstein widely varies throughout NorthWest Europe (Röhling 1991). We can divide the Buntsandstein into three main phases: the Lower Buntsandstein, Main Buntsandstein and Upper Buntsandstein (Geluk & Röhling 1999, van Adrichem Boogaert & Kouwe 1994). Main characteristics will be described below.

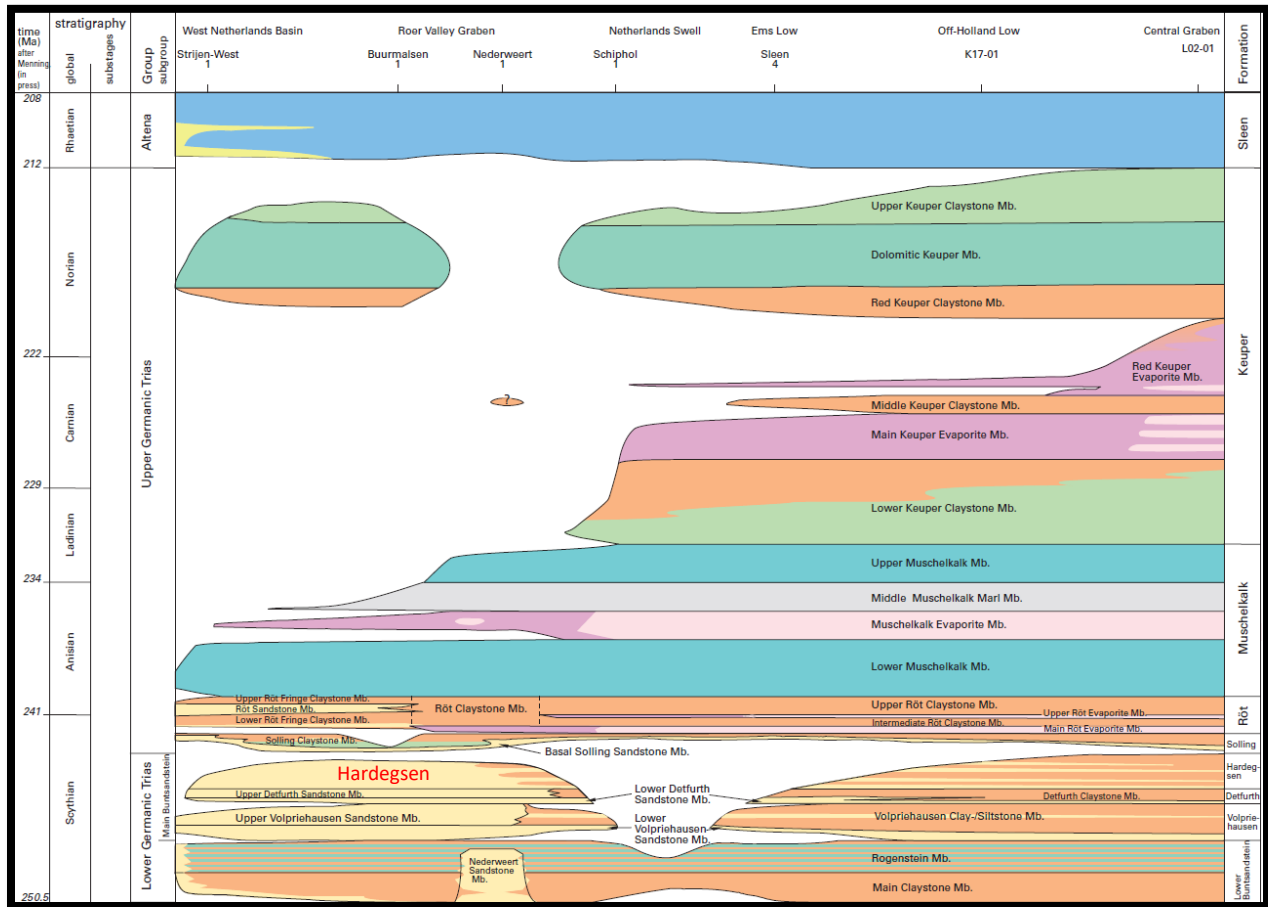


Figure 7. Stratigraphy of Netherlands' basins deposited during the Triassic. (After van Adrichem Boogaert & Kouwe 1993-1997)

Lower Buntsandstein

The Lower Buntsandstein consists following Röhling & Geluk (1997) out of a “cyclic alternation of fluviolacustrine fine-grained sandstones and clayey siltstones.” Because of relative uniform basin subsidence, the deposition is predominantly controlled by climate controlled humidity changes (Geluk & Röhling 1999).

Main Buntsandstein subgroup

The Main Buntsandstein subgroup consists out of cyclic alternations of reddish arkosic (at least 25% feldspar) sandstones (partly oolitic (Geluk & Röhling 1999) and clayey siltstones. The deposits are mainly from fluvial/lacustrine origin, with an exception (Aeolian origin) for the offshore part of the West Netherlands Basin (Ames & Farfan 1995). The Main Buntsandstein subgroup consists, following Van Adrichem Boogaert & Kouwe (1993-1997) from old to young out of the Lower Volpriehausen, Detfurth and Hardeggen formation. The bottom of the Volpriehausen formation is marked by an unconformity, although locally, in tectonic grabens and half-grabens, a sandstone unit is present in a part of this hiatus. In the Netherlands, this unit is incorporated within the Volpriehausen formation (Geluk & Röhling 1999). The thickness of the entire Main Buntsandstein group has strongly been influenced by the extensional tectonics of the Hardeggen phase. The Hardeggen is overlain by the Solling formation (Geluk, Plomp & van Doorn 1996). The strongest subsidence occurred in the Off Holland Low, but the other Dutch southern basins subsided nearly as much. Although the Volpriehausen unconformity is rather known, the Detfurth unconformity is predominant in the lows (Geluk, Plomp & van Doorn 1996).

Volpriehausen

The Volpriehausen Formation consists out of the Lower Volpriehausen Sandstone and the Upper Volpriehausen sandstone member which grades into the Volpriehausen Clay-Siltstone. The Lower Volpriehausen shows excellent reservoir properties with high porosity of 10% to 15%, although high cementation levels occur in the lowermost part. The Upper Volpriehausen Sandstone is a reddish brown, silty sandstone, with several claystone intercalations. The stacked fining upward cycles contain much anhydrite, dolomite and ankerite cement. Because of the Detfurth and Solling unconformity, the thickness of the member strongly varies, between less than 50 and up to 150 m (Geluk, Plomp & van Doorn 1996).

Detfurth

The Detfurth formation consists out of the Lower Detfurth, the Upper Detfurth claystone and in northern parts of the Netherlands, the Detfurth Claystone Member. The Lower Detfurth formation consist out of quartz cemented quartz sand (60%) with porosities in the West Netherlands Basin between 15 and 20%. The thickness of the layer in the West Netherlands Basin is strongly dependent on the position, but lies in the range of twenty to fifty metres (Geluk, Plomp & van Doorn 1996). The Upper Detfurth Sandstone shows rather worse reservoir properties, due to two main claystone intercalations in the sandstone (Geluk, Plomp & van Doorn 1996).

Hardeggen

The Hardeggen Formation is recognized by an alternation of sandstones and claystones. The West Netherlands Basin is an exception of this rule and has much larger sandbeds, with reported porosities up to 20%. The thickness (or even occurrence) of the Hardeggen is mainly dependent on the erosion of the Solling Unconformity (Geluk, Plomp & van Doorn 1996).

Upper Buntsandstein

In some papers (Geluk & Röhling 1999) the Solling and Röt formations are referred to as Upper Buntsandstein. The depositional environment changed due to transgression of the Tethys via the southeastern part of the basin in the southern part of the Permo-Triassic basin. This resulted in the deposition of sulphates and carbonates in Poland and large halite depositions in Northern Germany (Ziegler 1982). Even more westward in the basin, this caused the deposition of the Röt halites and mudstones (Ziegler 1982)

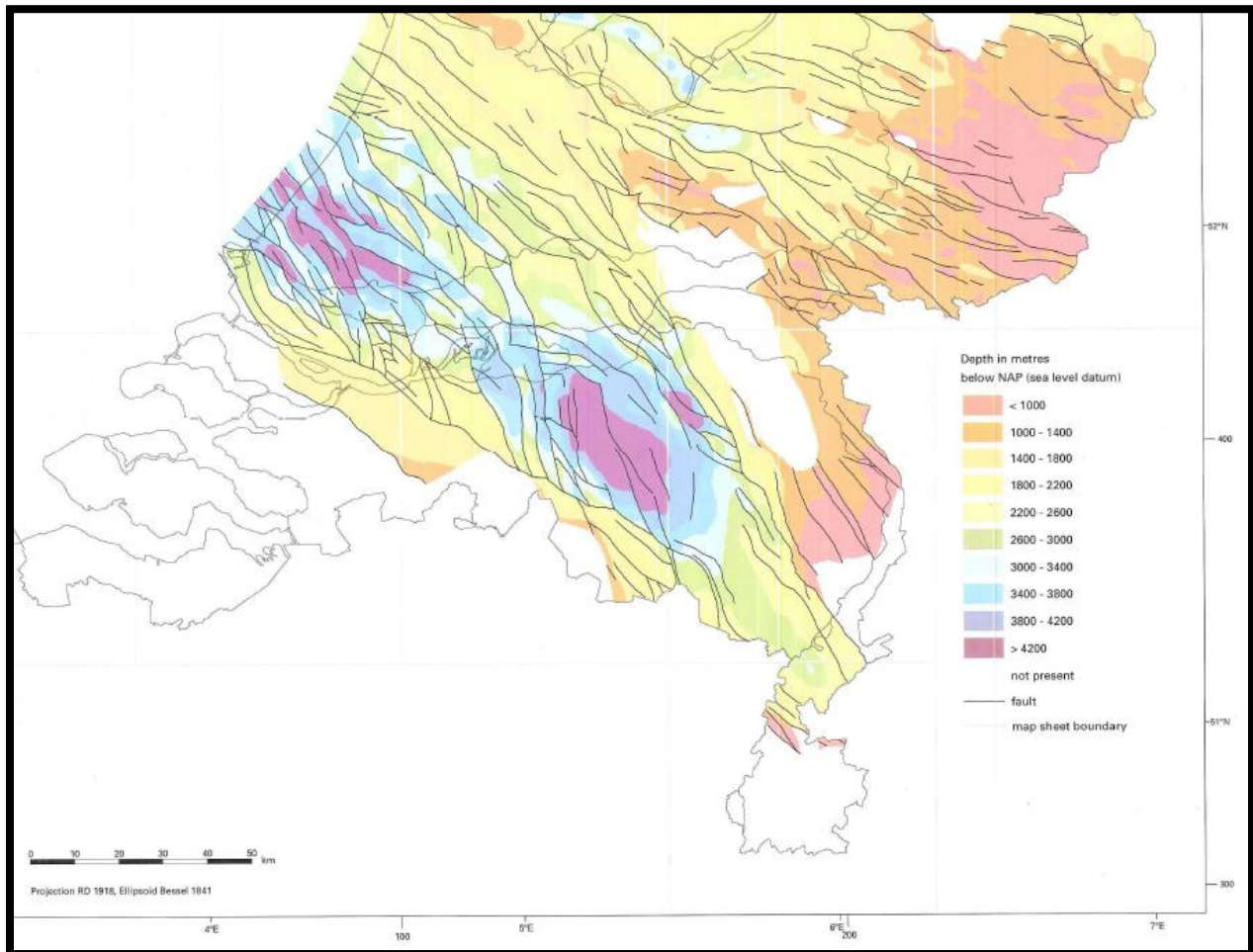


Figure 8. Depth of the base of the Lower Triassic (Lower Buntsandstein). (Detail from 'Geological atlas of the Subsurface of the Netherlands' 2004)

Muschelkalk

The start of the deposition of the Muschelkalk was caused by the transgression of the Tethys ocean and the accumulation of communications with the Tethys ocean. Therefore, open-marine conditions prevailed in the Basin (Ziegler 1982). For the West Netherlands Basin, this resulted in the deposition of evaporitic and dolomitic marls (Ziegler 1982). The Muschelkalk is subdivided into a lower, middle and an upper part. The lower part consists out of limestones, dolomites and claystones, the middle part out of evaporites and the upper part out of claystones and dolomites (Geluk, Plomp & van Doorn 1996). The whole formation is halite bearing, due to the evaporites that are present in the formation. The upper part of the Muschelkalk is absent the southern part of the Netherlands (and the West Netherlands Basin) due to erosion after the Triassic (Geluk, Plomp & van Doorn 1996).

Keuper Formation

The Muschelkalk formation ended with regional regression in Western and Central Europe. The termination of the carbonate regime followed by the Keuper clastic-evaporitic sedimentary regime. Eastern communications with the Tethys ocean became interrupted, but defined reasons are not certain. Only small marine incursions from the south were able to reach the southern basin. The return of the clastic infill, from eastern highs, of the basin marked the main difference between the Muschelkalk and the Keuper. The Keuper series could reach up to 2000m, although mainly in Northern Germany and the Polish Trough. In Late Triassic times, the Northwestern part of Europe was characterized by deltas, tidal flats and lagoons. Due to the still arid conditions also sabkhas were present. Subsidence and sedimentation was in balance with the cyclicity of rising sea-level. Conditions varied between arid to more humid and periods of extreme drought causing salt depositions to form (Ziegler 1982).

Jurassic, Cretaceous and Cenozoic times and the Alpine orogeny

Jurassic until Early Cretaceous

Rhaetian transgressions caused open-marine conditions to prevail in the West Netherlands Basin during most of Jurassic times. During Early Jurassic, shales and marls were deposited overlain by Middle and early Late Jurassic shales, marls, carbonates and minor clastic deposits. Deposition of coarser clastics in the deeper parts of the basin rarely occurred. Early Kimmerian uplifts caused minor unconformities to form during the Late Triassic and Early Jurassic. Although these unconformities are present on the basin margins and highs, the West Netherlands Basin shows highly uniform up fill during these times.

Intercalations between shallow marine and deep marine deposition change from time to time during Early and Middle Jurassic times, causing the deposition of shales, marls and carbonates (Van Adrichem Boogaert & Kouwe 1993-1997). The start of the Late Jurassic was marked by the mid-Kimmerian phase, that introduced a period of tectonic instability, that only would end in the Early Cretaceous, for most of Northwestern Europe. The increased rifting caused dextral NW-SE striking faults and induced differential subsidence of the basins (West Netherlands Basin) as well as uplift of the local highs. It is very likely that this rifting phase followed more or less the fault systems of the Late Hercynian faults. Due to the rapid subsidence of the basins, the highs were almost constantly subjected to erosion. The Late Kimmerian tectonic pulse was accompanied with a major eustatic regression, that formed a hiatus in the late Jurassic series in the West Netherlands Basin. During middle Early Cretaceous times, sedimentation continued, induced by a sea level rise. Sea level rise continued until late Early Cretaceous times when also on the highs on the borders of the basins, sediment was deposited (Van Wijhe 1986, Ziegler 1982).

Late Cretaceous and the Alpine orogeny

The Late Cretaceous was characterized by the progressive opening of the Atlantic Ocean and the start of the Alpine orogeny, causing major changes in the megatectonic regime. This was accompanied by a drastic rise of the eustatic sea level. The major transgression caused flooding of the shelves, as well as the surrounding highs. Estimates of the eustatic sea level range from 110 to 300 meters (Ziegler 1982). The tectonic quiescence of the West Netherlands Basin, regional subsidence, as well as the decrease of clastic influx caused huge chalk deposits to form (Ziegler 1982). The Sub-Hercynian tectonic phase induced the formation of huge anticlinoria and reactivated extensional faults that were formed during the Jurassic and Early Cretaceous times. The highs that arose were subjected to various degrees of erosion while in areas that had not been folded or reversed, sedimentation still continued (Ziegler 1982, Van Wijhe 1986). Small-scale thrust faults are evident along the margins of the strongly inverted West Netherlands Basin, following van Wijhe (1986) and Roos et al. (1983). Late Permian, and in a minor extent Triassic salts could have acted as the disharmonic layers in which the fault displacements have been dissipated (Van Wijhe 1986). This rural period was followed with decreased tectonic activity as well as advancing seas causing chalk deposition during the late Cretaceous in the inverted basins.

A second, more intense, tectonic phase occurred during the Paleocene. This event, the Laramide pulse, was the last extensional tectonic event in the West Netherlands Basin and caused, in combination with a major regression, a huge change in paleogeographic environment (Ziegler 1982, Van Wijhe 1986). The event reactivated the fault system that was already active during the Sub-Hercynian inversion. The combination of the very low sea level as well as the inverted basins, caused rapid erosion to occur. The

compressional as well as wrench movement caused steep reverse faults, small-scale overthrusts and flower structures to form especially in the West Netherlands Basin (figure 9) (Ziegler 1982). Inversion caused the floor of the West Netherlands Basin to be uplifted just below or even above areas that had not been subsided in Permian to Cretaceous times (Ziegler 1982). The structural relief in West Netherlands Basin at the Late Cretaceous level is 2000 meter, while it is only 500 meter for the base of the Zechstein (Ziegler 1982). Following van Wijhe (1986) and Ziegler (1982), inversion movements in the Broad Fourteens basin are even higher at 3000-3500 meter for shallower levels and 2000m at the base of the Zechstein.

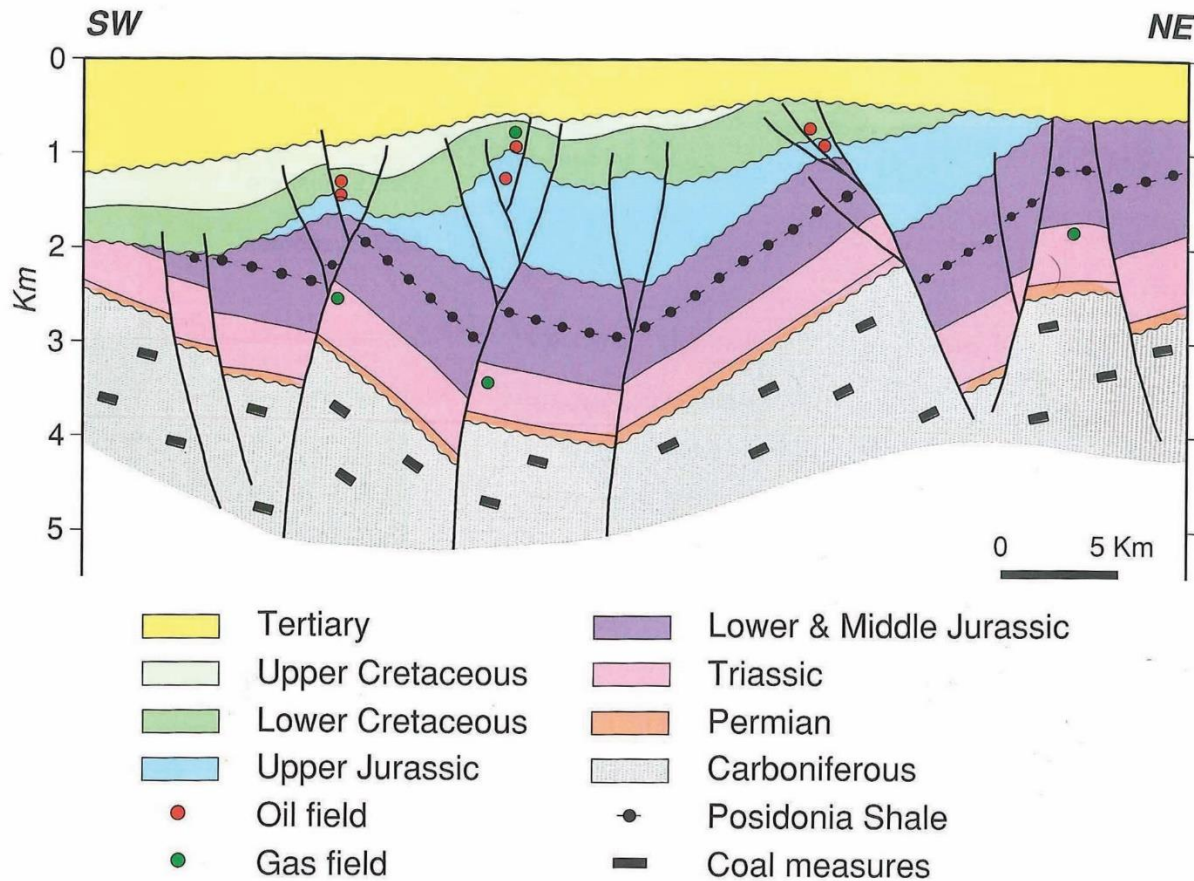


Figure 9. Cross-section of the West Netherlands Basin, passing through appr. Pernis, IJsselmonde/Ridderkerk and Moerkapelle. (De Jager et al. 1996)

After the Laramide phase, the tectonic activity ceased due to onset of seafloor spreading north of a fracture zone near Iceland (Charlie Gibbs fracture zone). The tectonic quiescence was accompanied with regional subsidence, which is still taking place (Ziegler 1982).

Data and Methods

NLog

The website NLog.nl contains all public data of every borehole in the Netherlands. From these data we created a database of wells penetrating the Buntsandstein. Of these wells only some have borehole cores of the Hardegens formation available. On these cores, core plug measurements were performed which are available on NLog. Also gamma ray logs and sedimentology reports are publicly available of most of the wells.

In total 9 exploration wells with cored intervals were studied. The locations of the wells are displayed in figure 10 and more information about the wells is given in table 1. Three of the wells are located off-shore in the North Sea. Six wells are located on-shore in the province Zuid-Holland near Rotterdam. This area has a rich history in hydrocarbon exploration which results in a large available data set.

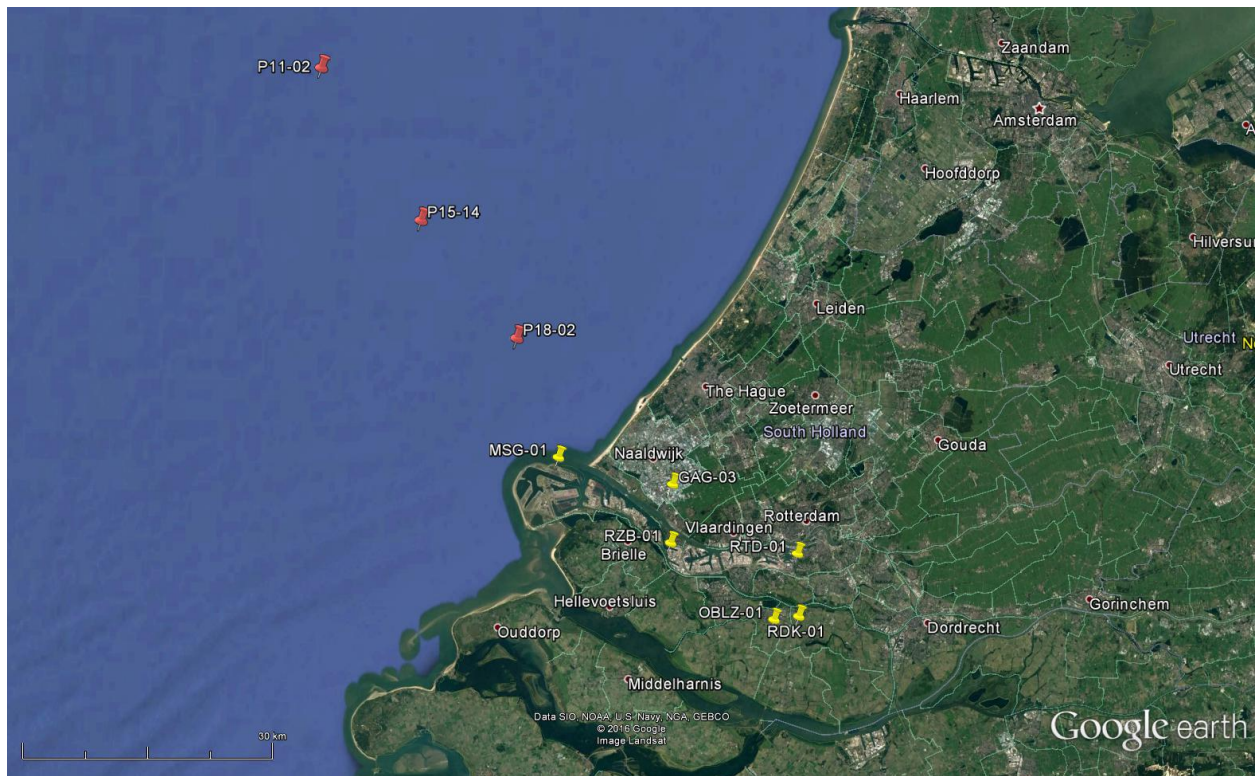


Figure 10. Geographic locations of on-shore wells (yellow) and off-shore wells (red) plotted on Google earth satellite images (Adapted from Google Earth)

Core description

During the research three core slabs of different borehole sites were described. The cores were made available by the well operators and stored by TNO at their storage location in Utrecht, Netherlands. The described cores, P11-02, P15-14 and P18-02, were all located off shore in the North Sea.

The core descriptions were performed by hand on a scale 1:50. Tools like a microscope, magnifying glass and grain size ruler were used. The entire cored interval and specific sedimentary structures were photographed for later reference. The core descriptions can be found in Appendix A.

Core plug measurements

The three off-shore wells with cored intervals, P11-02, P15-14 and P18-02, of which a core description was made were tested for their porosity and horizontal permeability. From the on-shore well database six wells with core measurements, GAG-03, MSG-01, OBLZ-01, RDK-01, RTD-01 and RZB-01, were selected to be studied for further reservoir properties. All on shore wells are located near Rotterdam in the Dutch province Zuid-Holland (figure 10). The core measurement data are presented in an excel file Appendix G, graphs of off-shore wells are displayed in Appendix B, graphs of on shore core measurements are displayed in Appendix C. The data was available and obtained from NLog.nl, a website from TNO.

well	Depth TVD (m)	Average porosity (%)	Average permeability (mD)	Standard deviation porosity	Standard deviation permeability
P11-02	2264-2319	19.0	161.8	5.47	233.7
P15-14	3106-3110.5	12.3	206.5	5.53	247.5
P18-02	3258-3275	10.6	136.1	2.69	574.5
OBLZ-01	2260-2280	20.3	1116	3.23	1334
RDK-01	2725-2750	12.1	177	4.06	611.0
RZB-01	2820-2836	14.1	235	3.23	264.5
RTD-01	2860-2880	14.0	51.4	3.86	58.3
GAG-03	2910-2938	15.5	465	3.79	568.7
MSG-01	2940-2970	15.7	967	3.58	2777.1

Table 1. True vertical depth and average core plug measurements with their standard deviations..

Well operator reports

Well operator reports were available on NLog for four wells. The reports were studied and summarized to determine the cause of high permeability and porosity sections in the cores at depths of three thousand meters. The findings of the researchers were studied get a better understanding of the grain size distribution, grain texture, composition of the clasts, cementation and diagenetic processes throughout the Hardeggen formation.

Gamma ray log

Gamma ray logs were available for all wells and made available on Nlog by the well operators of the concerned exploration well. The Gamma ray logs are presented in the composite well logs and show API values at specific depths. The logs were interpreted and linked to the well measurements to get a better understanding of their relation to each other. The data are displayed in Appendix D.

Field description

A field trip to the German province Thüringen was planned. Multiple outcrops of the Bunter formation were studied and described to give a better view on how the homogeneity and thickness of the separate layers behave over a larger unit and not just a specific location like a borehole does.

The field observations were used to relate core descriptions and measurements at a specific location to their surroundings. Giving a better view on what the surroundings of the well might look like. A good understanding of the rock in lateral direction is very important to make inferences about the reservoir properties.

Results

Core section description

65 on-shore wells and 68 off-shore wells were located in the region of interest, and reach the Bunter formation. Borehole cores were taken from several wells by the well operators and stored at TNO in Utrecht. These cored intervals were analyzed and described on their sediment structures and lithology by hand. This gives a detailed description of the potential reservoir at a specific borehole. Also detailed photos were taken for later use. Three wells were selected for core section description. All three wells are located off-shore and penetrate the Hardeggen formation.

The described cores consist of a continuous cored interval of the Hardeggen formation. The main objective is to give a detailed description of the Hardeggen formations sedimentary structures and an interpretation on the depositional environment. Also to obtain a clear view of the reservoir properties and a diagenetic interpretation.

P11-02

The core P11-02 is 29.5 meters. The dominant grainsize is fine to medium grained sandstone with a Net/Gross ratio of 0.92. The beds are 0.5-6 meters thick. Beds with visible cross-bedding, coarsening-up



Figure 11. Silty/clayey very fine sand with very small shale layers(1-3 mm), P11-02, 2374.00-2373.10 m.

and several fining-up sequences, are usually thinner(0.5-2 m) than beds that show no visible cross-bedding. This could either be caused by the fact that the different beds are not distinguishable because of the abundance of visible cross-bedding or that these beds actually have a different thickness, possibly caused by the different thickness and shape of sand dunes. A thick clayey very fine sand layer of 2 meters thick with some small clay layers of 1-3 mm thick is found in the bottom part of the core (figure 11).

P15-14 and P18-02

Core P15-14 and P18-02 are respectively 4.5 and 15 meters long. The dominant grainsize is fine to medium grained sandstone with minor coarse to very coarse (Figure 12) on the top of the beds with a Net/Gross ratio of 0.99. The beds are 0.25-5 meters thick and thicker (more than 1 meter) fine grained layers contain very small, up to 1 mm, greenish shale layers.



Figure 12. fining-up sequences from fine to medium/coarse grained sand. P18-02, 3287-3288 m.

Cores P15-14 and P18-02 show a more constant depositional environment since they both show cross-bedded fining-up and 1 coarsening-up sequence (see figure 12 and 13), with minor clay and silt (millimeters) intercalations.

Distance from the basin margin

The Hardeggen succession in P11-02 shows most of the types of depositions that were expected in the Hardeggen formation based on literature. Thick homogenous sandstone beds with fine to very fine grain sizes are alternated with cross-bedded coarsening-up and several fining-up sequences, both from alluvial as well as aeolian origin, intercalated with up to two meter thick silty/clayey very fine sand.

P11-02 gives the best representation on the general development of the Hardeggen succession. Since P11-02 is situated further away from the basin margin small changes in tectonic, climatic as well geomorphologic circumstances have much more influence on the depositional environment. P15-14 and P18-02 are deposited along the basin margin and show better potential reservoir properties in terms of grain size and sorting compared to the fine to very fine sands that were found in core P11-02. The very coarse sands that alternate with finer sand layers of well P18-02 show good reservoir potential. P18-02 and P15-14 do not show the small greenish clay layers that are so characteristic for the bottom part of core P11-02.



Figure 13. Fining-up sequences from fine to medium/coarse grained sand. P18-02, 3287-3288 m.

Silt and Clay Deposits

The bottom part of core P11-02 (figure 14) shows clay layers that have been intercalated by sands. These layers, that are very likely to be from playa lake or wet sand flat origin, have a high clay content resulting in clayey layers up to a cm thick. These clay/silt layers are heavily disrupted with desiccation or syneresis cracks. This syneresis should affect the vertical permeability of the clay layers in a positive way. Therefore the expected vertical permeability could be better than was beforehand expected.



Figure 14. Clay and sand layers with desiccation or syneresis cracks. P11-02, 2376 m.

Well operator reports

P11-02

Thin slab, XRD and microscopy analysis has been obtained by G.A.P.S. B.V. prepared for AMOCO B.V.

MSG-01

Thin slab and microscopy analysis has been obtained by NAM Stratigraphical and Sedimentological services prepared for NAM B.V.

OBLZ-01

Thin slab, XRD and microscopy analysis has been obtained by G.A.P.S. B.V. prepared for NAM B.V.

RDK-01

Thin slab, XRD and microscopy analysis has been obtained by G.A.P.S. B.V. prepared for NAM B.V.

Core plug measurements

The core plug measurements are available in Appendix B and C average values and their standard deviation are displayed in table 2.

well	Depth TVD (m)	Average porosity (%)	Average permeability (mD)	Standard deviation porosity	Standard deviation permeability
P11-02	2264-2319	19.0	161.8	5.47	233.7
P15-14	3106-3110.5	12.3	206.5	5.53	247.5
P18-02	3258-3275	10.6	136.1	2.69	574.5
OBLZ-01	2260-2280	20.3	1116	3.23	1334
RDK-01	2725-2750	12.1	177	4.06	611.0
RZB-01	2820-2836	14.1	235	3.23	264.5
RTD-01	2860-2880	14.0	51.4	3.86	58.3
GAG-03	2910-2938	15.5	465	3.79	568.7
MSG-01	2940-2970	15.7	967	3.58	2777.1

Table 2. Average properties of the core plug measurement of the evaluated wells.

Field description

In the field trip we were able to define a description of sedimentary structures in the Hardegsen on a large scale. Location and pictures of the individual stops can be found in Appendix E. These descriptions can be linked to the core descriptions which results in a better understanding of the lateral continuity of the sedimentary structures.



Figure 15. 1-2 meter thick cross-beds from the Hardegsen formation in Thüringen (Germany). (the spring rule is 1 m in length)

In the field study the Hardegsen outcrops show thick homogenous sandbanks of ca. 1 to 2 meters thick with clearly visible cross-bedding (figure 15). Thick laterally consistent shale layers of 10-50 centimeters (figure 16) are found with sharp transitions between the sandstones. These layers are laterally consistent over the entire outcrop. A similar sediment layer was present in the core section of well P11-02 at 2376 m (figures 11 and 14). It is assumed that thicker (more than 10 cm) shale layers found in the core description generally are continuous in the horizontal direction.

All Hardegsen outcrops investigated during the field trip show very clear cross-bedding patterns over the entire length of the outcrop. Many core descriptions also clearly show cross-bedding, but this not count for all of them. Absence of visible cross-bedding could either be caused by the homogeneity of the beds or the actual absence of it at all. Since this is very hard to define this based on the field work findings, this will be discussed later with the integration of geographic orientation.



Figure 16. Laterally consistent 10-30 cm thick silty/clayey very fine sand layers overlain by thick cross-bedded sandstones from Thüringen (Germany).

The core descriptions show occasionally very small very fine sand banks or clayey layers of maximum several mm thick. These layers can be linked to the not continuously small clay lenses that were found in between the cross-bedded sand layers. However, outcrops rarely showed smaller (1 mm) laterally consistent clayey layers. We cannot be entirely sure whether the small clayey layers in the core descriptions are continuous or not. However the clay lenses tend to be a little bit thicker than the continuous very fine sand and clayey layers which means we can make an assumption on continuity of the layers. Also the presence of these layers in between cross-beds will give you a high certainty that they follow the bedding planes and are therefore not laterally consistent.

One outcrop of the field study showed layers of 1.5 cm thick with a high mica content. These layers were not continuous over the entire length of the outcrop but continued for around 1-5 meters. Similar layers were found in the core of well P15-14.

The entire field trip report is presented in Appendix E.

Interpretation

Core plug measurement interpretation

Of all wells the permeability and porosity measurements at a certain depth are plotted against each other in a figure. This results in a scatter of data points. When the data points are close together it means the entire cored interval shows about the same porosity and permeability values at a specific depth and thus indicates a homogenous reservoir. A wide scatter shows a non-homogenous reservoir. The reservoir quality is restricted by the data points that are in the lower left corner since these represent the lowest permeability/porosity values. Through the set of points a trend line is fitted which indicates the positive correlation between porosity and permeability.

Continuous core plug measurement plot

The porosities and permeabilities of the samples has been plotted continuous instead of scattered. This is not a true representation of the reality. Core plug measurements are generally taken every 30 centimeter. They are therefore not continuous and show only point measurements. The choice for a continuous plot has been made for visibility reasons, since it is easier to see lower and higher porosity/permeability zones on a larger scale. The fact that layers between two measurements could show either worse or better qualities should always be taken into account.

P11-02

Based on permeability and porosity measurements the cored interval of P11-2 can be divided in 3 sections.

The lower part of the core, unit [A] (2376.5-2379 m)

The middle part of the core, unit [B] (2366-2376.5 m)

The upper part of the core, unit [C] (2350-2366 m)

Unit [A] (2376.5-2379m) has high horizontal permeability ranging from 50-675 mD, and porosity values around 15% (mean 15.5%). The values are increasing as depth decreases.

Unit [B] (2366-2376.5m) shows lower permeabilities ranging from 0.04-10 mD with occasionally higher permeabilities of around 50 mD. Unit B has a lower vertical permeability due to its more impermeable layers and has fluctuating porosity values between 10-20% (mean 15.7%)

unit [C] (2350-2366m) has high permeability's ranging from 50-1300 mD. And high porosity values of 20-25% (mean 21.7%)

The porosity and permeability against depth is plotted in figure 17 and porosity-permeability plot (figure 18) shows the relation between porosity and permeability.

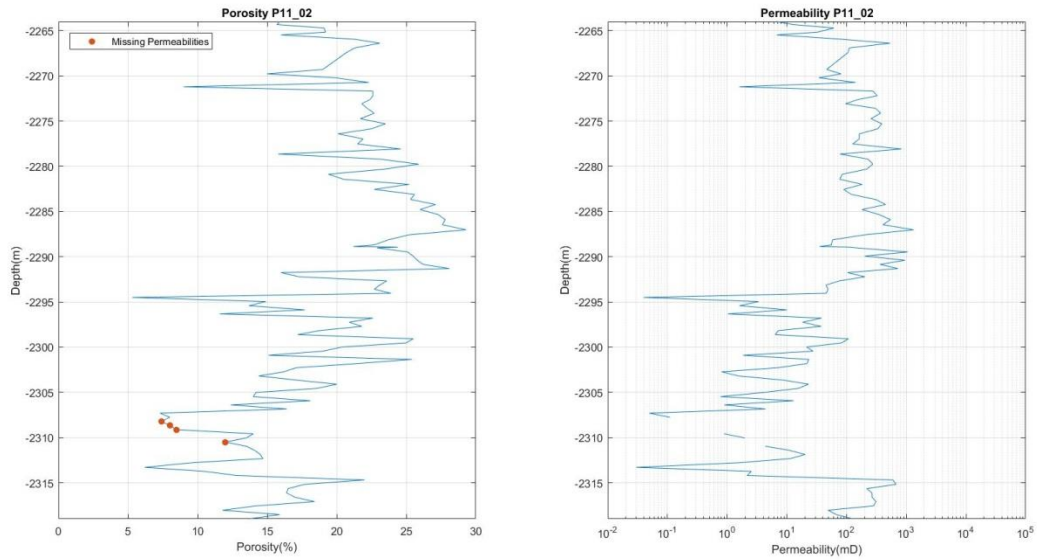


Figure 17. Porosity and permeability core plug measurement of well P11-02 plotted against depth. Red dots show missing permeability values due to either very low permeability or damaged samples.

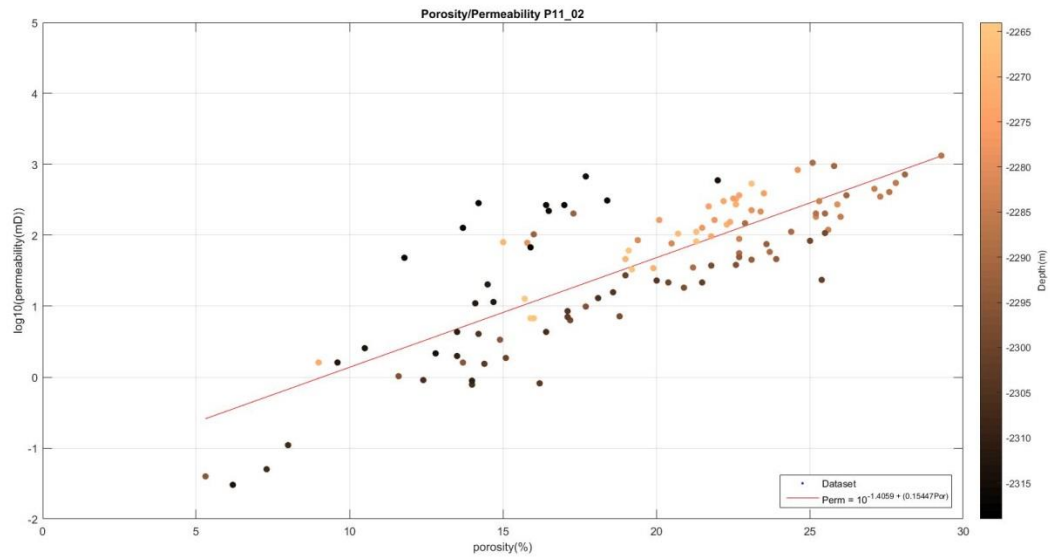


Figure 18. Porosity/permeability plot of P11-02 with trend line. Depth of the sample is plotted with color with the corresponding color bar at the right.

P15-14

Based on permeability and porosity values the cored interval P15-14 can be divided into four units.

Unit [A] (3151.7-3152.7 m)

Unit [B] (3149.3-3151.7 m)

Unit [C] (3146-3149.3 m)

Unit [D] (3145-3146 m)

The lower part of the core Unit [A] (3151.7-3152.7m) has a low permeability (mean 0.4 mD) and low porosity (mean 5.8%).

Unit [B] has higher permeability (mean 295 mD) and porosity values (mean 13.4%).

Unit [C] has low permeability and porosity values (mean 5 mD and 7% respectively) that are very low and show similar values with unit [A] which suggests that the type of sediments of unit [C] are comparable with the deposits of unit [A].

Unit [D] shows better permeability (mean 280 mD) and porosity (mean 18%) values. Of this section there were no cores available.

The porosity and permeability against depth is plotted in figure 19 and porosity-permeability plot (figure 10) shows the relation between porosity and permeability.

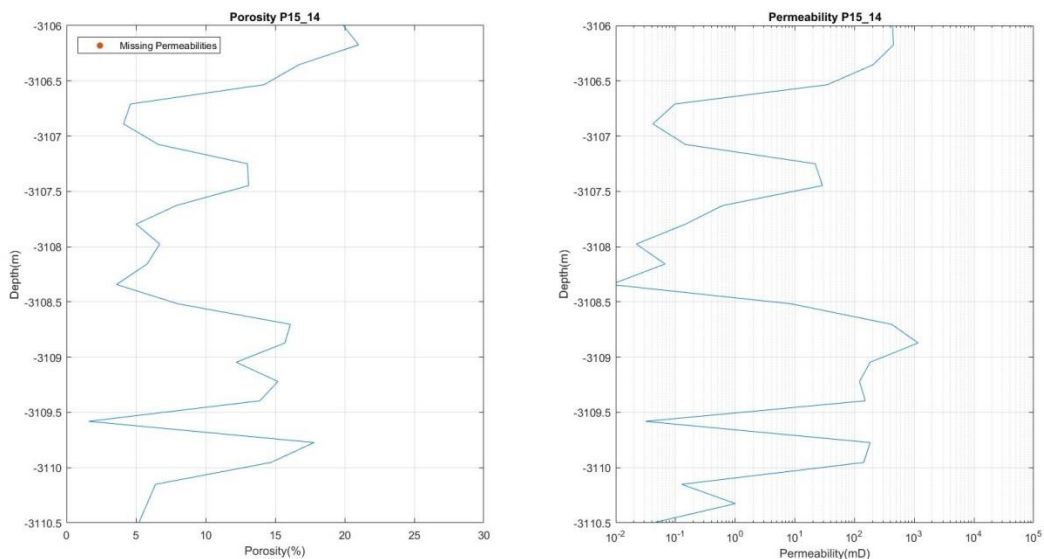


Figure 19. Porosity and permeability core plug measurement of well P15-14 plotted against depth. Red dots show missing permeability values due to either very low permeability or damaged samples.

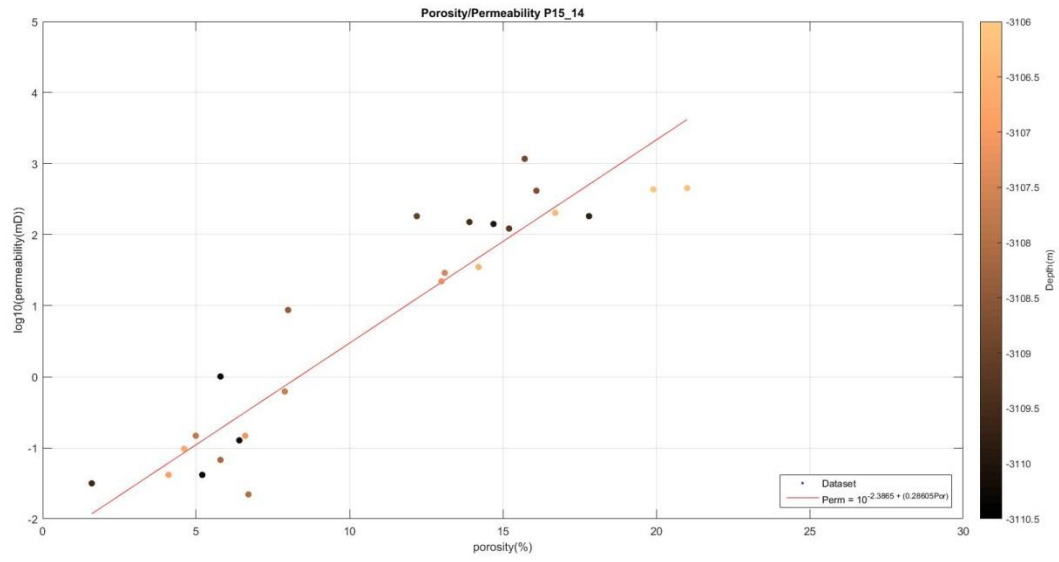


Figure 20. Porosity/permeability plot of P15-14 with trend line. Depth of the sample is plotted with color with the corresponding color bar at the right.

P18-02

Based on permeability and porosity values the cored interval P18-02 cannot be divided in different units. The permeability is high and fluctuating throughout the entire core between 50-300 mD (mean 206 mD). The porosity gives values between 10-15% (mean 12.3%). The bottom part of the cored interval (3297-3298.75 m) generally shows lower permeability and porosity values (mean 5.6 mD and 8% respectively)

The porosity and permeability against depth is plotted in figure 21 and porosity-permeability plot (figure 22) shows the relation between porosity and permeability.

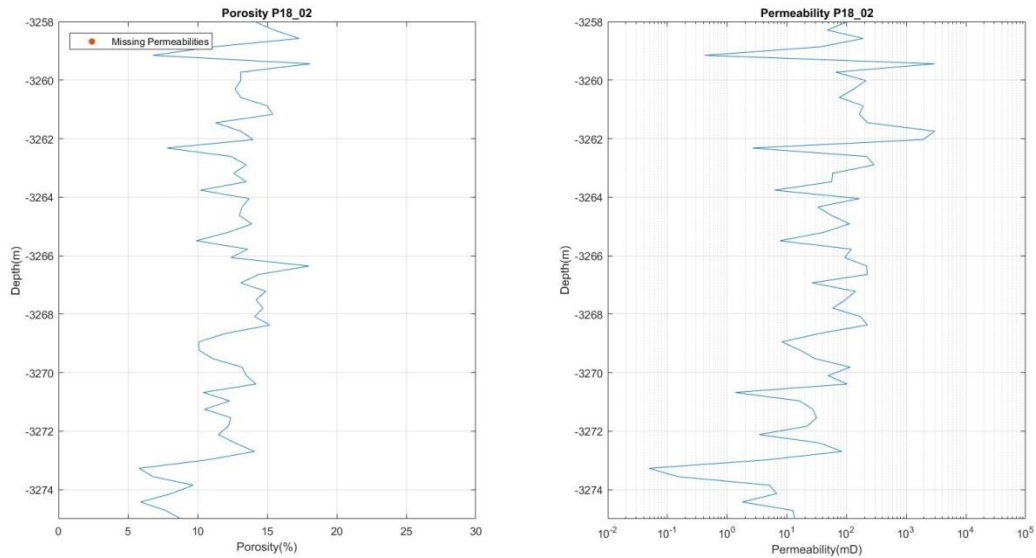


Figure 21. Porosity and permeability core plug measurement of well P18-02 plotted against depth. Red dots show missing permeability values due to either very low permeability or damaged samples.

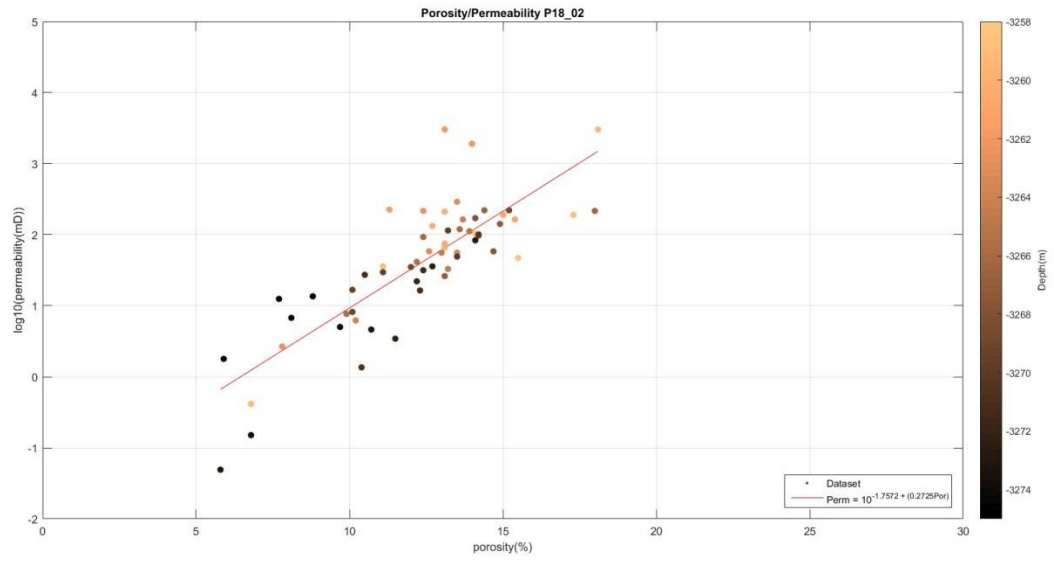


Figure 22. Porosity/permeability plot of P18-02 with trend line. Depth of the sample is plotted with color with the corresponding color bar at the right.

RDK-01

The depth of the cored interval is at 2725-2750 m TVD and 2800-2825 m ABH.

The cored interval of Reedijk-01 is not very homogenous in permeability and porosity. Sections with a low permeability and low porosity alternate with porous, high permeable layers. The porosity values typically range between 10-15% but at some depths reach values as low as 3% or as high as 20%. The average porosity of the core is 12%. Permeability is fluctuating strongly and ranges from 0.1 mD in low permeable layers to 300 mD in high permeable layers. The mean permeability over the entire length of the core is 177 mD.

These alternations of sections with high porosity and permeability with sections with low porosity and permeability can drastically influence the vertical permeability of the reservoir, when layers are continuous throughout the entire reservoir.

The porosity and permeability against depth is plotted in figure 23 and porosity-permeability plot (figure 24) shows the relation between porosity and permeability.

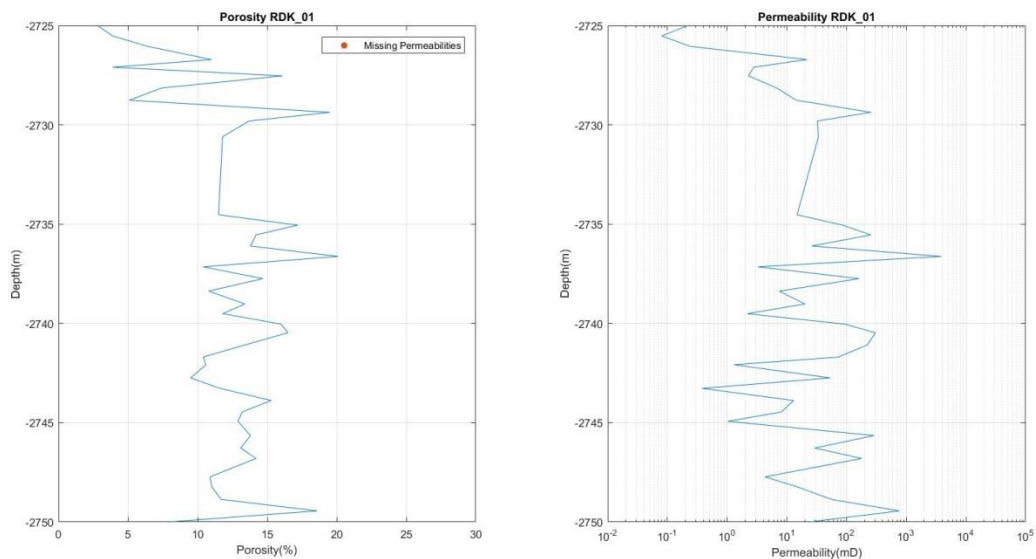


Figure 23. Porosity and permeability core plug measurement of well RDK-01 plotted against depth. Red dots show missing permeability values due to either very low permeability or damaged samples.

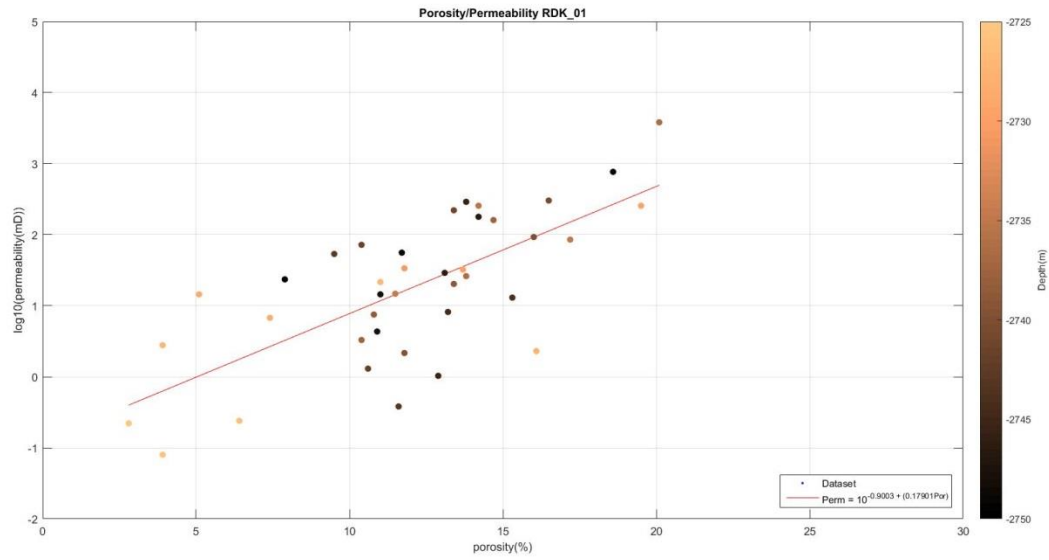


Figure 24. Porosity/permeability plot of RDK-01 with trend line. Depth of the sample is plotted with color with the corresponding color bar at the right.

MSG-01

The depth of the cored interval is at 2940-2970 m TVD and 3753-3783 m ABH.

The cored interval of Maasgeul-01 can be divided in three units based on the porosity and permeability measurements.

Unit [A] (3788.9-3780 m) is porous and permeable. The section has an average permeability of 74.5 mD. The porosities range between 10-15% (mean 12.3%). In this part of the cored interval there are however some low permeable layers for example at a depth of 3780 m where the permeability drops significantly.

Unit [B] (3780-3766.5 m) is porous and permeable. The section is very constant in porosity. The permeability is more variable. Unit B has an average permeability of 140.5 mD. The porosity ranges between 15-20% (mean 16.4%) and are slightly increasing with decreasing depth.

Unit [C] (3755-3766.5 m) consists of porous layers (mean 17.6%) with very high permeabilities (mean 2645 mD). At 3764.3 m there is one small low permeable (1.54 mD) layer in the interval. There are some fluctuations in permeability and porosity which could be the result of differences in grain sizes or cementation.

The porosity and permeability against depth is plotted in figure 25 and porosity-permeability plot (figure 26) shows the relation between porosity and permeability.

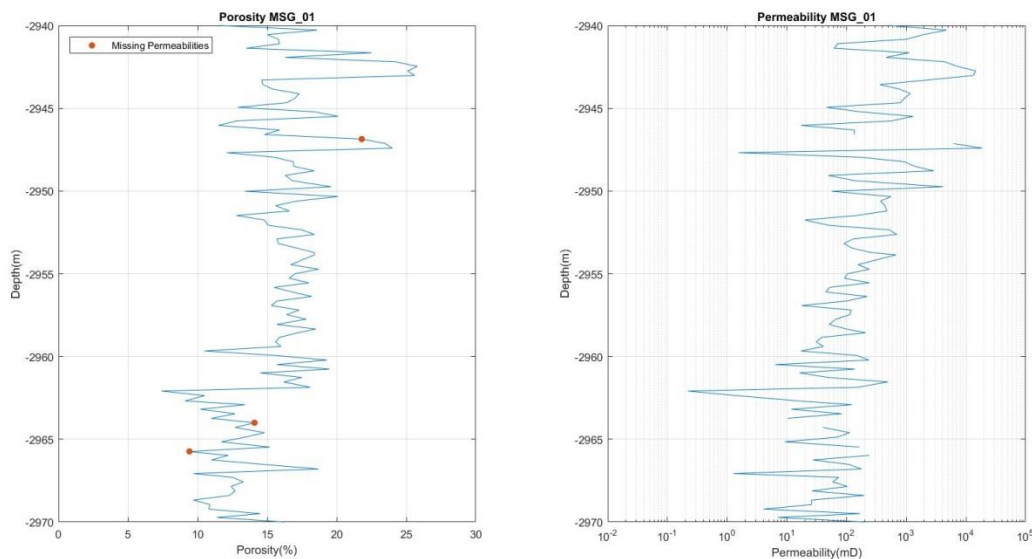


Figure 25. Porosity and permeability core plug measurement of well MSG-01 plotted against depth. Red dots show missing permeability values due to either very low permeability or damaged samples.

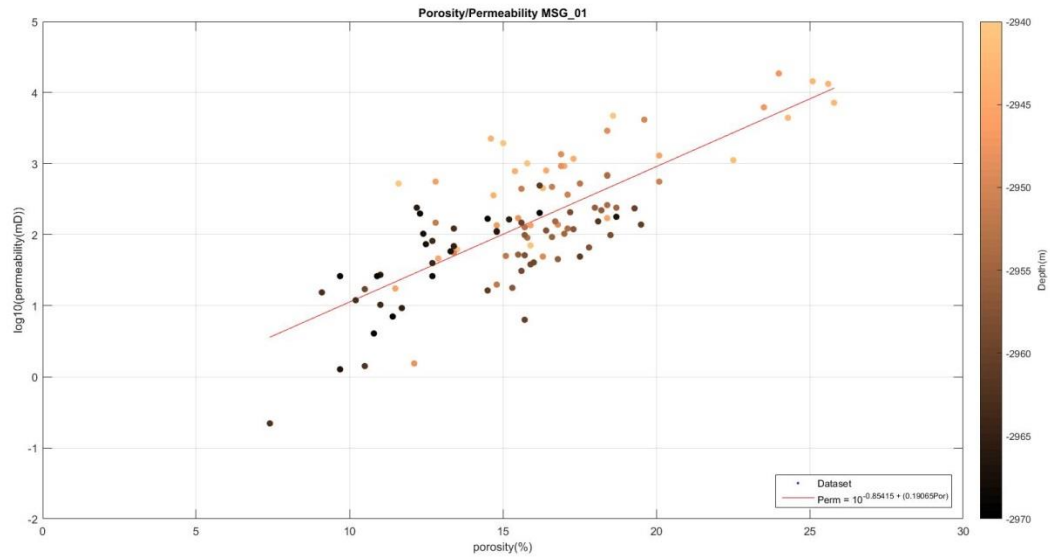


Figure 26. Porosity/permeability plot of MSG-01 with trend line. Depth of the sample is plotted with color with the corresponding color bar at the right.

RTD-01

The depth of the cored interval is at 2860-2880 m TVD and 3103-3122 m ABH.

Rotterdam-01 can be divided in two units based on the porosity and permeability measurements.

The lower part, unit [A] (3122.7-3114 m) shows porosity's between 15-20% with some low measurements below 10% (mean 15.3%). The average permeability is 65.7 mD what stands out are the 2 very low measurements.

The upper part, unit [B] (3114-3105.3 m) shows 2 sequences of decreasing porosities with decreasing depth. The permeability measurements do not show any patterns but are fluctuating strongly throughout this section. The average porosity of unit [B] is 12.8% and the average permeability is 37.6 mD.

The overall average permeability of the cored interval is 51.4 mD and the overall average porosity is 14%.

The porosity and permeability against depth is plotted in figure 27 and porosity-permeability plot (figure 28) shows the relation between porosity and permeability.

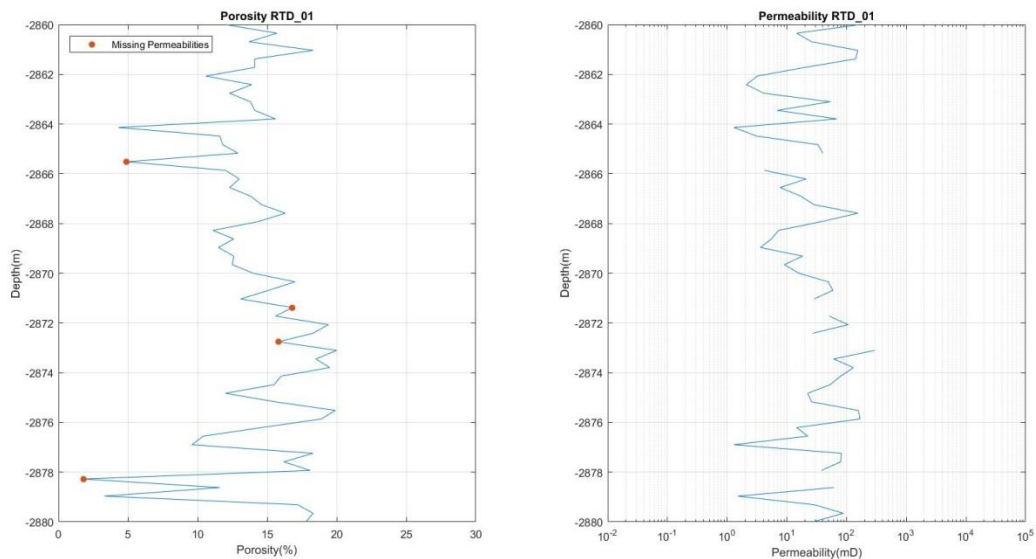


Figure 27. Porosity and permeability core plug measurement of well RTD-01 plotted against depth. Red dots show missing permeability values due to either very low permeability or damaged samples.

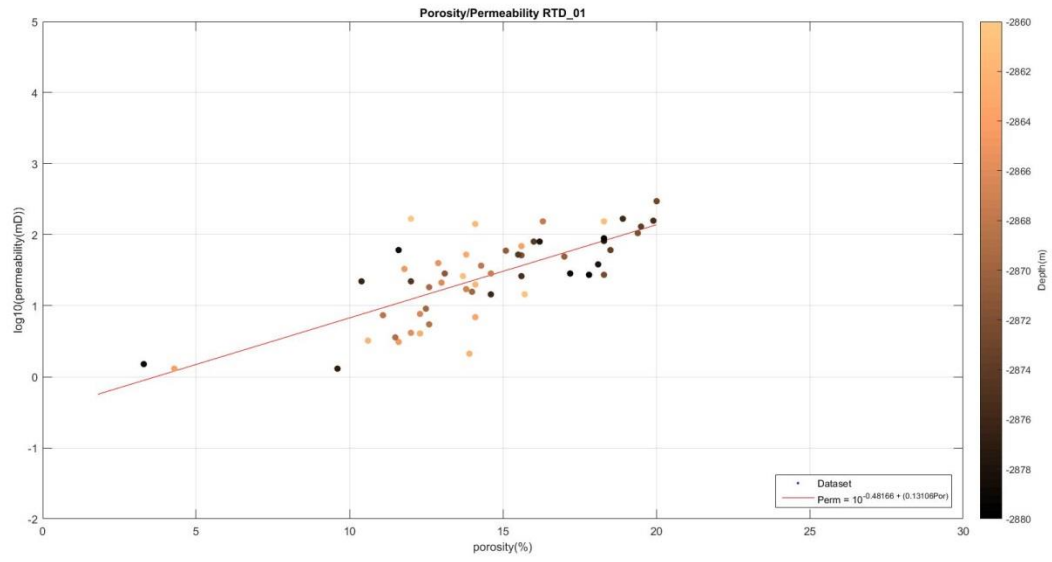


Figure 28. Porosity/permeability plot of RTD-01 with trend line. Depth of the sample is plotted with color with the corresponding color bar at the right.

RZB-01

The depth of the cored interval is at 2820-2836 m TVD and 2989-3005 m ABH.

Rozenburg-01 is a cored interval with homogeneous porosity values between 10-20% (mean 14%) and permeabilities of around 100-300 mD (mean 235 mD). There is one small section with a lower permeability and porosity at 2990 m. With decreasing depth the values are increasingly fluctuating.

The porosity and permeability against depth is plotted in figure 29 and porosity-permeability plot (figure 30) shows the relation between porosity and permeability.

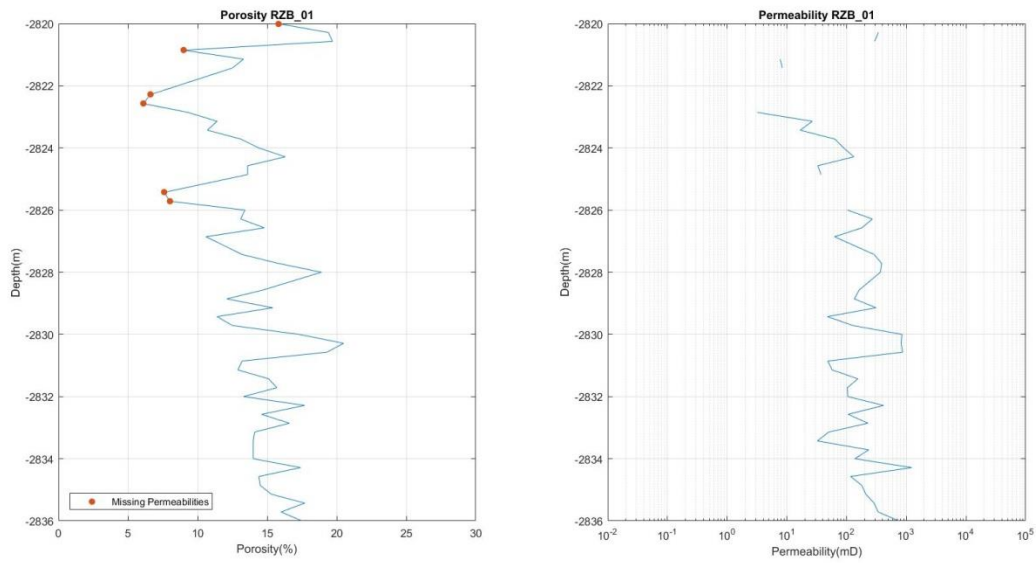


Figure 29. Porosity and permeability core plug measurement of well RZB-01 plotted against depth. Red dots show missing permeability values due to either very low permeability or damaged samples.

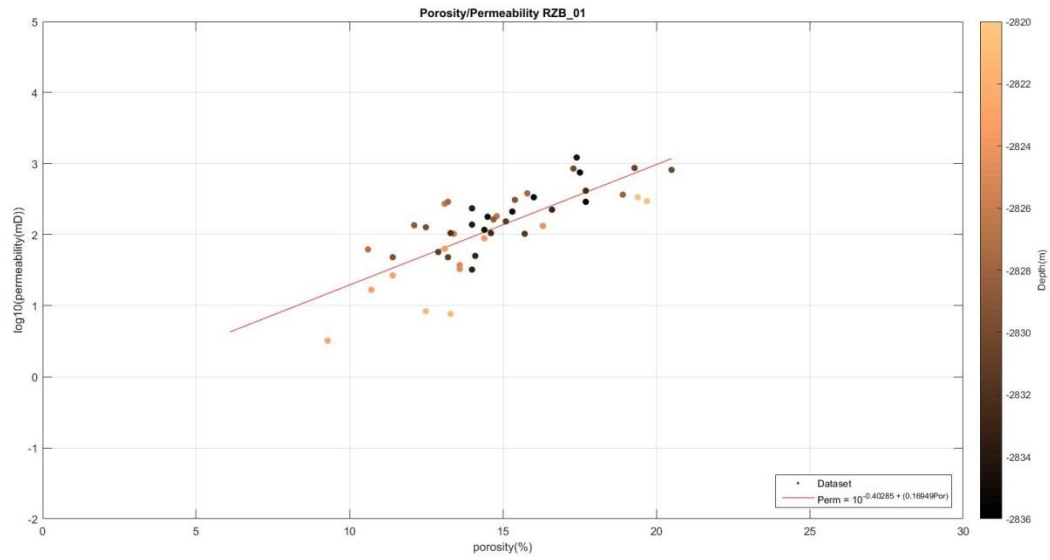


Figure 30. Porosity/permeability plot of RZB-01 with trend line. Depth of the sample is plotted with color with the corresponding color bar at the right.

OBLZ-01

The depth of the cored interval is at 2260-2280 m TVD and 2275-2295 m ABH.

Oud Beijerlandzuid-01 is a core interval with a mean porosity of 20% and large permeability's in the hundreds and some intervals thousands mD (mean 1116 mD). The measurements are very constant with only two measurements with very low permeability's. When these impermeable sections are small local clay lenses or mud pebbles it wouldn't affect the reservoir properties a lot however when these are continuous horizontally stratified impermeable layers they can become of great influence.

The porosity and permeability against depth is plotted in figure 31 and porosity-permeability plot (figure 32) shows the relation between porosity and permeability.

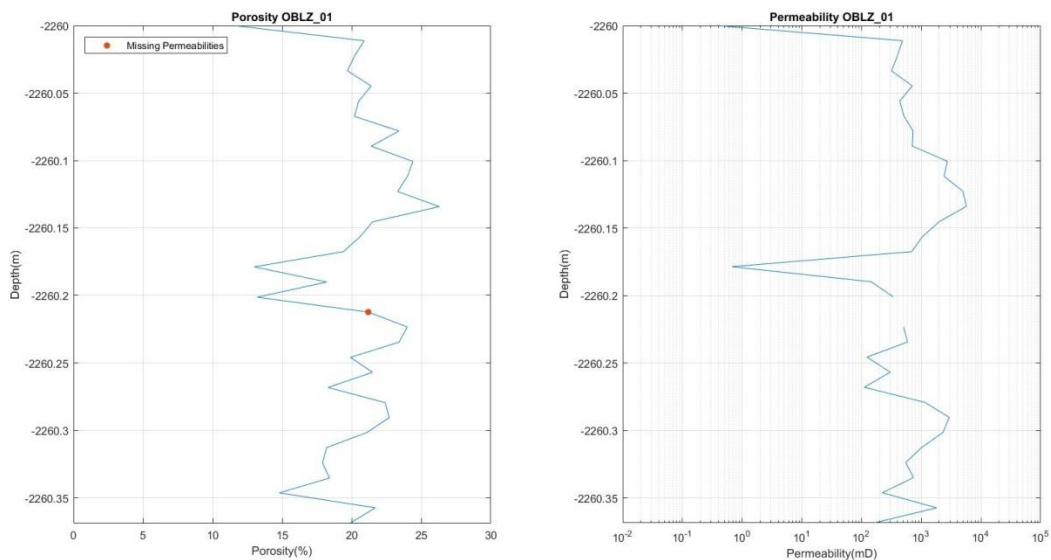


Figure 31. Porosity and permeability core plug measurement of well OBLZ-01 plotted against depth. Red dots show missing permeability values due to either very low permeability or damaged samples.

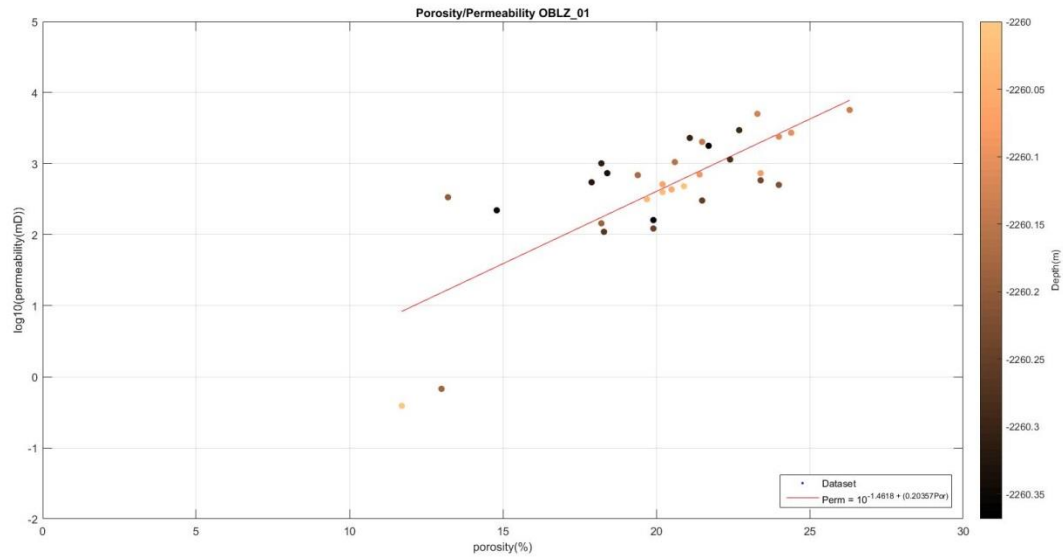


Figure 32. Porosity/permeability plot of OBLZ-01 with trend line. Depth of the sample is plotted with color with the corresponding color bar at the right.

GAG-03

The depth of the cored interval is at 2910-2938 m TVD and 3645-3674 m ABH.

Gaag-03 is a core interval with homogeneous porosities of around 15% (mean 15.5%) and large permeabilities in the hundreds and some intervals thousands mD (mean 465 mD). Very occasionally a small low permeable layer interrupts the continuous high permeable layers.

The porosity and permeability against depth is plotted in figure 33 and porosity-permeability plot (figure 34) shows the relation between porosity and permeability.

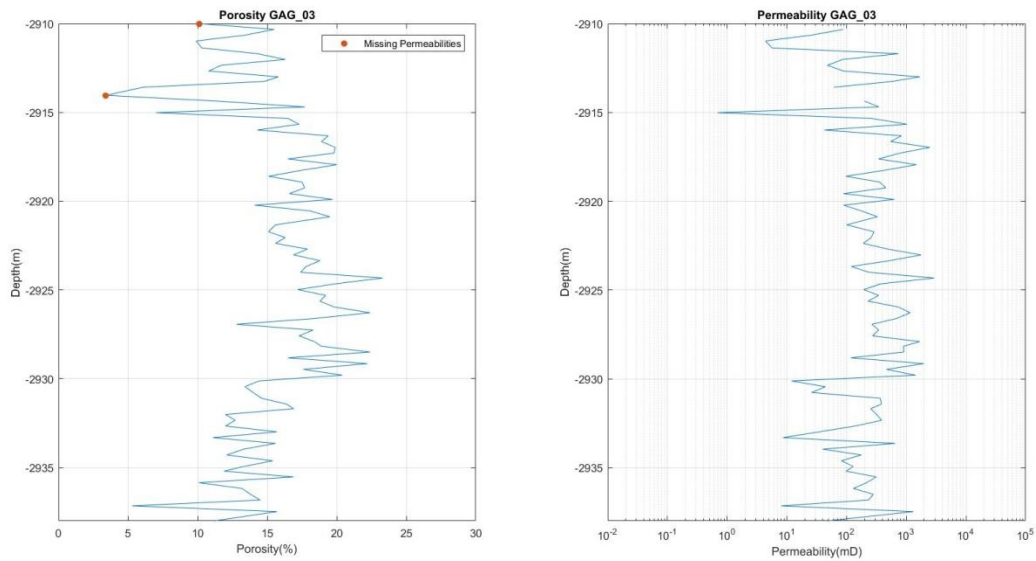


Figure 33. Porosity and permeability core plug measurement of well GAG-03 plotted against depth. Red dots show missing permeability values due to either very low permeability or damaged samples.

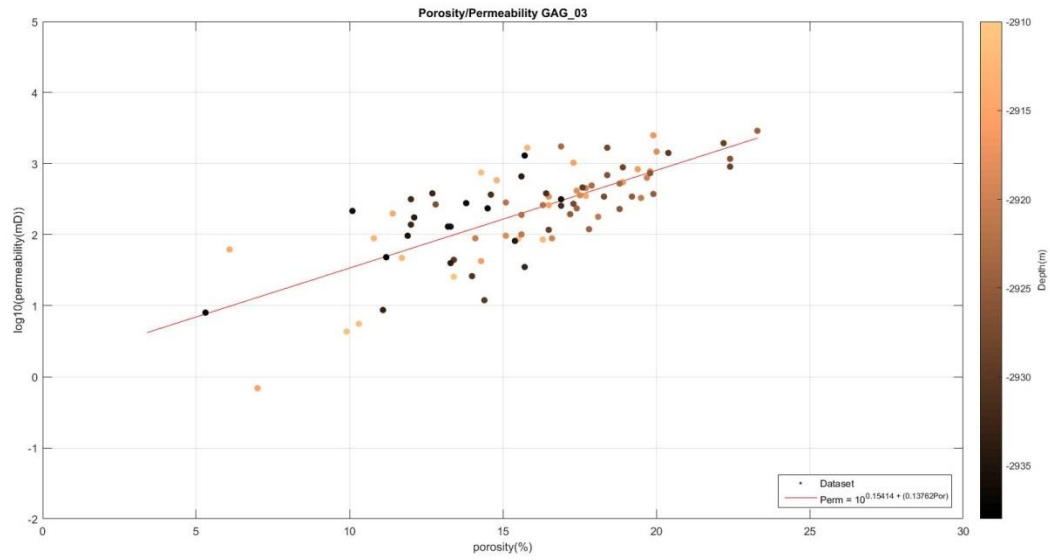


Figure 34. Porosity/permeability plot of GAG-03 with trend line. Depth of the sample is plotted with color with the corresponding color bar at the right.

Well operator reports interpretations

P11-02

G.A.P.S. B.V. Interprets the Hardeggen in P11-02 using thin slab, XRD and microscopy analyses as: ‘... fine grained horizontally, low angle to high-angle cross-bedded and structureless sandstone deposited in sheetflood Dry Aeolian Dune environments, with minor intercalations of wavy to ripple laminated argillaceous and silty sandstone deposited in Wet and Damp Sandflat environments.’

Diagenesis has mainly been controlled by: ‘precipitation of quartz, calcite and dolomite cement and pore-filling and grain replacive kaolinite and illite clay minerals.’ It is also suggested that the calcite cement is an effect of dedolomitisation, caused by invasive meteoric water that dissolved early anhydrite cement. This theory is fortified by the fact that, especially in the lower part of the Hardeggen, there is a very high minus cement porosity, probably caused by early precipitation of anhydrite cement.

G.A.P.S. concludes that the Hardeggen shows excellent reservoir properties (porosity 19% and permeability 45 mD on average) due to very good intergranular porosity. Only locally it has been affected by cements and clays. The clays that are present mainly consist out of kaolinite and platy illite. The fibrous pore-bridging illite, that has devastating effects on reservoir quality is absent.

MSG-01

The Hardeggen interval of MSG-01 consists out of deposits from ‘distal ephemeral stream, clay playa/ephemeral lake, ephemeral stream and proximal ephemeral stream deposits.’ The core is gradual coarsening-upward in terms of grain size as well as sedimentary structures.

Diagenesis is, as we also know from literature, complex and the main cementing minerals are: quartz, chlorite, dolomite, anhydrite, kaolinite and pyrite. The effects of compaction are suggested to be moderate to strong and the preservation of porosity is mainly due by gas charge as well as overpressure.

The reservoir properties are moderate to good and average porosities over different units range from 12.5 to 17.1 % with permeabilities from 79.9 mD to 572.3 mD These well-developed reservoir properties are due to the ‘lack of matrix’ and ‘large secondary intergranular and intragranular porosity.’

At a depth of 3757.4 meters along the borehole chlorite cement was found as a grain coating. The cement was corroded but still present to some extent. At this depth also a high porosity was measured. This may be due to the presence of the chlorite cement which reduces the growth of other pore filling cements (Ehrenberg 1993).

OBLZ-01

Following the conclusions from G.A.P.S. prepared for N.A.M. B.V., the Hardeggen succession shows: ‘a fining-upward trend from relatively proximal sands, via distal sands and anhydritic/dolomitic lake margin deposits, to lacustrine clays.’

Most of the researched samples are very fine to medium grained arkosic and lithic sandstones. Sorting increases with decreasing grain size and maturity. Diagenesis varies with lithology. ‘Mudstones have been indurated with carbonates and hematite.’ Sandstones have varying clay infiltration, pseudomatrix, dolomite cement and minor pyrite and quartz cement. Most of these minerals have been formed during

early diagenesis. Dolomite, a main authigenic mineral, formed as a precipitate in sabkha-like lake margins. It was formed by recrystallization of calcretes that were formed on alluvial fans with interrupted sediment depositions. Therefore, dolomitic cement is much less present in areas with a continuous deposition of sediment.

Porosities are mainly intergranular with both primary and secondary pores. The minor intragranular porosity comes from K-feldspar dissolution voids and moulds. The sandstones show good reservoir properties. The highest porosities, up to 26% with permeability up to 6000 mD, are found in well-stratified fine and medium grained sandstones.

RDK-01

The Hardegsen succession consists, following G.A.P.S., out of: ‘relatively clean wavy bedded sandstones which are believed to result from deposition by adhesive processes on a damp Aeolian sandflat.’ The depositional environment is ‘in the spectrum of desert plain depositional systems’ that ranges from fringing alluvial plain to a desert lake margin (See figure 35).

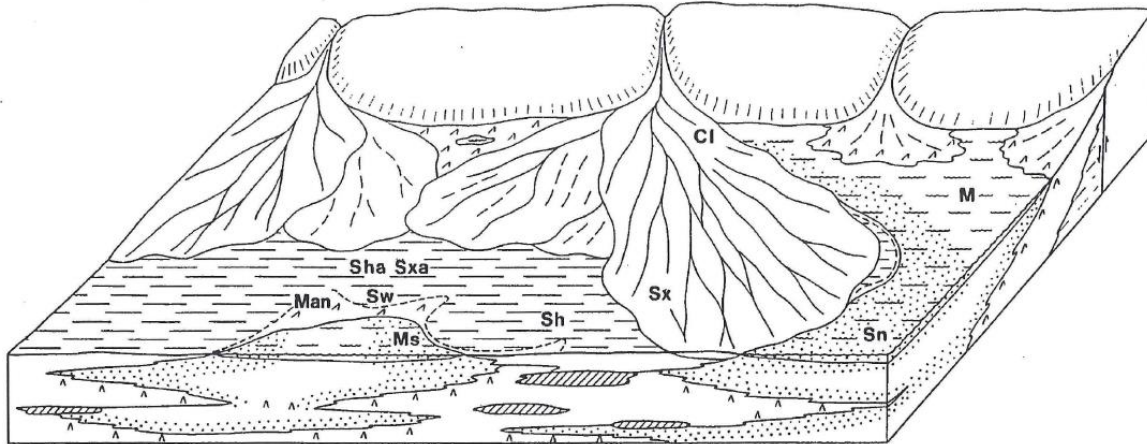


Figure 1: Approximate locations of the lithofacies associations encountered in Buntsandstein deposits.

M:	argillaceous sequence		Inner fan with fluvial channels
Man:	argillaceous sequence with anhydrite		Outer fan/desert plain with sheetfloods and aeolian processes
Ms:	argillaceous sequence with common sandstone/claystone beds		Inland sabkha with anhydrite precipitation
Sh:	sandstone sequence, mainly horizontally bedded		Desert lake
Sha:	sandstone sequence, mainly horizontally bedded, aeolian		Lake margin
Sw:	sandstone sequence, mainly wavy bedded		Fluvial deposits
Sn:	sandstone sequence, mainly homogeneous		
Sx:	sandstone sequence, mainly cross-bedded		
Sxa:	sandstone sequence, mainly cross-bedded, aeolian		
Cl:	sequence of intraformational conglomerates		

NAM, Reedijk-1

Figure 35. Approximate locations of the lithofacies associations in the Buntsandstein. (Well report, MSG-01)

The Hardegsen core shows mature sandstones with less compaction compared to the cores of the sandstones above the Hardegsen. The diagenesis of the core shows: ‘early formation of clay rims and titaniferous oxides; degradation of labile grains (feldspars), crystallization of quartz and feldspar overgrowths, an early phase of secondary porosity generation.’ With further burial of the rock, kaolinite, quartz, dolomite illite and siderite precipitated. This succeeded with emplacement of bitumen, pyrite crystallization and anhydrite cementation. Several phases of secondary porosity generation have been

observed. By dissolution of framework grains and cements, primary porosity improved and enhanced pore channeling locally.

The reservoir properties ranges from poor to good, 'with a porosity range of 2.4 to 20.1% (averaging 10.7%), and permeability range of 0.01 to 3841.17 mD(geometric mean of 4.72 mD).' The main processes decreasing reservoir properties are compaction and quartz and anhydrite cementation. Damp Aeolian sandflats usually show the best quality due to good sorting and rounding, therefore a high primary intergranular porosity and a lower anhydrite cement content.

Gamma ray log interpretation

The gamma ray log is a tool to detect radioactive minerals like clay minerals. Generally the gamma ray tool gives a high value in rock that has a high clay content and a smaller value in rock with less clay content. This means that a sandstone that contains clay or mud in its matrix will give a higher gamma ray value compared to a clean sandstone. This is a simple and fast way to get an indication of the reservoir properties of an exploration well since the porosity and permeability of a rock are often correlated with the clay content. An example of gamma ray log interpretation is given below on well P11-02.

P11-02

At the bottom of the cored interval at 2379m the gamma ray starts at 60 API after which the log immediately sharply increases to 90 API with 3 peaks as high as 110-120 API. These values suggest there is an increased amount of clay minerals present in throughout this section with 3 clay layers at the gamma ray peaks.

This increase in gamma ray value and thus clay content continues for 6 meters to a depth of 2373m. At this depth the gamma ray value drops back to 70 API and stays more or less constant throughout the rest of the cored interval, fluctuating between 60 and 75 API.

Integration

Influence of clay content on reservoir properties

Generally an increase of clay content in a reservoir rock is shown as a peak in the gamma ray log. This increase in clay content results in a decrease of reservoir quality of that rock. In the case of well P11-02 this hypothesis is confirmed (comparison of core plug measurements, gamma ray log values and core description) . The gamma ray shows an increased value in the bottom part of the cored interval at a depth of 2379-2376 m which suggests there should be a significant increase in clay material in this part of the core. The core description shows greenish clay layers between 2377-2376 meters which confirms the increase in clay content. This increase of clay results in a decrease in reservoir quality which is confirmed by the core plug measurements (section Results) that show decreased values in permeability and porosity at this depth.

Since an increase of clay content results in a significant increase of the gamma ray values and a decrease in reservoir properties. Therefore, gamma ray logs give a very good estimation of the location of sections of shaly layers with bad reservoir properties. When we look at the gamma ray log of well P18-02 a significant drop in the gamma ray value is found at a depth of 3287m. The core description at this depth shows very coarse sandstone with no clay content that is almost falling apart at this depth. This confirms the absence of clay. The core measurements at this depth shows a permeability of 3000 mD and a porosity of 13%. This confirms the increase in reservoir properties that was expected at this depth based on the gamma ray log.

These results strongly suggest there is a relation between the gamma ray values and reservoir properties. Since this is based on only 2 wells, and other factors that don't appear on the gamma ray log can influence the reservoir properties too, for now the gamma ray can only be used as an indication tool for reservoir quality of the Hardeggen formation.

Overall this means that a high value in the gamma ray log is very likely to result in poor reservoir properties. However a low value of the gamma ray log does not have to result in good reservoir properties since for example diagenetic processes like cementation, which influence the reservoir properties in a negative way, are not picked up by the gamma ray logging.

Influence of geographic orientation on homogeneity of Hardegsen reservoirs

The Hardegsen formation has been formed near the edge of the West Netherlands basin. Not all wells are deposited in exactly the same depositional environment. Generally it is believed that the further away from the basin edge the more clay content is found in the sediments that were deposited. This is the result of a calmer flow regime with higher water levels away from the basin edge which allows more fine material to settle.

Since the homogeneity of the Hardegsen is believed to be correlated to its orientation to the basin margin, the reservoir quality is not only dependent on depth and diagenetic influences but also on its deposition location within the West Netherlands basin (figure 36).

When a reservoir is containing continuous impermeable layers this will drastically influence the (vertical) permeability of the reservoir. Some of the investigated wells show an impermeable section in the cored intervals. It is unknown if these impermeable sections are continuous throughout the reservoir. When this is the case they will be of large influence on the reservoir quality.

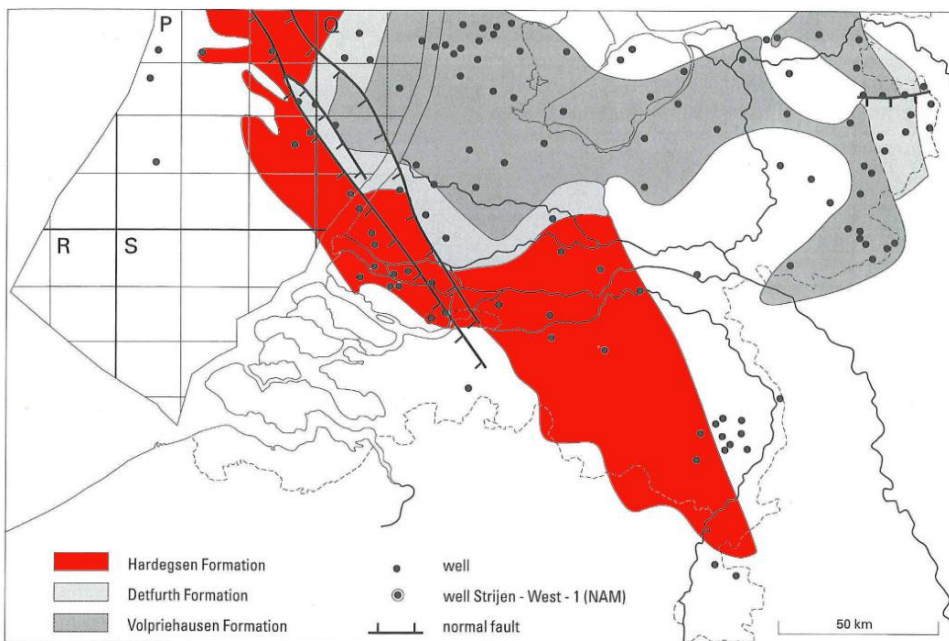


Figure 36. Subcrop map at the base of the Solling formation. (Geluk, Plomp & van Doorn, 1996)

on a larger scale. During this field description multiple sedimentary structures were found that could show as impermeable layers in the core measurements. For example mud pebbles, clay lenses and continuously stratified horizontal clay layers were found. The mud pebbles and clay lenses only effect the permeability of the reservoir locally since they are relatively small structures and thus will not dramatically influence the overall permeability of the reservoir. The continuously stratified horizontal clay layers however are limiting the permeability throughout the reservoir and will influence the overall reservoir quality.

Based on only the core descriptions no conclusions on the continuity of the impermeable layers can be made. The field study does give more insight on how sedimentary structures are oriented

A core description gives the best insight on what specific sedimentary structure is causing the impermeable section in the core measurements. Since only of three wells core descriptions were made we cannot explain all impermeable sections in the core measurements.

Influence of diagenesis on reservoir quality

Diagenesis is, like depositional environment, burial history and tectonic history, heavily dependent on the location within the reservoir. In the case of the Hardegsen the differences in diagenesis is mainly dependent on its location from the basin margin. The thickness of the Hardegsen is mainly dependent on the distance from the base to the Solling/Hardegsen unconformity. It is therefore that we try to link general assumptions for the diagenesis to depositional environment as well as distance to the basin margin.

Chemical diagenesis

Almost everywhere in the Hardegsen early diagenesis was accompanied with precipitation of illite. Also feldspar replacement with illite and mica replacement with kaolinite has occurred.

Following Purvis & Okkerman (1996), anhydrite and halite have also been major early diagenetic cements. Originating from the underlying evaporates as well as meteoric waters, they cemented the rocks with the highest original porosity and permeability. Calcites, either in nodules or as cement, in the West Netherlands Basin are associated with the dedolomitisation and leaching of anhydrite. The theory of Purvis & Okkerman (1996) is substantiated by the very high minus porosities that are found in the West Netherlands Basin. Although this theory is widespread in literature, the West Netherlands Basin does not show higher cementation of rocks with the highest porosity and permeability as on the scale that occurs north of the Waddenzee (Geluk, 2005). Either way, both the calcites and the high-minus porosity give good arguments to presume this theory.

Locally calcretes were deposited. These calcretes were formed mainly on the basin margin and are marginal around sabhka's and playa lakes. The minor calcretes that are present around these environments are mainly dolomitised. Early dolomite precipitation is associated with inland sabkha's and playa lakes.

Uplift and exposure at the unconformity led to dissolution of unstable minerals as feldspars and micas (kaolinite precipitation) and, due to invasion of fresh meteoric water, dedolomitisation. Precipitation of Kaolinite is also associated with the time of uplift and exposure.

Burial diagenesis is associated with precipitation of ferroan dolomite rhombs (leading locally to pore-filling kaolinite), minor precipitation of illite and over the whole reservoir minor and major quartz cementation. Well operators suggest that quartz cementation has played a role in the high minus cement porosities found in the West Netherlands Basin by reinforcing the grain replacing minerals through cementation.

The local dissolution of components has probably been after quartz cementation. The most convincing prove is the presence of pore bridging clay streaks, which could have been grain coating clays that have been left after grain dissolution. Since the effects of cementation vary so much over the West Netherlands Basin, studies of local wells and depositional environment patterns are important to get a better understanding of the local diagenesis.

Physical processes

The depth of the Hardegsen formation in the investigated wells range in depth. Depth can have a large influence on the reservoir properties of a rock. Generally a rock formation found at a greater depth will show more compaction. This leads to a lower porosity and lower connectivity of the pores which leads to a decrease in permeability. Since the depth of the Hardegsen formation in the wells range between 2000-3000 meters a difference in reservoir properties can be expected. Table 3 shows the true vertical depth of the wells and the average porosity and permeability and figure 37 shows all permeability values plotted against porosity and depth.

well	Depth TVD (m)	Average porosity (%)	Average permeability (mD)	Standard deviation porosity	Standard deviation permeability
P11-02	2264-2319	19.0	161.8	5.47	233.7
P15-14	3106-3110.5	12.3	206.5	5.53	247.5
P18-02	3258-3275	10.6	136.1	2.69	574.5
OBLZ-01	2260-2280	20.3	1116	3.23	1334
RDK-01	2725-2750	12.1	177	4.06	611.0
RZB-01	2820-2836	14.1	235	3.23	264.5
RTD-01	2860-2880	14.0	51.4	3.86	58.3
GAG-03	2910-2938	15.5	465	3.79	568.7
MSG-01	2940-2970	15.7	967	3.58	2777.1

Table 3. True vertical depth and average core plug measurements with their standard deviations.

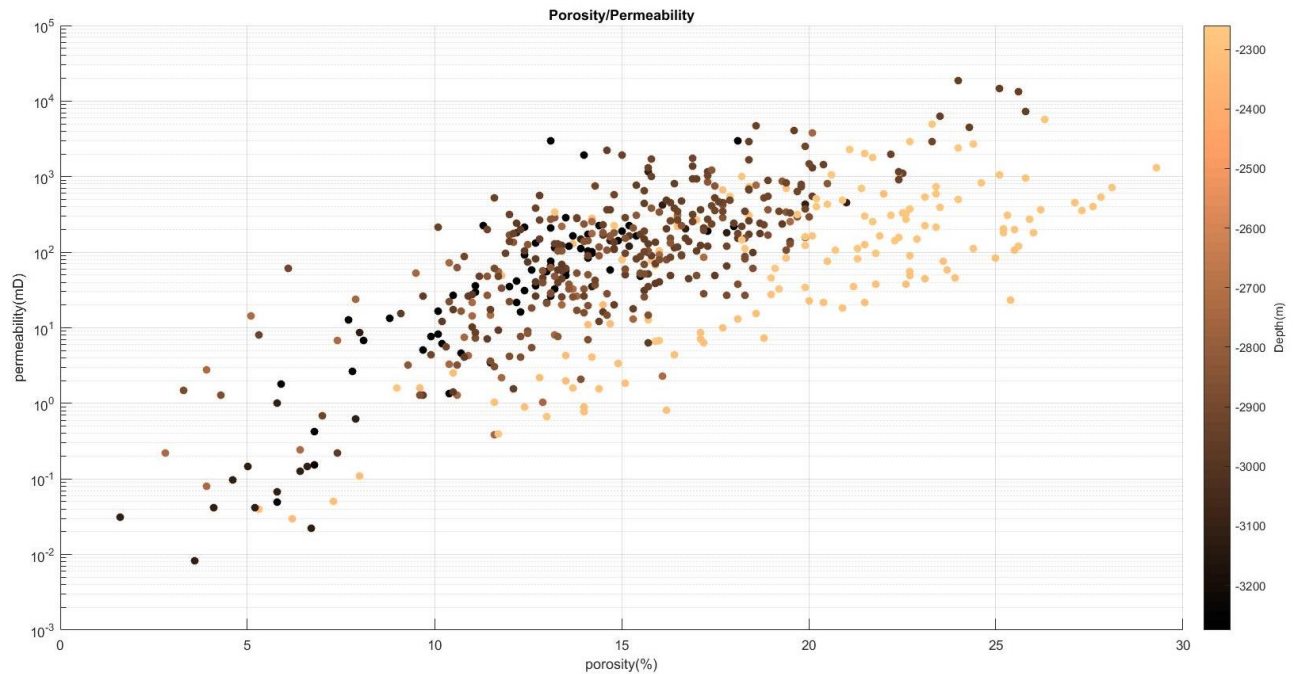


Figure 37. Permeability, Porosity, Depth scatter plot of all the researched plugs.

As expected OBLZ-01 and P11-02 at a depth of 2260 meter show better reservoir properties compared to deeper Hardeggen reservoirs. What stands out is that the onshore wells at a depth greater than 2700 meter tend to have lower porosities, but do not have much lower permeabilities compared to the shallower reservoirs. This could be due to the fact that the arkosic sandstones deposited in semi-arid to arid environment have large amounts of feldspar that could have played an important role in the development of secondary porosities. Since depositional environment widely varies in between the Hardeggen by, for example, distance from the basin margin or amount of erosion by the Solling unconformity, it is hard to find a straight relationship, but what can generally be said about the effects of depth on porosity and permeability is that it is more dependent on the distance from the basin margin than it is on depth itself. Since this development of the Hardeggen in the West Netherlands Basin is rather complex, a detailed study of thin sections of these reservoirs could give valuable information about the cause of these differences.

Influence of depositional environment on reservoir quality

In the onshore part of our study area of the West Netherlands Basin, following our conclusions as well as widespread literature, the formation mainly consists out of fluvio-lacustrine and aeolian sandstones and shales. It is quite hard to differentiate if the reservoir rock is from aeolian or fluvial origin. Following the conclusions from Geluk (2005), the sandstones are mainly from fluvial origin in the West Netherlands Basin. Following Ames & Farfan (1996) the thick sandbeds of the Hardeggen formation are mainly from aeolian origin in the southern part of the West Netherlands Basin. Ames & Farfan do conclude that distinction between aeolian dolomitic sandstones and fluvial sandstones is hard and has a high uncertainty when evaluated on horizon predictions. Either way, reservoir properties are very much alike. There is no doubt that thicker sand beds that occur in the Hardeggen formation occur mainly on the basin margins, which is especially the case for the area near Delft. In figure 38, a schematic view of the area is given during the deposition of the Buntsandstein.

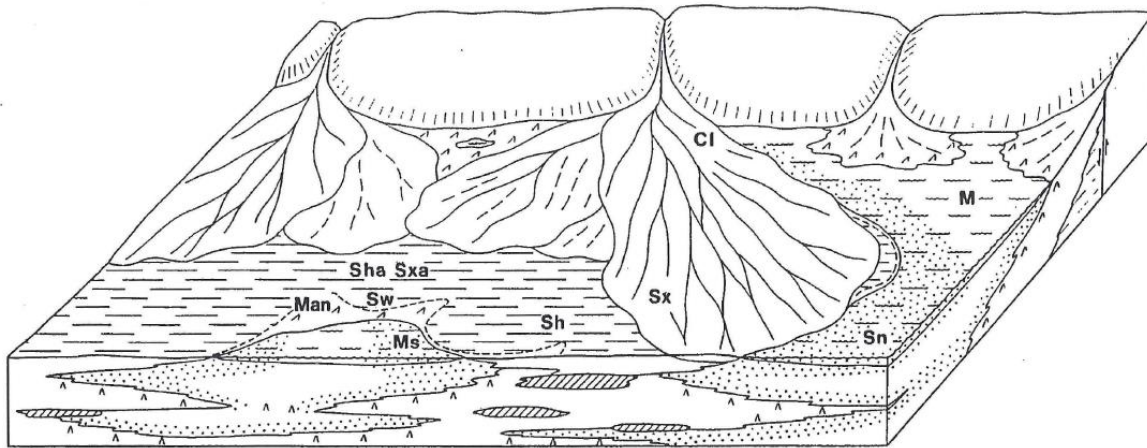


Figure 1: Approximate locations of the lithofacies associations encountered in Buntsandstein deposits.

M:	argillaceous sequence
Man:	argillaceous sequence with anhydrite
Ms:	argillaceous sequence with common sandstone/claystone beds
Sh:	sandstone sequence, mainly horizontally bedded
Sha:	sandstone sequence, mainly horizontally bedded, aeolian
Sw:	sandstone sequence, mainly wavy bedded
Sn:	sandstone sequence, mainly homogeneous
Sx:	sandstone sequence, mainly cross-bedded
Sxa:	sandstone sequence, mainly cross-bedded, aeolian
CI:	sequence of intraformational conglomerates

	Inner fan with fluvial channels
	Outer fan/desert plain with sheetfloods and aeolian processes
	Inland sabkha with anhydrite precipitation
	Desert lake
	Lake margin
	Fluvial deposits

NAM, Reedijk-1

Figure 38. Schematic view of the depositional environment of the Buntsandstein. (Well report, MSG-01)

From the fieldwork as well as depositional environment, we can conclude that thicker (more than 20 cm) shale, and sandy shale layers are continuous in lateral direction. These shale and sandy shale layers are mainly from shallow marine (sabkha) as well as lacustrine (Playa Lakes, floodplains) origin and have a negative influence on vertical permeability. Thinner clay layers that are present in the cores, especially in between cross bedding, are only very locally present, and have therefore much less disastrous influence on reservoir permeability.

We have also found signs of desiccation and synaeris cracks in the shale layers, with a sandy and shaly sand filling. If synaeris is widespread throughout larger regions in the Hardeggen this could enhance vertical permeability of a reservoir.

Permeability to porosity, depth model

A very good example for the dependency of both depth and depositional environment is the difference between well OBLZ-01 and RDK-01. These wells are located just two kilometres apart, but show major differences in depth, porosity and permeability. This large difference could be caused by diagenesis, depositional environment, amount of compaction and effects of secondary porosity generation or a combination of these. Depositional environment could differ much on a very small scale (several hundreds of metres) since lakes, streams, rivers and floodplains could be restricted to rather small areas.

A model has been obtained to get a very global idea of the expected permeability for known porosity and depth and an estimation of the error in the dataset. The formula takes porosity as well as depth into account in order to determine an estimation of the surface permeability of the reservoir rock. Since we have a limited dataset as well as a limited depth range, firm conclusions are difficult and would need a larger dataset.

From the dataset from figure 39 as to be seen in the integration, a general formula has been established, depending on porosity and depth:

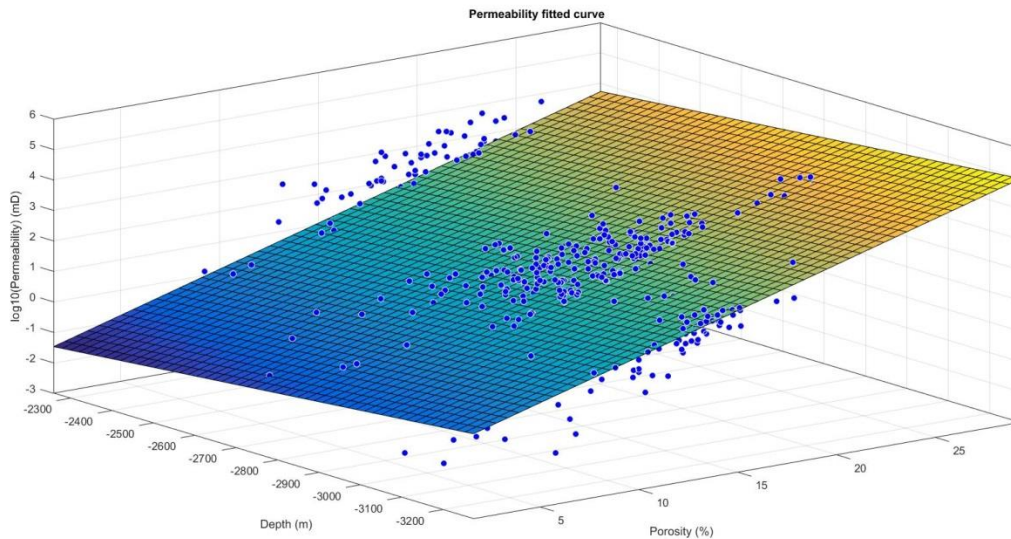


Figure 39. Permeability (porosity, depth) relationship

$$Perm(Por, D) = 10^{(-4.582 + 0.1879 * Por - 0.001245 * Depth)}$$

With median: 1.00% and standard deviation 1000%.

Since it is a weighted dataset, the mean is not representative for the expected error. It is therefore that we take the median and the relative standard deviation. In figure 40, you can see the histogram of the relative and absolute error.

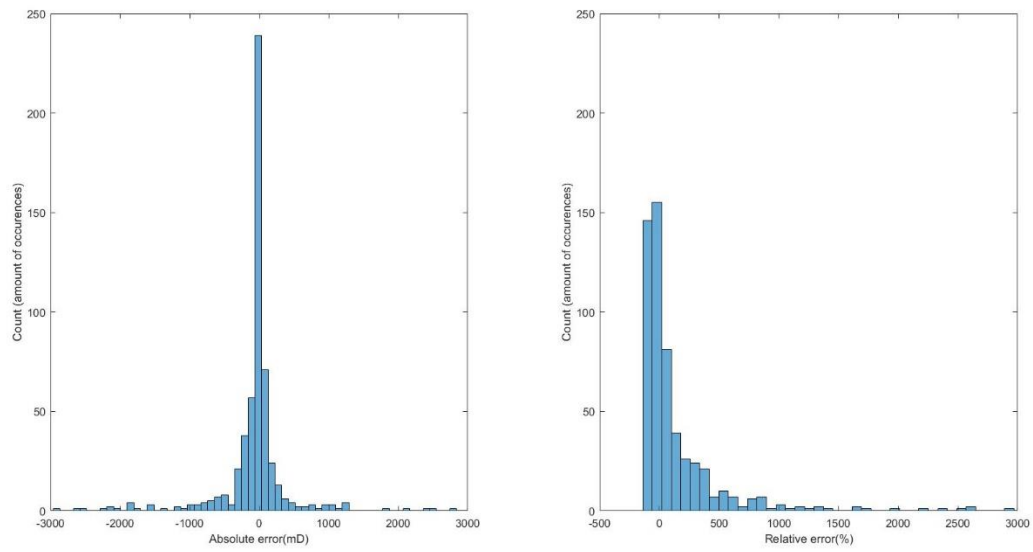


Figure 40. Absolute error (left) and relative error (right) of the permeability to porosity depth model.

From the errors between the model and the actual permeability values (Figure 40) we can see that it gives a global idea of the expected permeabilities in on the southern margin of the West Netherlands Basin.

Discussion and recommendations

The main subject of the project was to provide a general view on the reservoir properties, related to its geological background, of the Hardeggen succession in the West Netherlands Basin. Since the Hardeggen does not form a stratigraphic entity and its sedimentology is heavily dependent on the location in the basin, we have tried to provide a more general approach.

The location of the reservoir compared to the margins of the basin tends to be very important for the deposits that are found in the reservoir. As figure 29 in the chapter 'Influence of depositional environment' suggests is that a large range of deposits occur in the succession, ranging from alluvial, aeolian to shallow marine. Through changes in subsidence patterns, change of climatological circumstances, tectonic circumstances and transgressions, these depositional environments change places regularly and it is very hard to tell the range on which certain depositions occur. In order to get a better understanding of the distribution of these depositional environment in the West Netherlands Basin, a study including all (or more) of the available cores of the West Netherlands Basin would be necessary. Ames & Farfan, 1996, performed such a study for the Buntsandstein reservoirs in the Broad Fourteens basin (P and Q quadrants of the Dutch offshore).

Also the thickness, reduced by the Solling unconformity, depends heavily on location. A general study about the thickness of the Permo-Triassic succession has been done by Geluk, Plomp & van Doorn, 1996, but a rather detailed study about the thickness of the Hardeggen would be favorable to determine the reservoir potential of the Hardeggen laying more north in the West Netherlands Basin (figure 41).

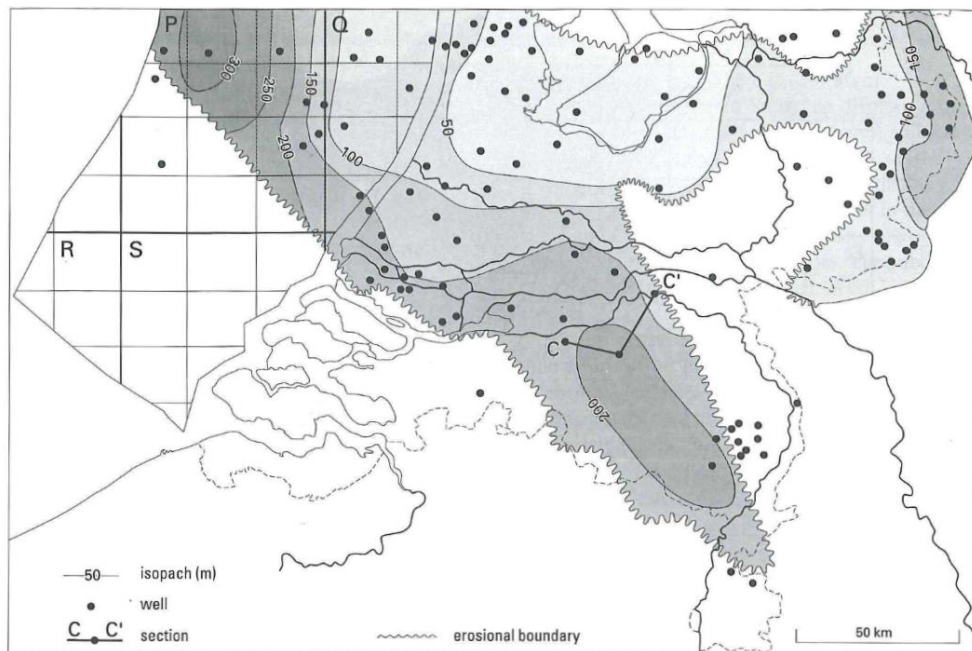


Figure 41. Thickness of the Main Buntsandstein in the West Netherlands Basin. (Geluk, Plomp & van Doorn, 1996)

Since the tectonic development of the West Netherlands Basin is rather complex (figure 9), the diagenesis and burial depth of the different reservoirs is heavily dependent on the location in the

reservoir. It is said in both literature (Purvis & Okkerman, 1996; Geluk, 2005) as well as our own findings that the reservoir properties are more dependent on depositional environment and secondary porosity generation than on the effects of compaction due to burial depth. This is only one side of the medal. It is hard to prove that deeper reservoirs, that occur north of the researched wells in West Netherlands Basin, do show the same trend, since we do not have data of those reservoirs.

A main problem for the quality of the reservoir is the presence of very fine grained sand, silt and clay layers related to playa lakes and floodplains. As said in the discussion about depositional environment, the locations of these layers are hard to predict, but they can be recognized in gamma ray logs, by the presence of high gamma ray values. The effects on vertical and horizontal permeability over large areas as well as horizontal continuity of these layers is unknown. The expected positive effects on vertical permeability of desiccation and syneresis cracks on the properties of the reservoir have to be investigated further. Further study of these deposits and its effects on the properties of the reservoir as a whole would be advisable to get a better prediction of the feasibility of reservoirs with these layers.

Conclusion

The subject of the paper is to characterize the Hardegsen succession in the West Netherlands Basin to determine its reservoir potential.

- The thick fluvial and aeolian sandbeds of the Hardegsen formation show excellent reservoir properties. Vertical flow in the reservoir is mainly restricted by the presence of thick, more than 10 cm, laterally consistent shale and shaly sand/silt layers. These layers, mainly from lacustrine origin, do not occur in every Hardegsen alternation and vary with location in the basin.
- Diagenesis in the Hardegsen is rather complex. Main cement components are illite, kaolinite, halite, anhydrite, dolomite and quartz. Although the amount of cementation varies within location as well as deposition, all sandstones show moderate to well reservoir qualities.
- Early cementation and matrix strengthening with quartz cement prevented heavy compaction to occur. The Hardegsen in the West Netherlands Basin shows very little compaction compared to average reservoirs at a depth between 2000-3000 meters. This is strengthened by the minus-cement porosities found by well operators in the Hardegsen.
- Secondary porosity could have played an important role in the porosity and permeability preservation of generation of the Hardegsen. Reservoir properties in terms of permeability in the range between 2000 and 3000 meters do not tend to decrease with depth.
- Major variations in depositional environment, depth and diagenetic history make it rather complex to give one general prediction for the expected reservoir quality of the Hardegsen. Data from wells with comparable distances from the basin margin and comparable depth give the best information of the expected quality of the targeted reservoir.
- The southern margin of the West Netherlands Basin shows very good reservoir properties for geothermal exploitation. Firm conclusions about Hardegsen reservoir north of the researched wells are hard to make, but quality as well as thickness is expected to decrease.

Acknowledgements

We would like to thank our mentor Dr. M.E. Donselaar for his time, help and constructive criticism and PhD student K.A. van Tooreenburg for his help during our research. We would like to thank the institution TNO for providing the cores that were used for core description and all well contractors for providing the well data. We would also like to thank the TU Delft for funding the field trip which gave an extra dimension to our research. At last we would like to thank Jan Kees Blom for his final corrections in order to get a better conclusion out of our research.

References

- Ames, R. & Farfan, P.F. 1996. The environment of deposition of the Triassic Main Buntsandstein Formation in the P and Q quadrants, offshore the Netherlands. In: Rondeel, H.E., Batjes, D.A.J., Nieuwenhuijs, W.H. (eds), *Geology of gas and oil under the Netherlands*, Kluwer Academic Publishers (Dordrecht): 167–178.
- Autran, A., & Cogné, J. 1980. La zone interne de l’orogène varisque dans l’Ouest de la France et sa place dans le développement de la chaîne hercynienne. In: *Congrès Géologique International, XXVI, Colloque C* (Vol. 6, pp. 90-111).
- Beckhoff, B., Kanngießer, B., Langhoff, N., Wedell, R., Wolff, H., *Handbook of Practical X-Ray Fluorescence Analysis*, Springer, 2006
- De Jager, J., Doyle, M. A., Grantham, P. J., & Mabillard, J. E. 1996. Hydrocarbon habitat of the West Netherlands Basin. In *Geology of gas and oil under the Netherlands* (pp. 191-209). Springer Netherlands.
- Fuglewicz, R. (1980). Stratigraphy and palaeogeography of Lower Triassic in Poland on the basis of megaspores. *Acta Geologica Polonica*, 30(4): 417-470.
- Geluk, M.C. 2005. Stratigraphy and tectonics of Permo-Triassic basins in the Netherlands and surrounding areas, University of Utrecht, PhD Thesis.
- Geluk, M.C., Plomp, A. & Van Doorn, T.H.M. 1996. Development of the Permo-Triassic succession in the basin fringe area, southern Netherlands. In: Rondeel, H.E., Batjes, D.A.J., Nieuwenhuijs, W.H. (eds): *Geology of gas and oil under the Netherlands*, Kluwer Academic Publishers (Dordrecht): 57–78.
- Geluk, M.C. & Röhlting, H.-G. 1997. High-resolution sequence stratigraphy of the Lower Triassic ‘Buntsandstein’ in the Netherlands and Northwestern Germany. *Geologie en Mijnbouw* 76: 227–246.
- Geluk M.C. & Röhlting H.-G. 1999. High-resolution sequence stratigraphy of the Lower Triassic Buntsandstein: a new tool for basin analysis. In: Bachmann, G.H. & I. Lerche *Epicontinental Triassic, Zentralblatt für Geologie und Paläontologie* 1998: 545–570.
- Glennie, K.W. 1998. Lower Permian – Rotliegend. In: Glennie, K.W. (ed.) *Petroleum Geology of the North Sea*, Fourth Edition, Blackwell Science: 137–174.
- Habicht, J. K. A., 1979. Paleoclimate, Paleomagnetism and Continental Drift. *American Association of Petroleum Geology*. In: *Studies in Geology* No. 9, 31 pp.
- Kockel, F. (ed.), 1995. Structural and palaeogeographical development of the German North Sea sector. *Beiträge zur regionalen Geologie der Erde* 26:1–96.
- McKie, T. & Williams, B., 2009. Triassic palaeogeography and fluvial dispersal across the northwest European Basins. *Geological Journal*, 44(6), 711-741.
- Peryt, T.M. 1975. Significance of stromatolites for the environmental interpretation of the

Buntsandstein (Lower Triassic) rocks. Geol. Rundschau 64: 143–158.

Plein, E. (ed.) 1995. Norddeutsches Rotliegendbecken; Rotliegend-Monographie Teil II. Stratigraphie von Deutschland I. Courier Forschungsinstitut. Senckenberg 183 (Frankfurt): 193 pp.

Purvis, K. & Okkerman, J.A. 1996. Inversion of reservoir quality by early diagenesis: an example from the Triassic Buntsandstein, offshore the Netherlands. In: Rondeel, H.E., Batjes, D.A.J., 146 Nieuwenhuijs, W.H. (eds): Geology of gas and oil under the Netherlands, Kluwer Academic Publishers (Dordrecht): 179–189.

Röhling, H.-G. 1991. A Lithostratigraphic subdivision of the Early Triassic in the Northwest German Lowlands and the German Sector of the North Sea, based on Gamma Ray and Sonic Logs. Geologisches Jahrbuch A 119: 3–23.

Roos, B.M. & Smits, B.J. 1983. Rotliegend and Main Buntsandstein gasfields in block K13, a case history. Geologie en Mijnbouw 62: 75–82.

Van Adrichem Boogaert, H.A. & Kouwe, W.F.P. 1994b. Stratigraphic nomenclature of the Netherlands; revision and update by RGD and NOGPA, Section E Triassic. Mededelingen Rijks Geologische Dienst 50, 28 pp.

Van Wijhe, D.H. 1987. Structural evolution of inverted basins in the Dutch offshore. Tectonophysics 137: 171–219.

Ziegler, P.A. 1982 Geological Atlas of Western and Central Europe - Shell Internationale Petroleum Maatschappij: pp 13-99

www.nlog.nl – Netherlands Oil and Gas Portal, source for all wireline logs and core measurements.





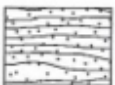



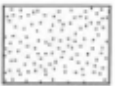
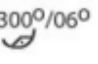





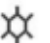


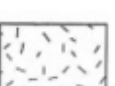
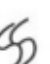


<http://wiki.aapg.org/> - Website of the American Association of Petroleum Geologists.

Well report MSG-01

Appendix

Appendix A – Core section description

Legend to logs

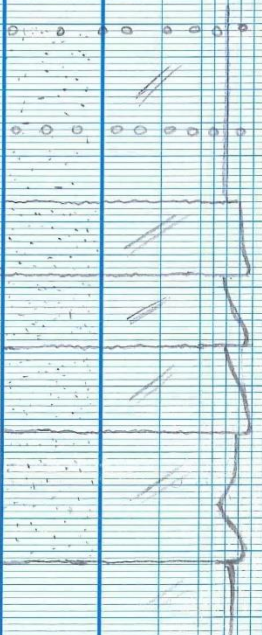
	Claystone		Tabular cross-bedding
	Shale		Trough cross-bedding
	Heterolithic sandstone/shale beds		Wave ripple lamination
	Parallel laminated sandstone		Current ripple lamination
	Sandstone		Lateral accretion with dip direction/angle
	Trough x-bedded sandstone		Transport direction
	Conglomeratic sandstone		Bioturbation
	Polymict conglomerate		Mottling
	Monomict breccia		Roots
	Granite basement		Deformed bedding
	Pebble stringers		Cement (nodules)

		Macroscopic Description		TL en BTM 11/12/15 1:50 PM/02													
Stratigr. units	Photo	Samples	Depth	Lithofacies log						Sedimentary structures			Additional Description (e.g. strike & dip, bed thickness, colour)	Fossil content			
				m	Relief	Composition & Texture	Grain size					Transport direction			Sedimentary/diagenetic structures	Bio-turb.	
						clay	silt	vf	f	mc	vc	gravel					
			2367			//										homogenous grad sands	
			2368														
			2369			//											
			2370														
			2371													Occasionally greenish very fine sand, or clays < 1mm	
			2372														
			2373													greenish very fine sand with some clay layers < 1mm	
			2374													reddish brown very fine sand with clay layers < 2mm and smaller synaeresis occasionally small greenish clay layers < 1mm	
			2375													occasionally very fine greenish sand layers < 1mm	
			2376													clay layers with synaeresis greenish < 1-2mm increasing clay content and synaeresis (detail photo)	
			2377														
			2378			//											
			2379			//										fine sand pebble ϕ 1mm fine layered greenish bank < 5mm	

P15-14

1#

Macroscopic Description TL & BTM 9/12/15 1:50 P15-14															
Stratigr. units	Photo	Samples	Depth	Lithofacies log					Sedimentary structures			Additional Description [e.g. strike & dip, bed thickness, colour]	Fossil content		
				m	Relief	Composition & Texture	Grain size				Transport direction			Sedimentary/diagenetic structures	Bio-turb.
						clay	silt	v f	f m	c	vc	g			
				3145											
				3146											
				3147											
				3148											
				3149											
				3150											
				3151											
				3152											
				3153											

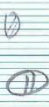


matrix is fine but contains some coarse grains. also small layers of greenish sand/clay

looks like cement with mica s.

fining up, then median

alternating finer and coarser layers.



P18-02

1#2

Macroscopic Description TL 2 BTM 10/12/15 1:50 P18-02																				
Stratigr. units	Photo	Samples	Depth	Lithofacies log						Sedimentary structures			Additional Description (e.g. strike & dip, bed thickness, colour)	Fossil content						
				m	Relief	Composition & Texture	Grain size					Transport direction			Sedimentary/diagenetic structures	Bio-turb.				
						clay	silt	v/f	f	m	c	v/c	gravel							
			3287																	
			3288																	
			3289																	
			3290																	
			3291																	
			3292																	
			3293																	
			3294																	
			3295																	
			3296																	
			3297																	
			3298																	
			3299																	

fast striae

alternating with very small very fine layers (greenish)

some finer layers in bed bases

small clay layers

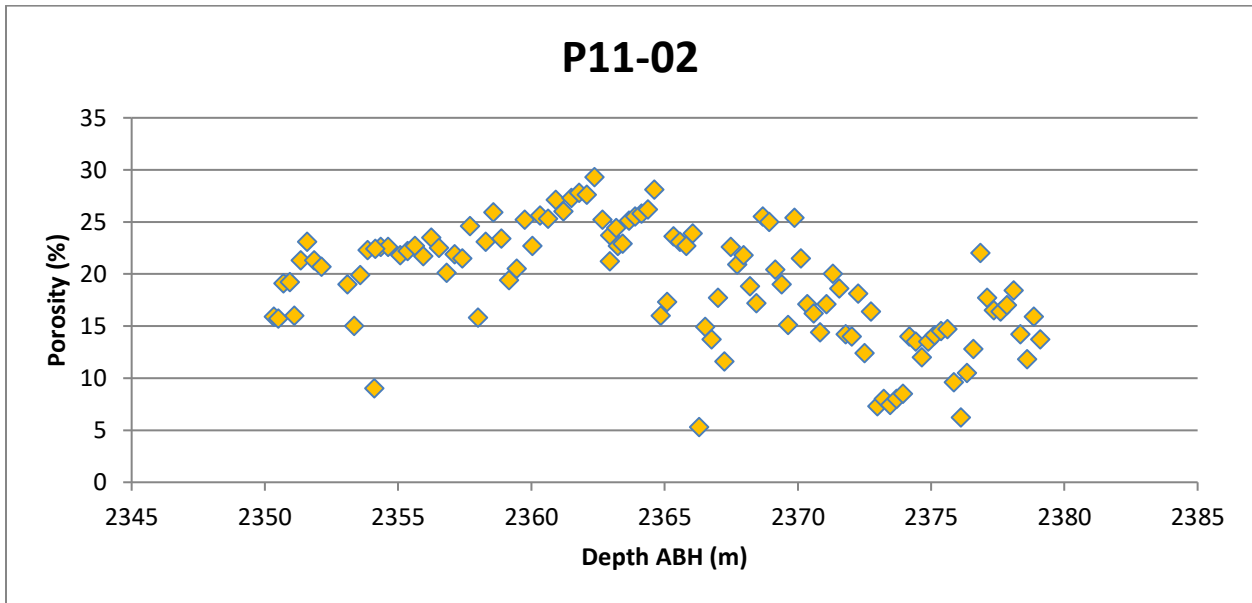
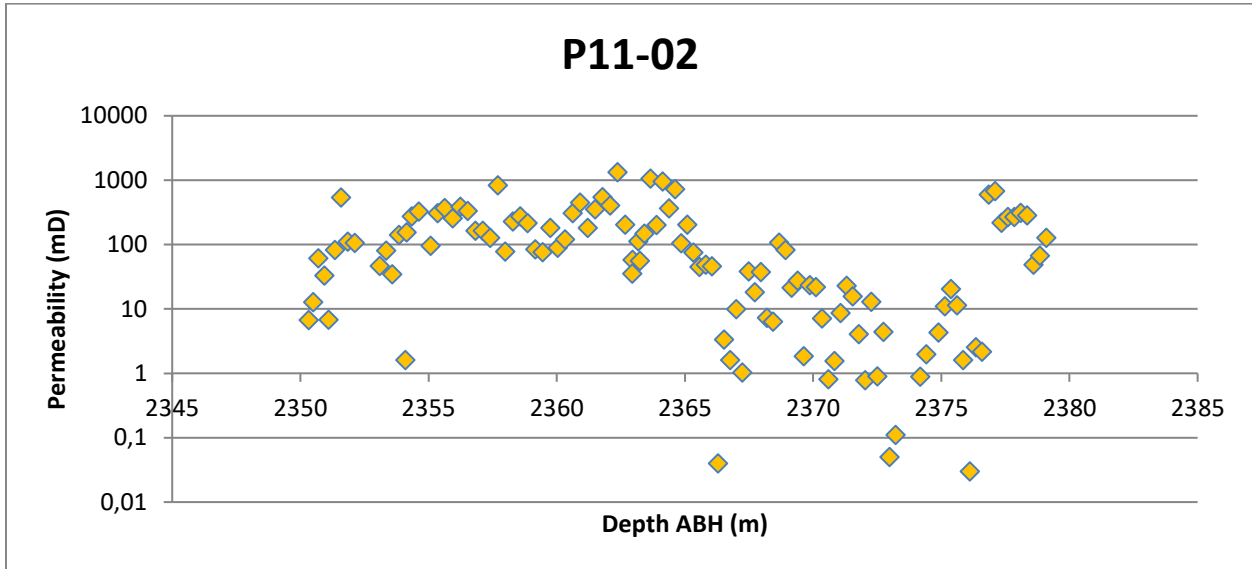
some coarser layers between fine sands

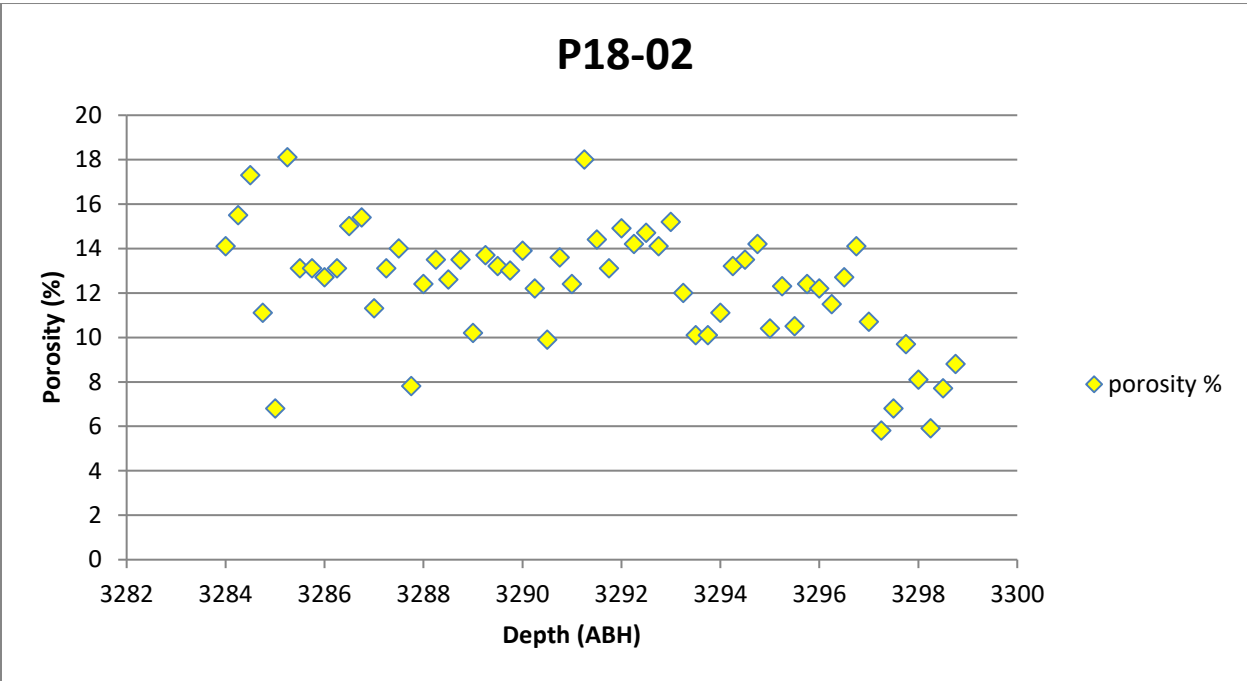
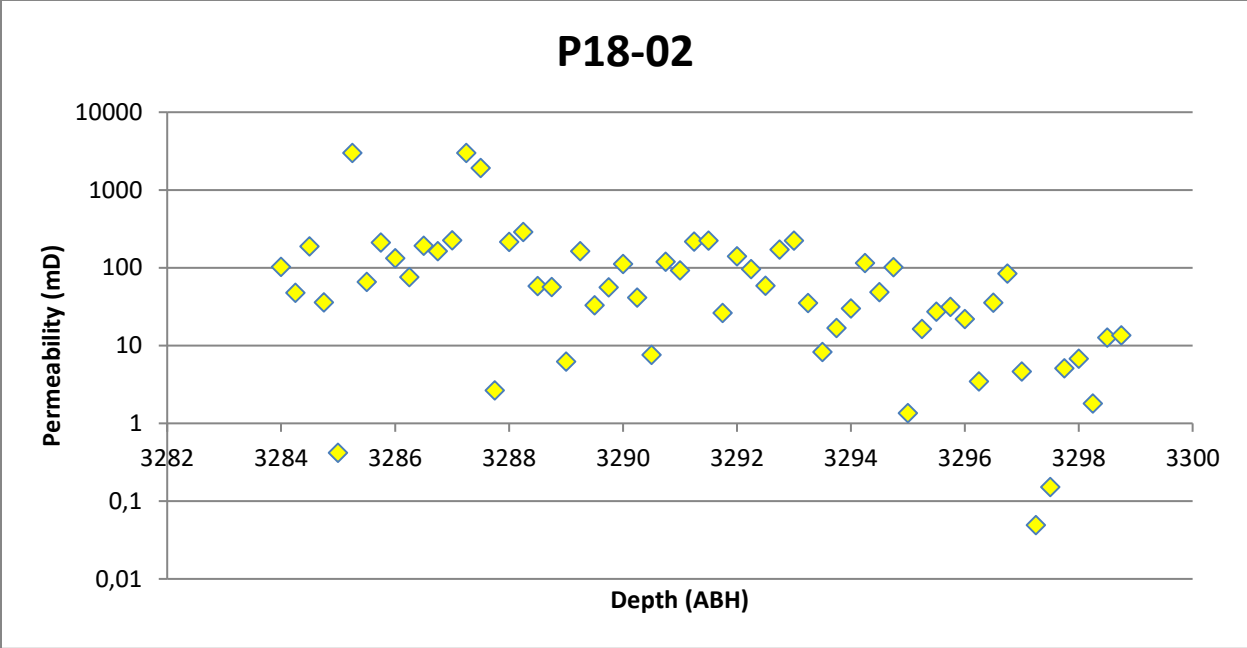
green layers (clay layers)

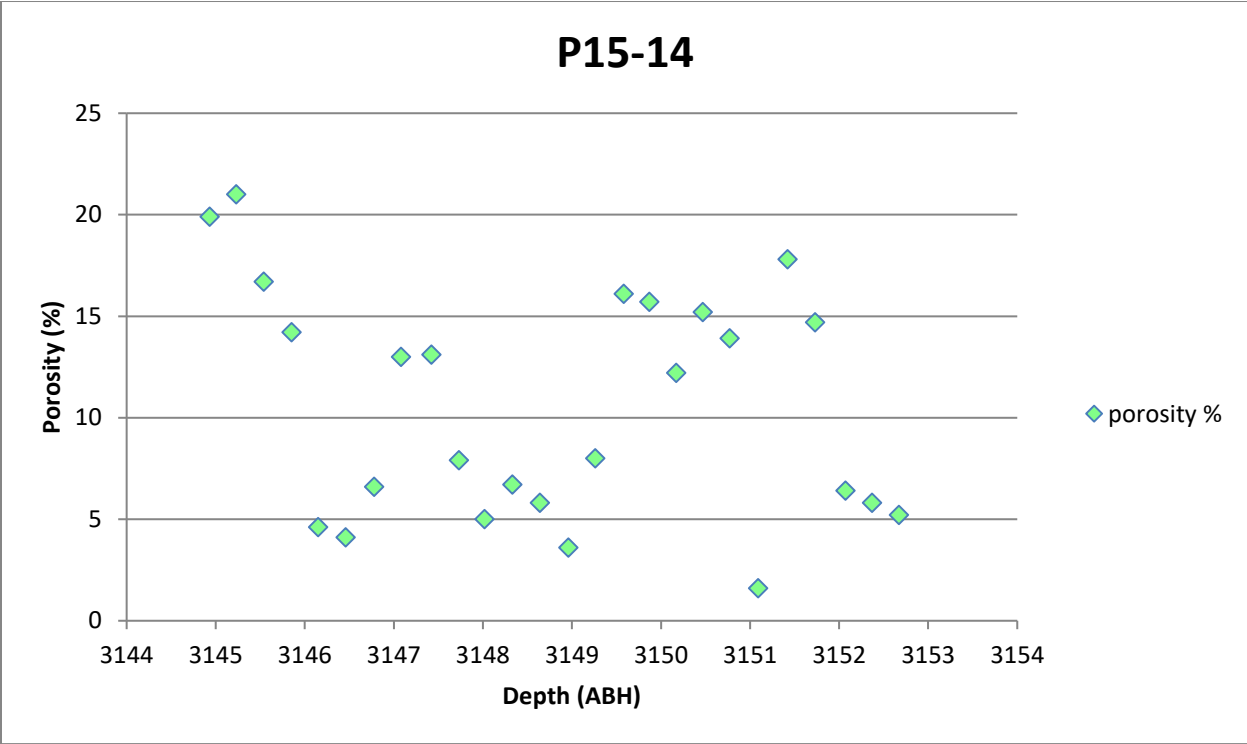
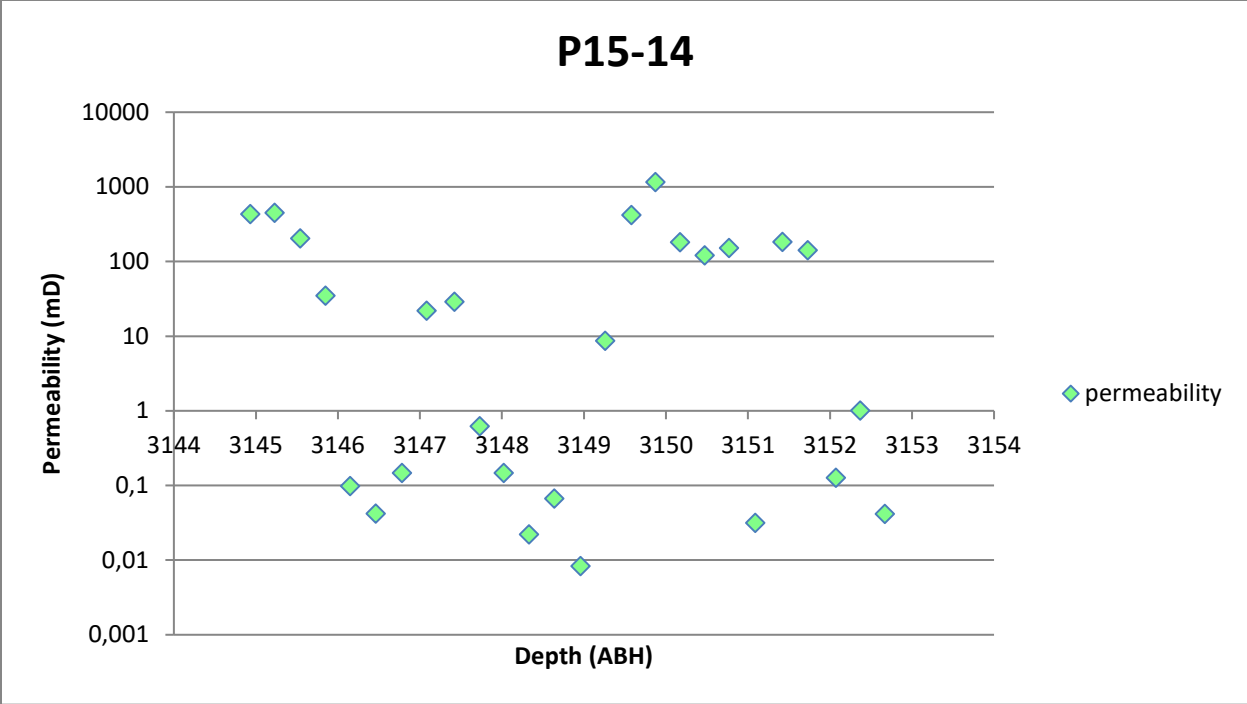
clay layers green

Appendix B – Off shore core plug measurements

The following graphs present the permeability and porosity as function of depth.

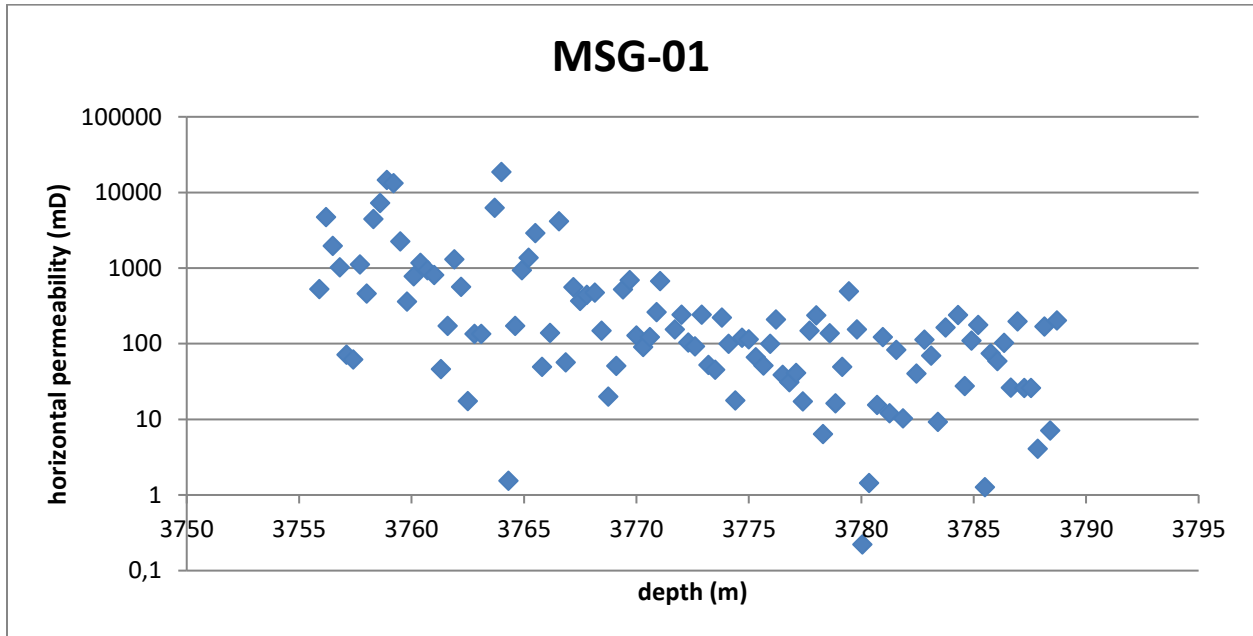
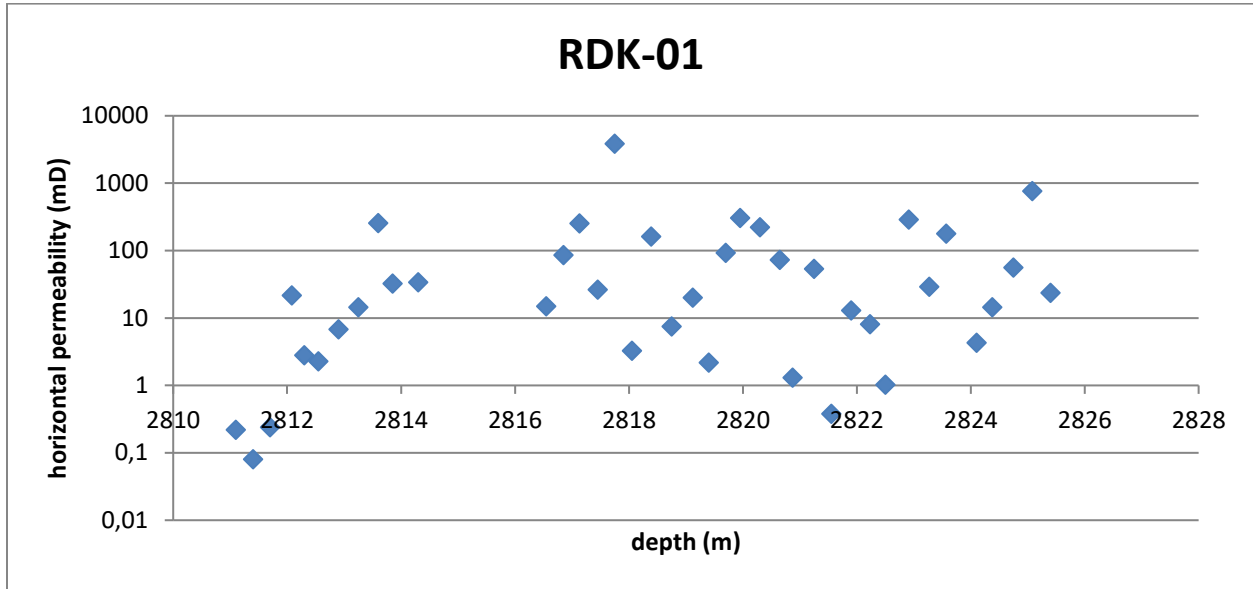


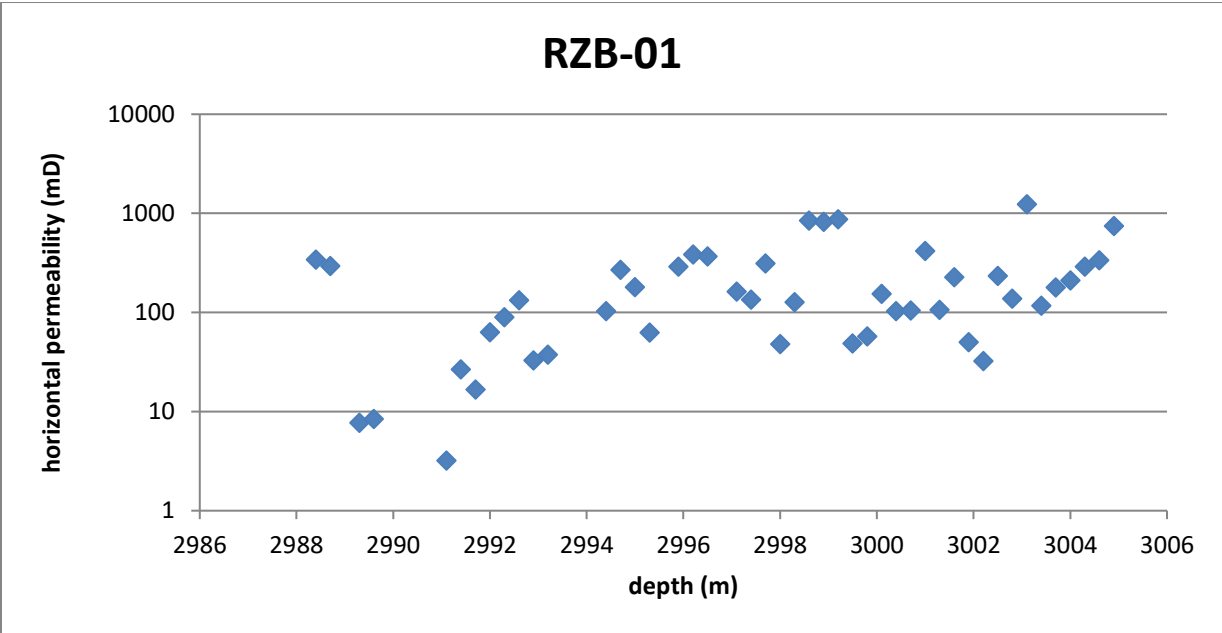
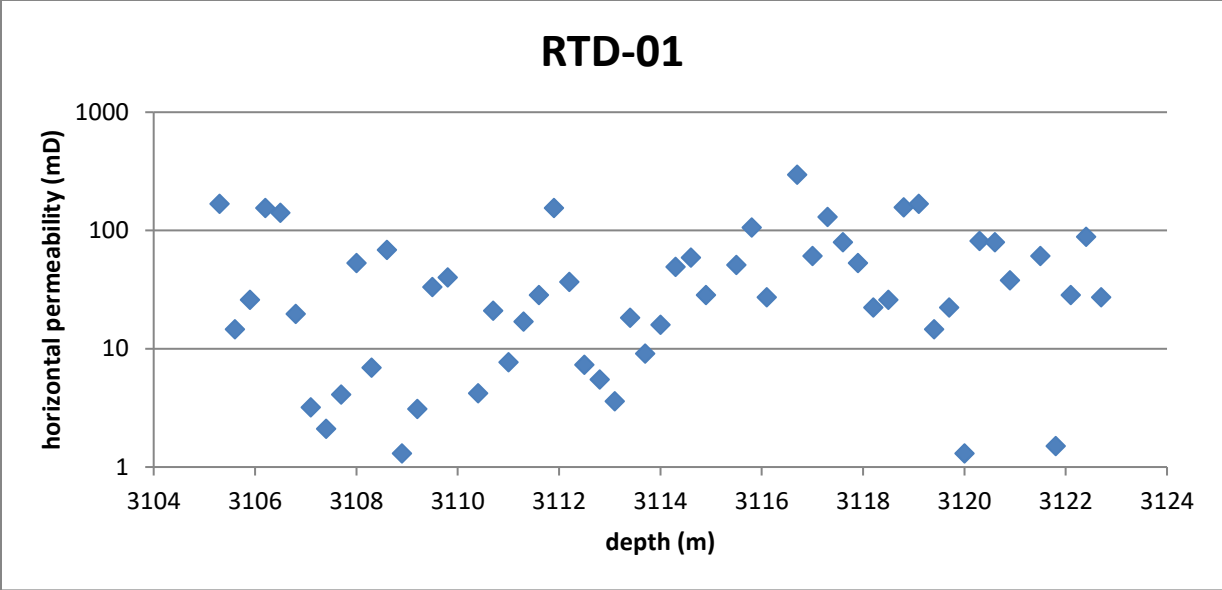


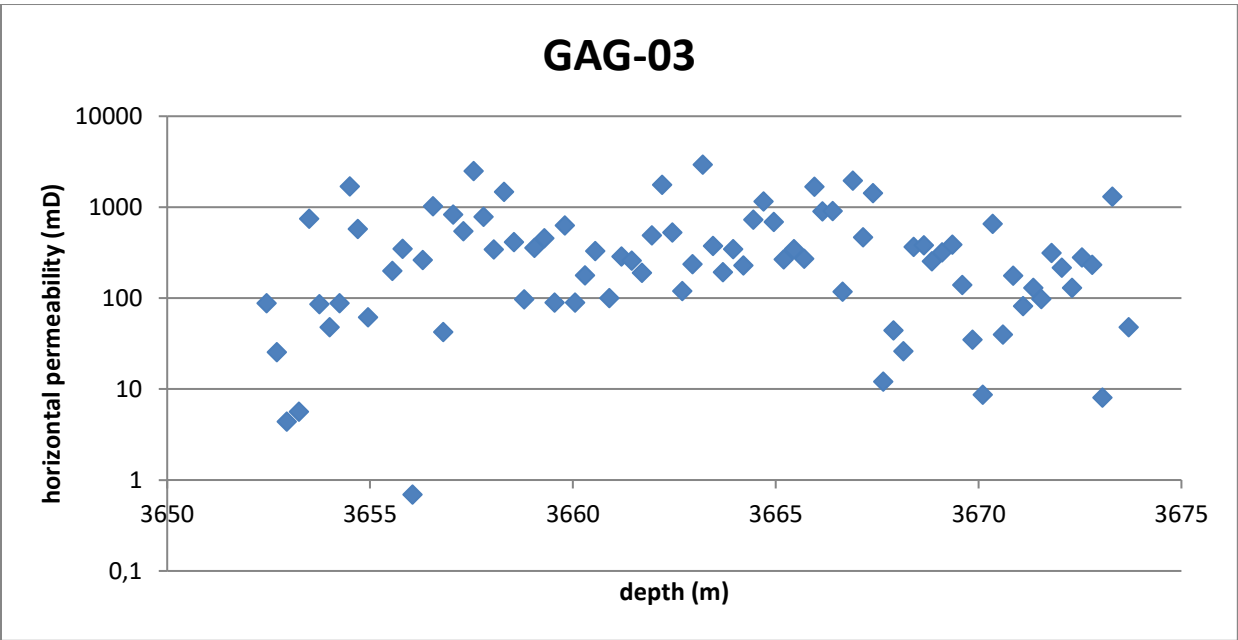
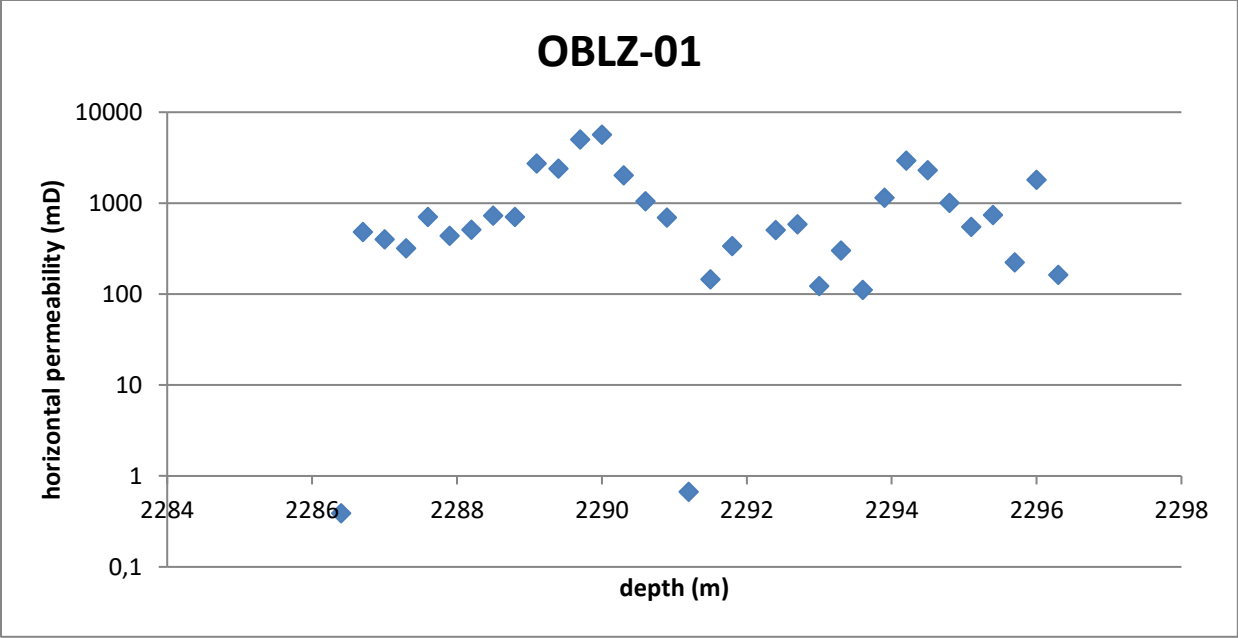


Appendix C – On shore core plug measurements

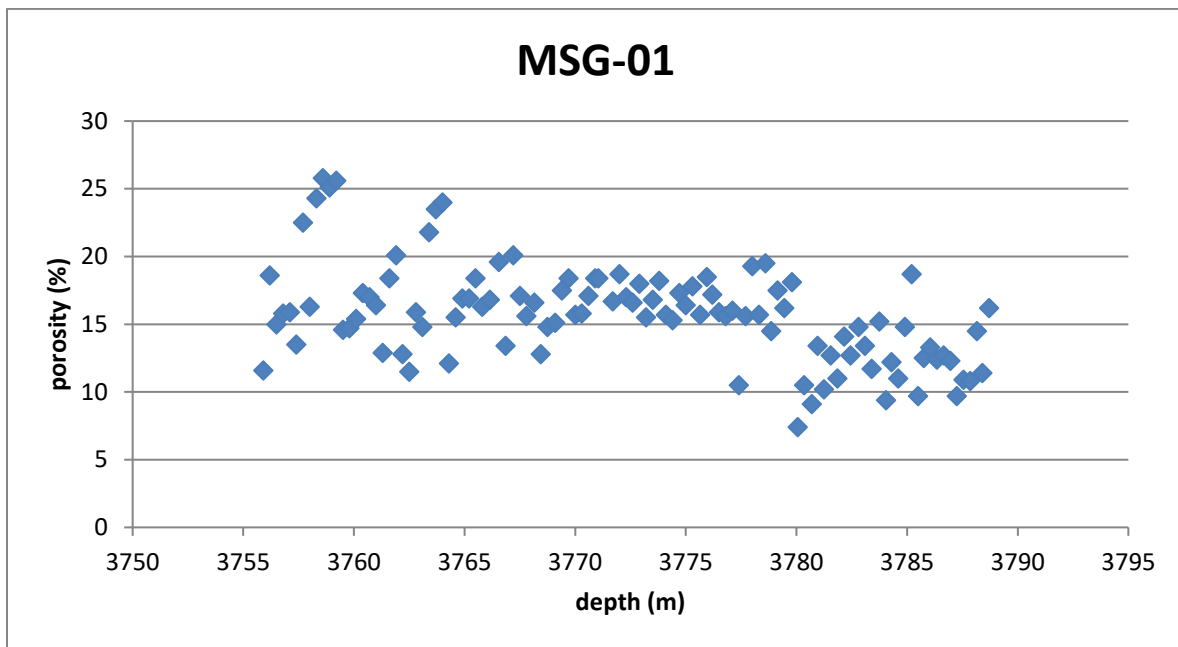
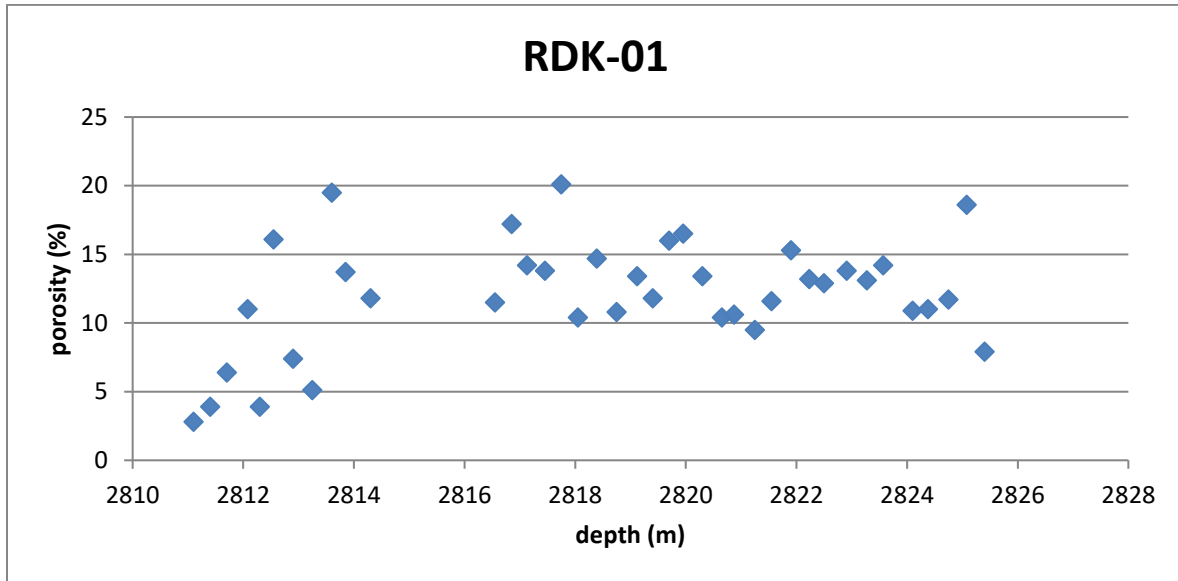
On-shore permeability measurements on the cored intervals are presented by the following graphs.

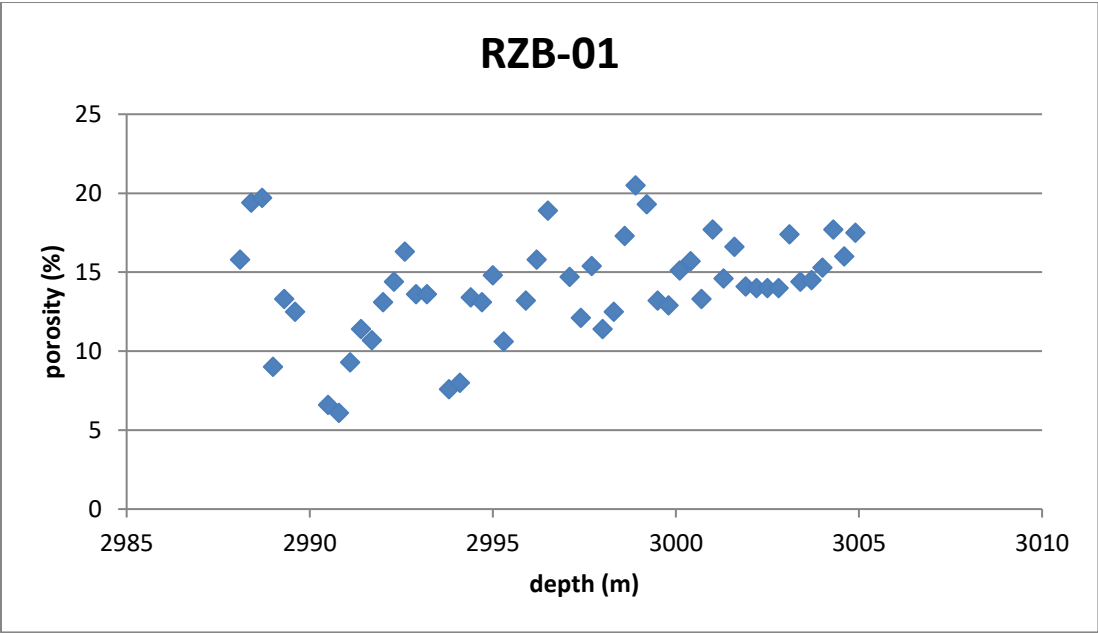
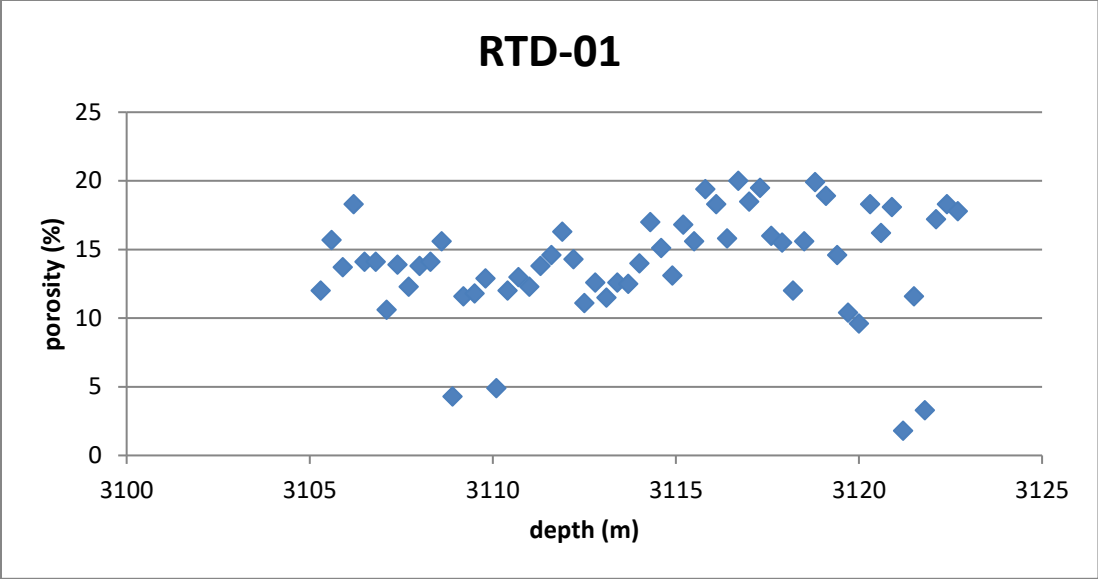


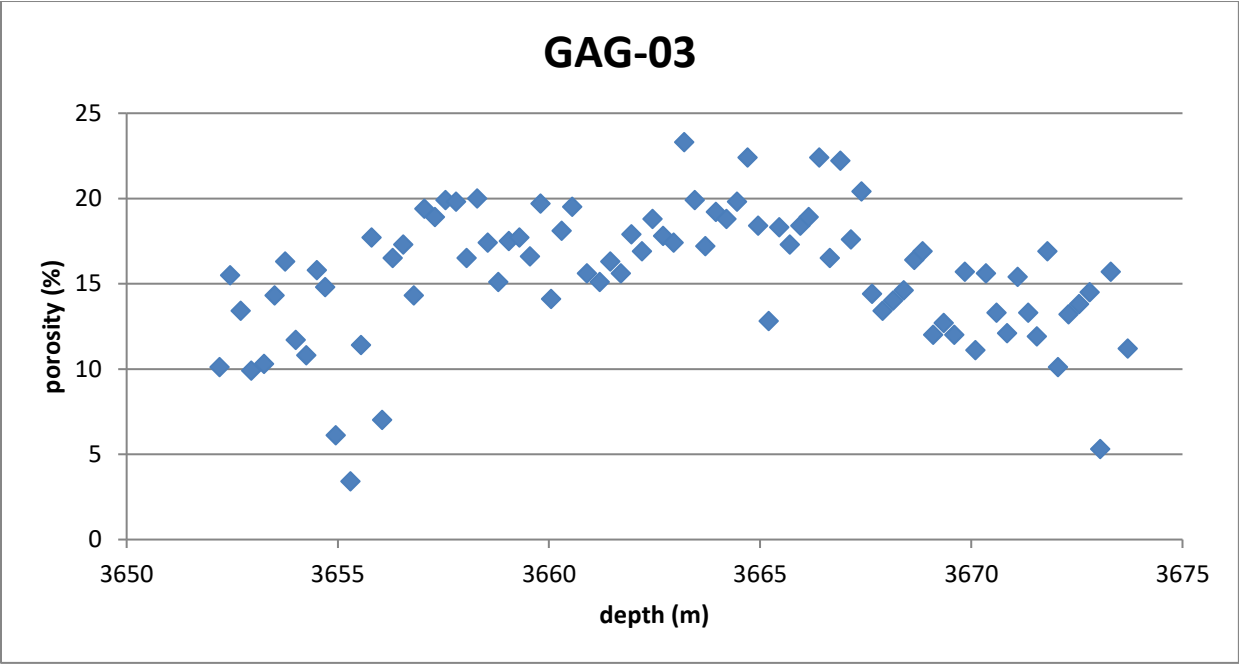
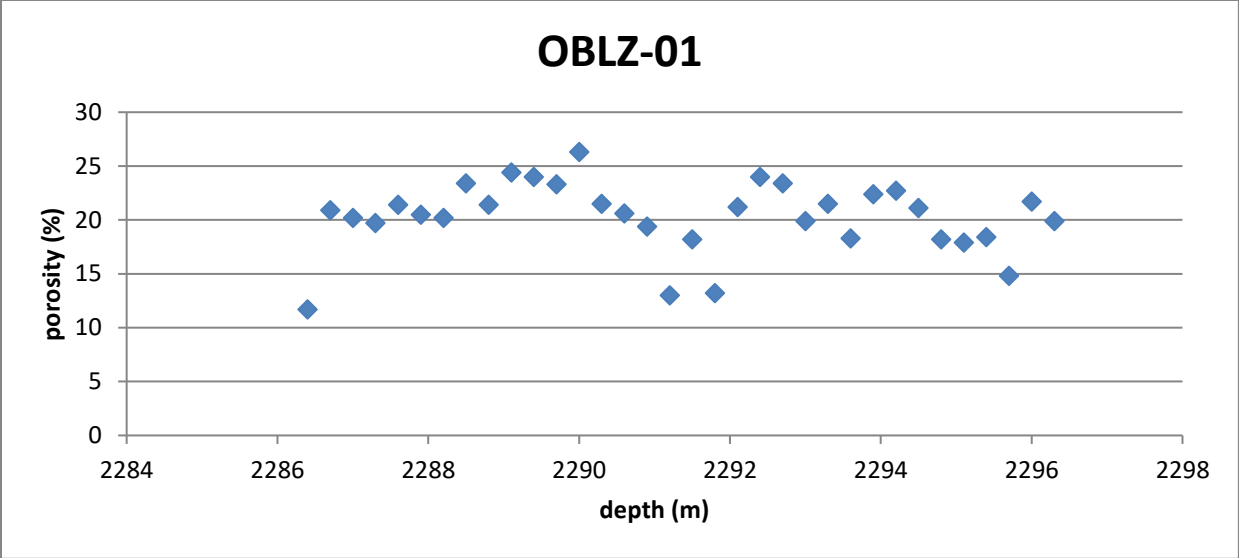




On-shore Porosity measurements on the cored intervals are presented by the following graphs.

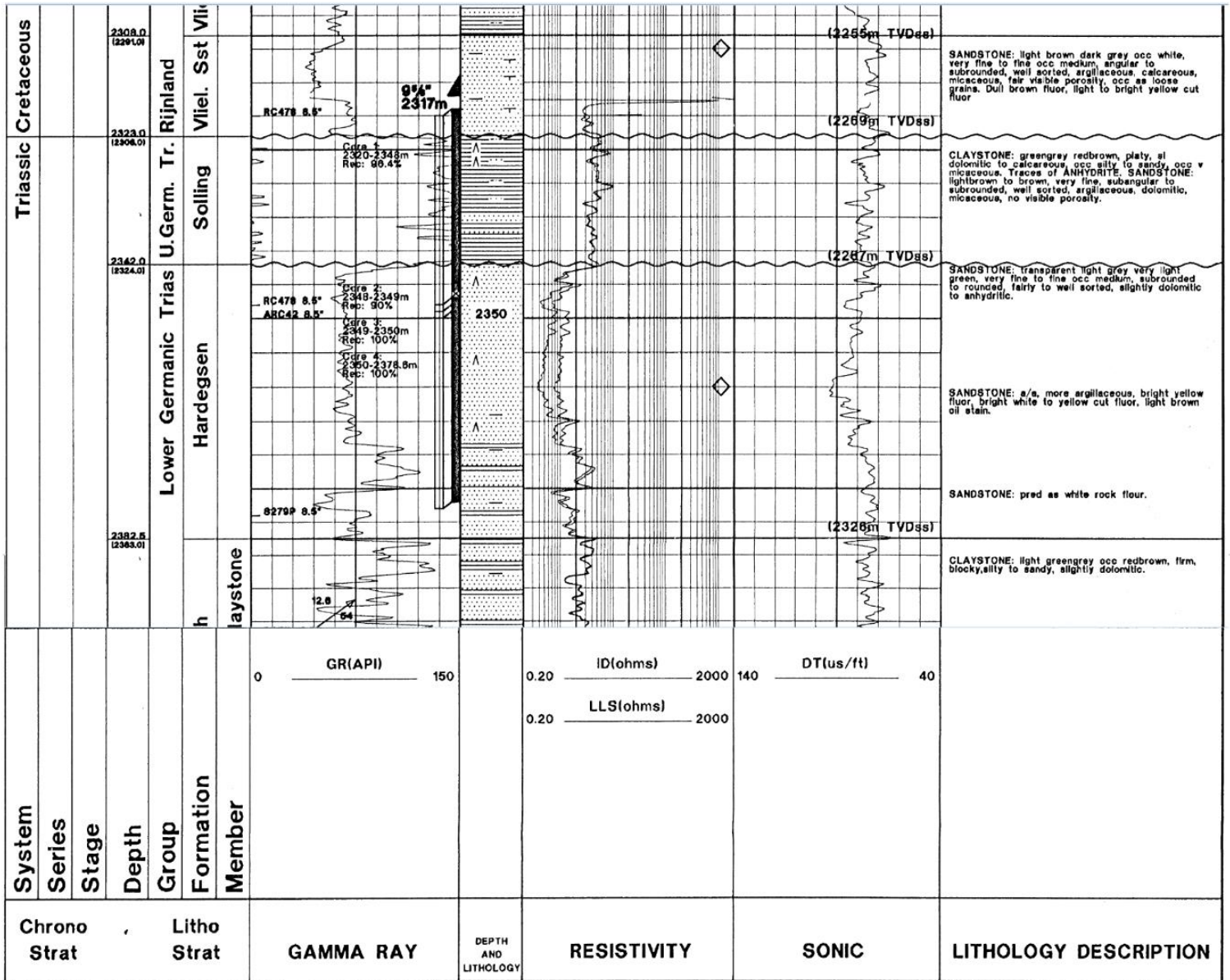


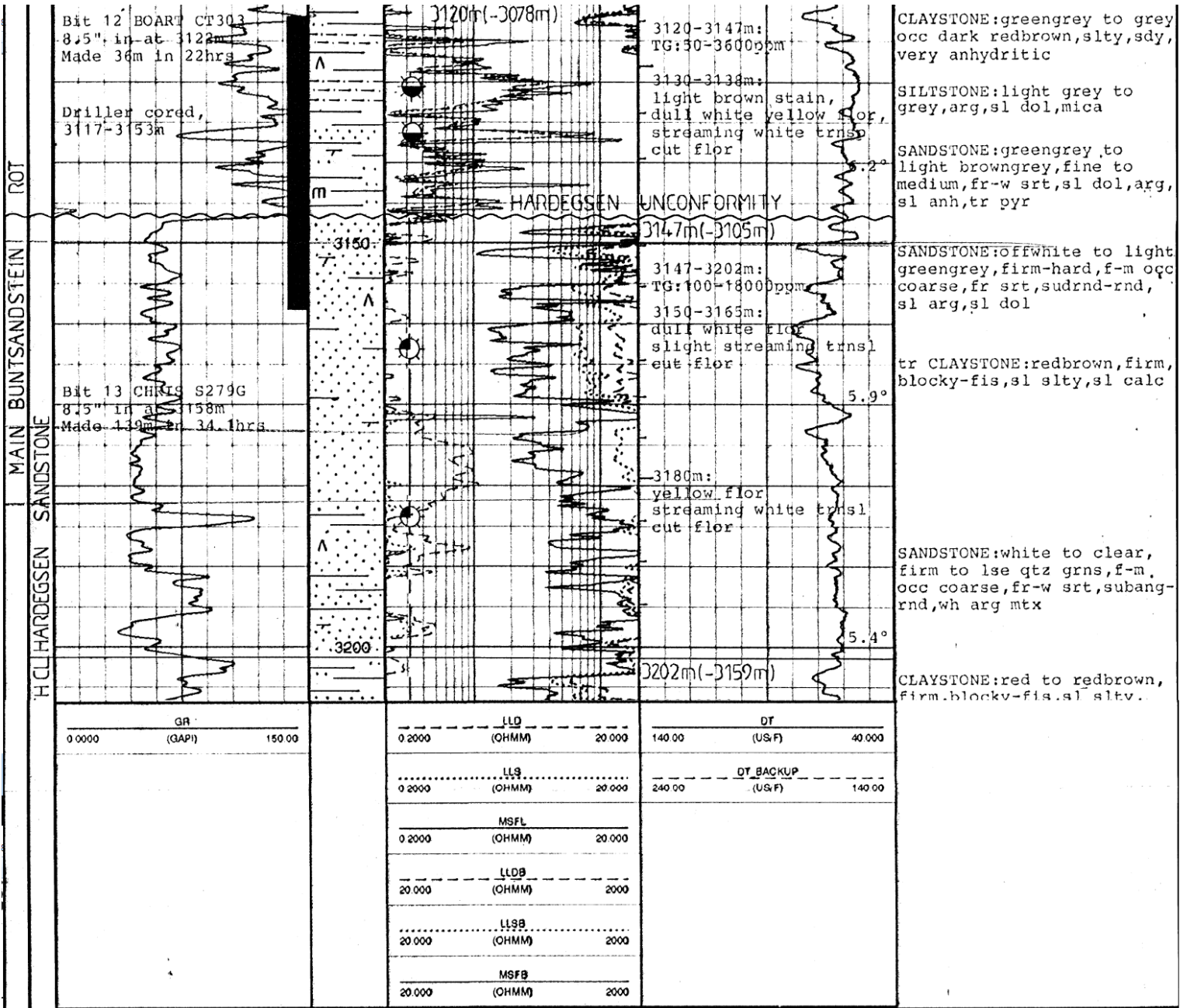


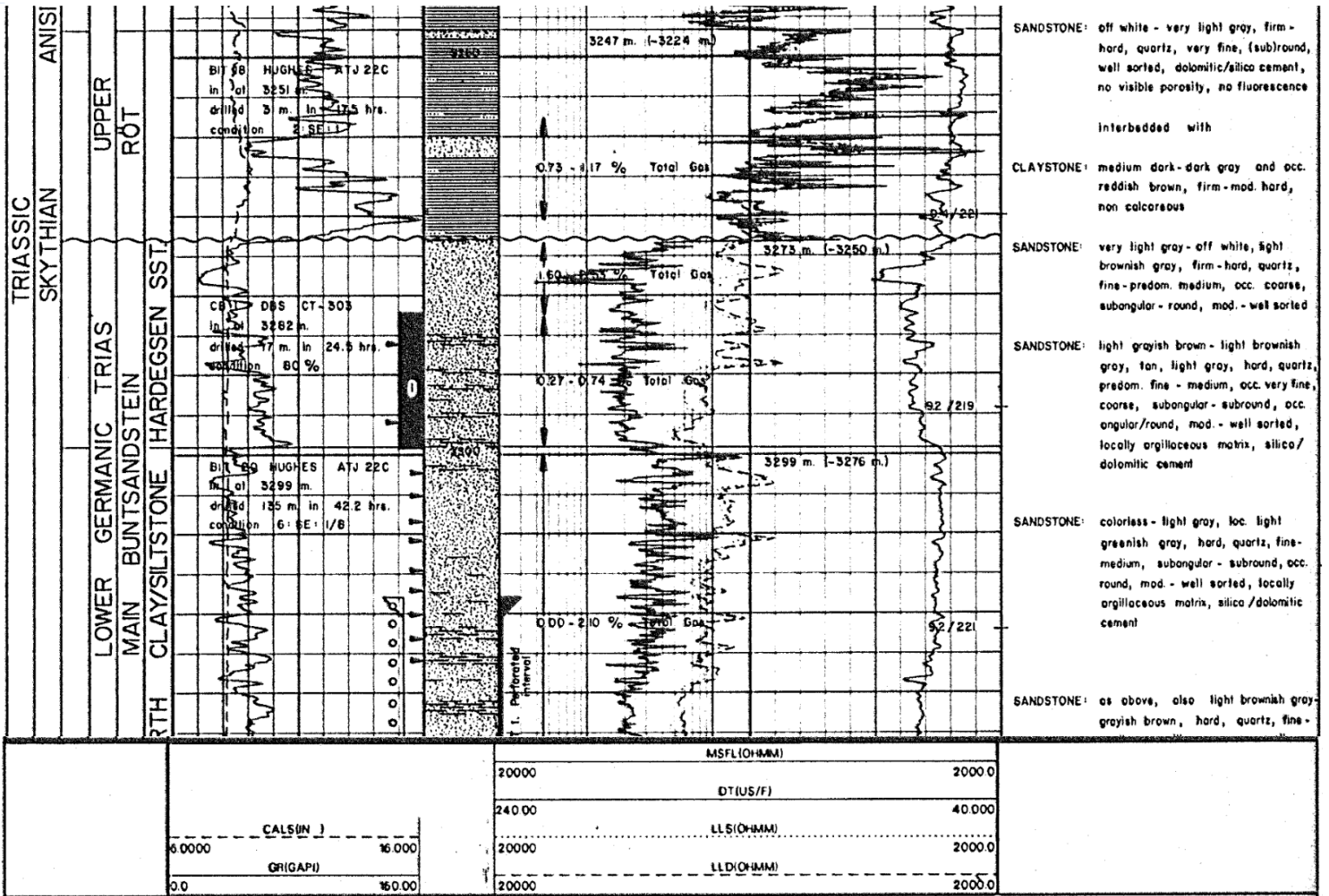


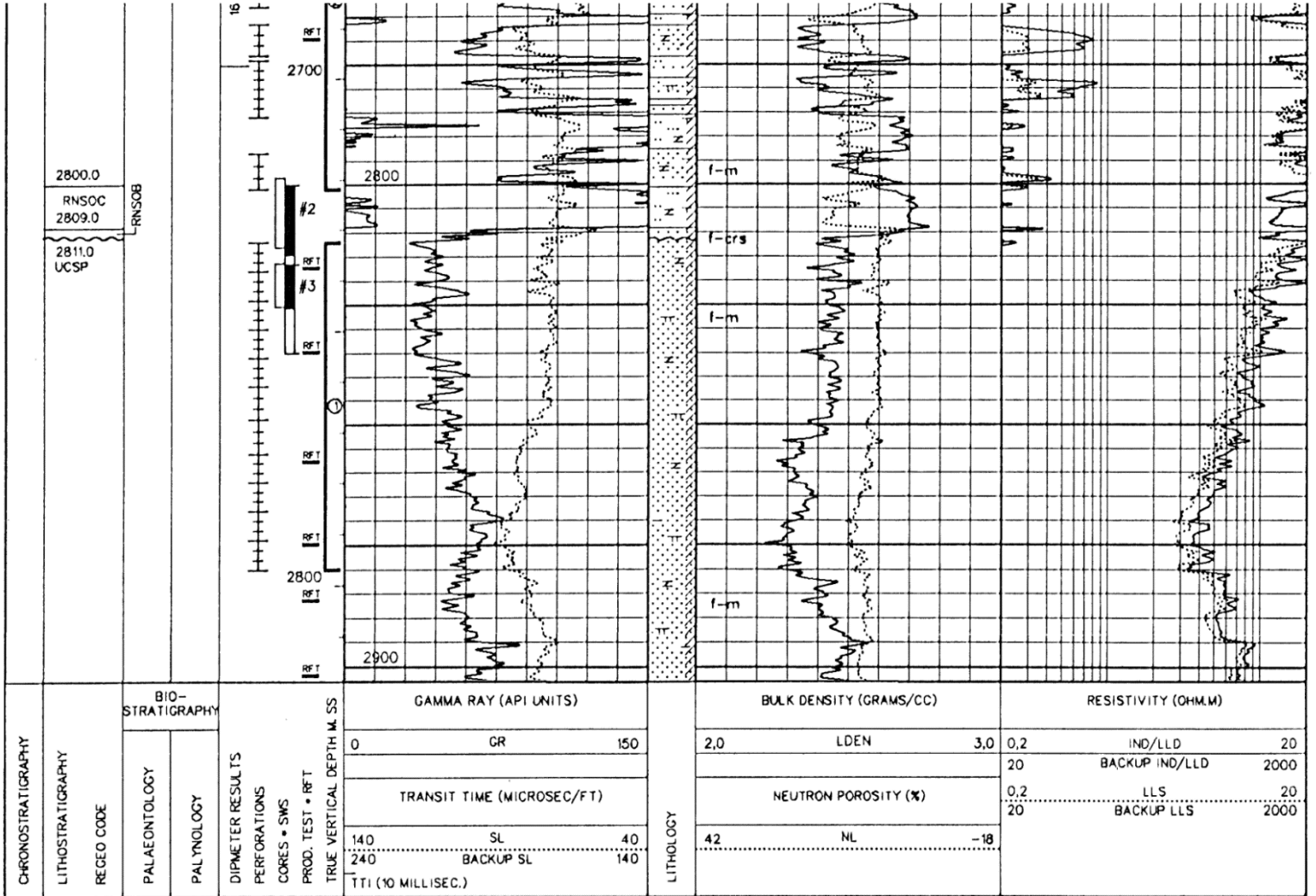
Appendix D - Composite well logs

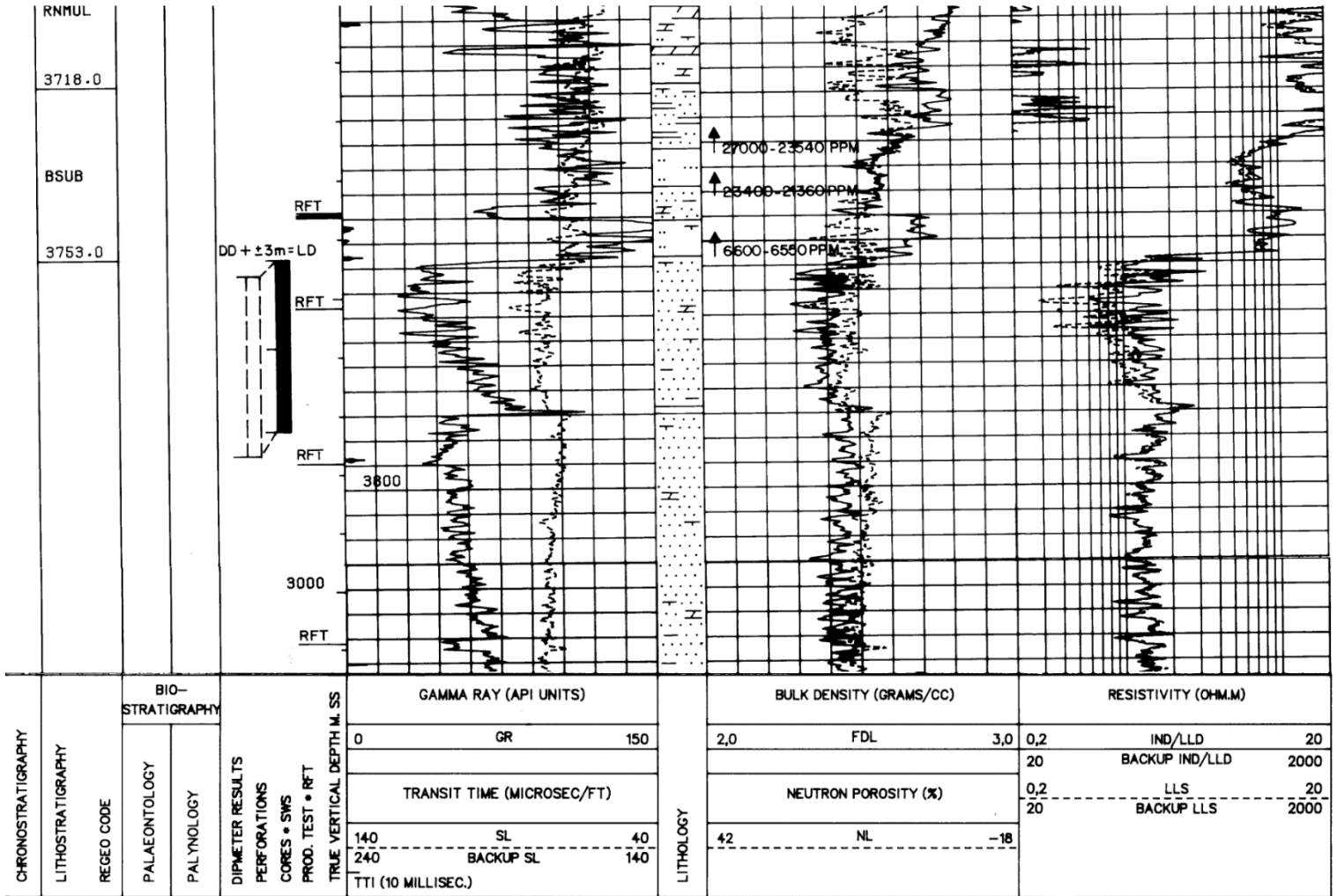
P11-02



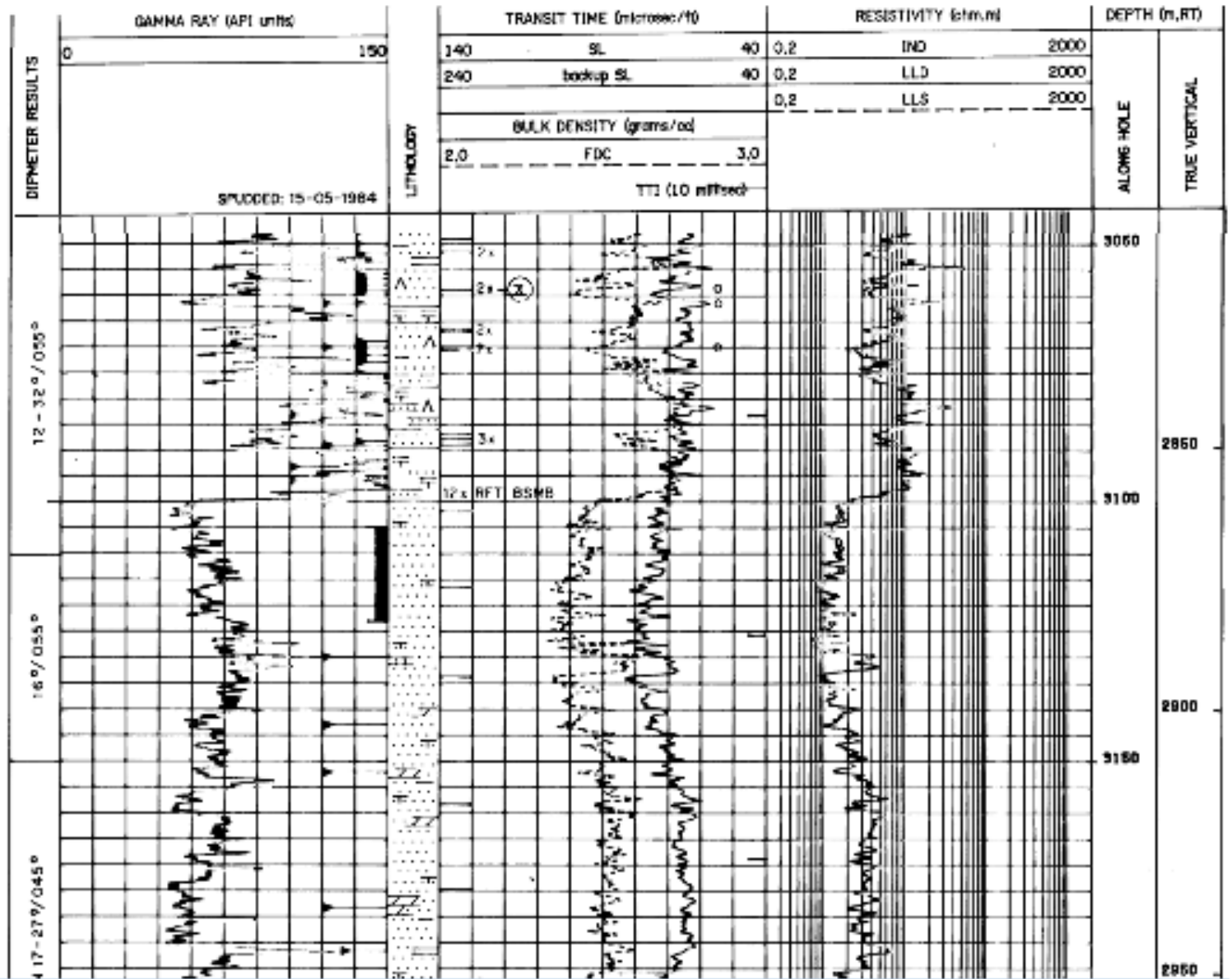


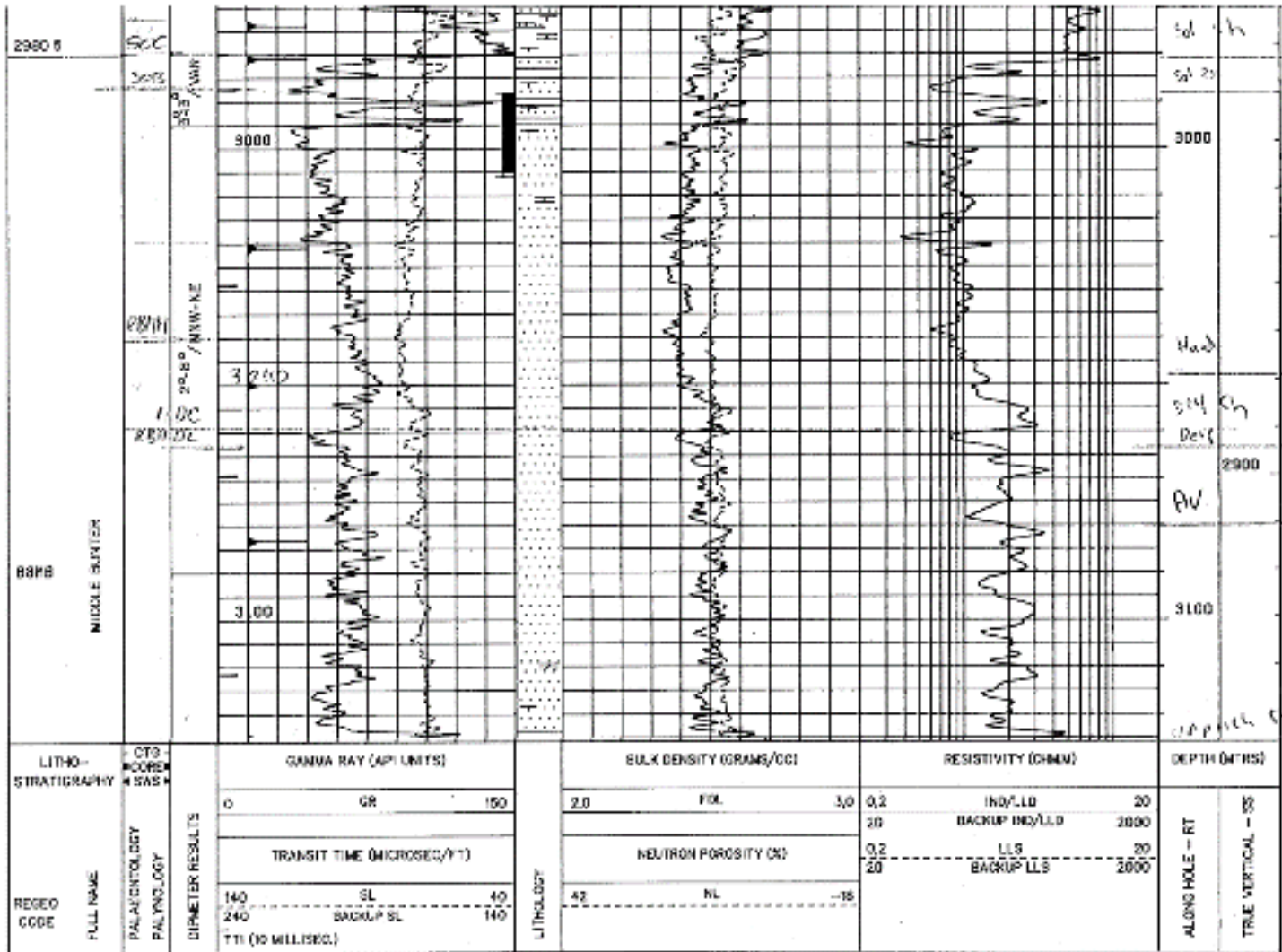


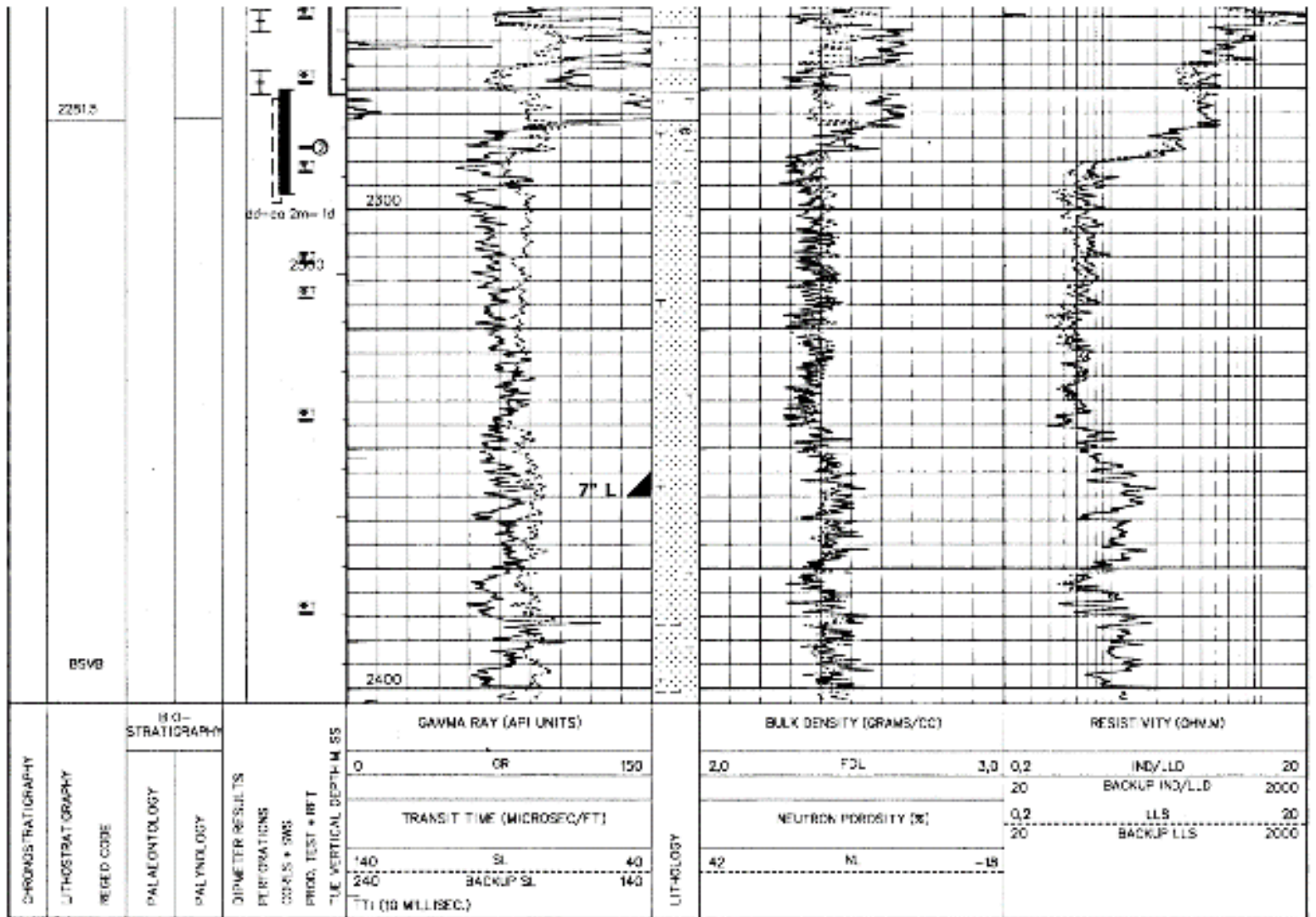


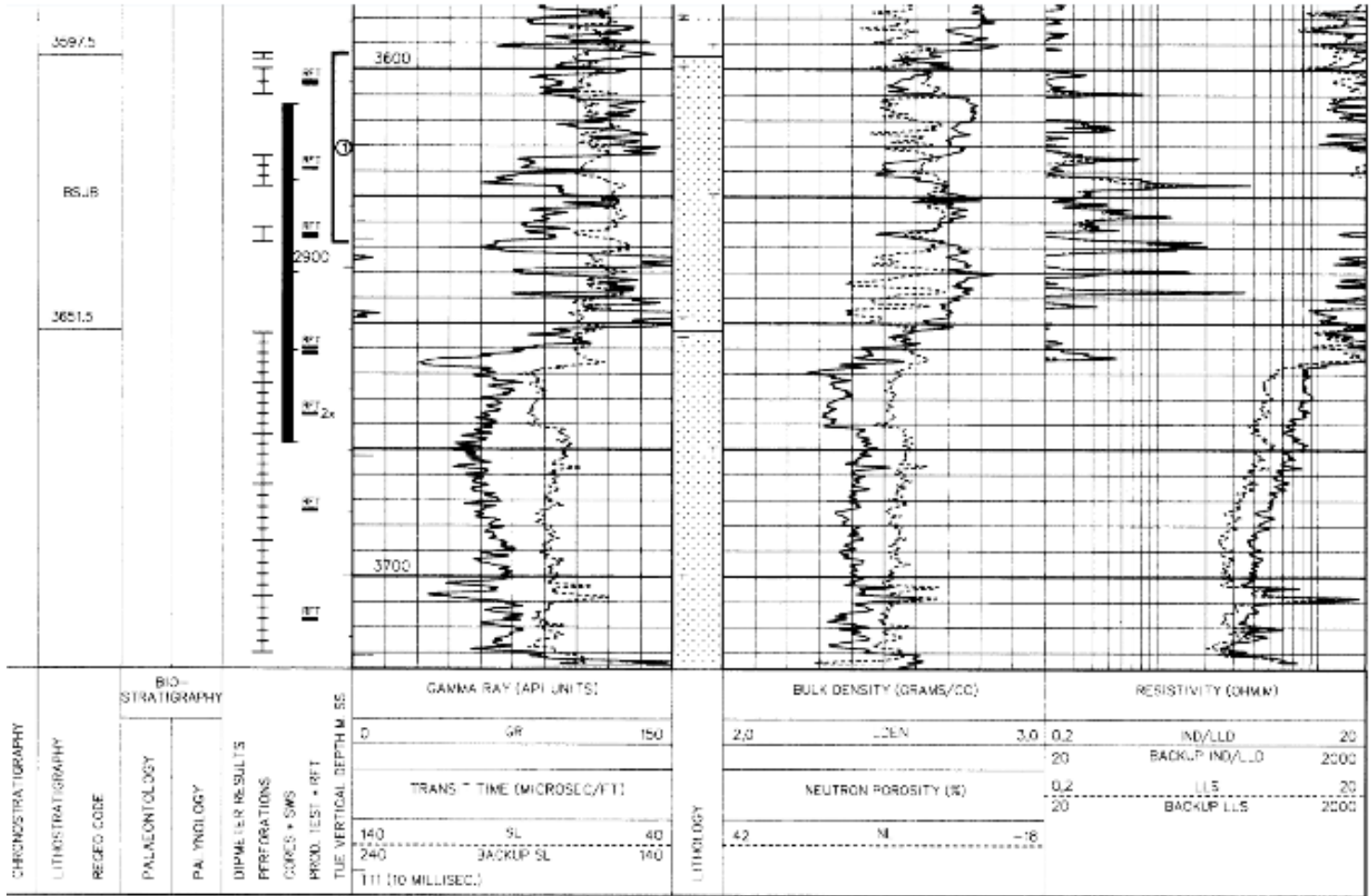


RTD-01









Appendix E – Field description

The locations of the visited outcrops are presented below. They are sorted by stops.

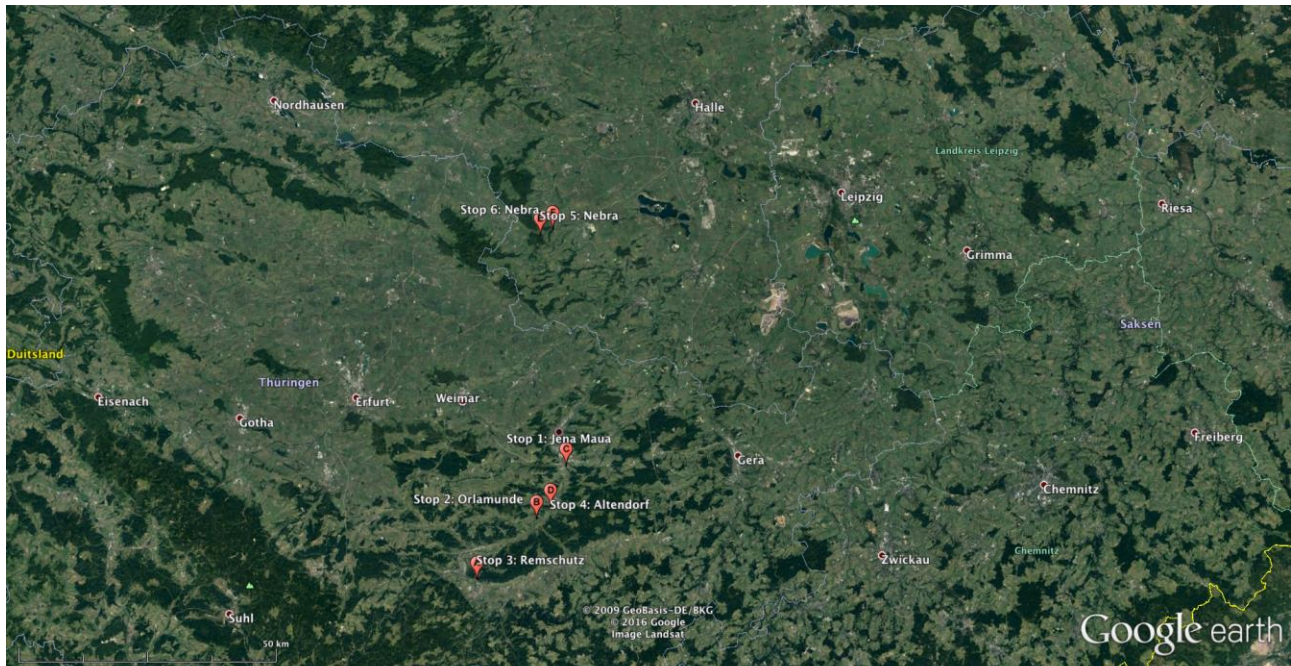


Figure 42. Visited outcrops during fieldwork. (Thuringen, Germany) (Google Earth, 2016)

	breedte	lengte
stop 1	50°52'3.34"N	11°36'29.93"O
stop 2	50°46'33.42"N	11°31'40.19"O
stop 3	50°40'11.98"N	11°21'52.50"O
stop 4	50°47'47.09"N	11°33'56.46"O
stop 5	51°16'0.88"N	11°32'11.72"O
stop 6	51°16'38.10"N	11°34'15.66"O



Figure 44. Detail from visited outcrops during fieldwork. (Jena, Thuringen, Germany) (Google Earth, 2016)

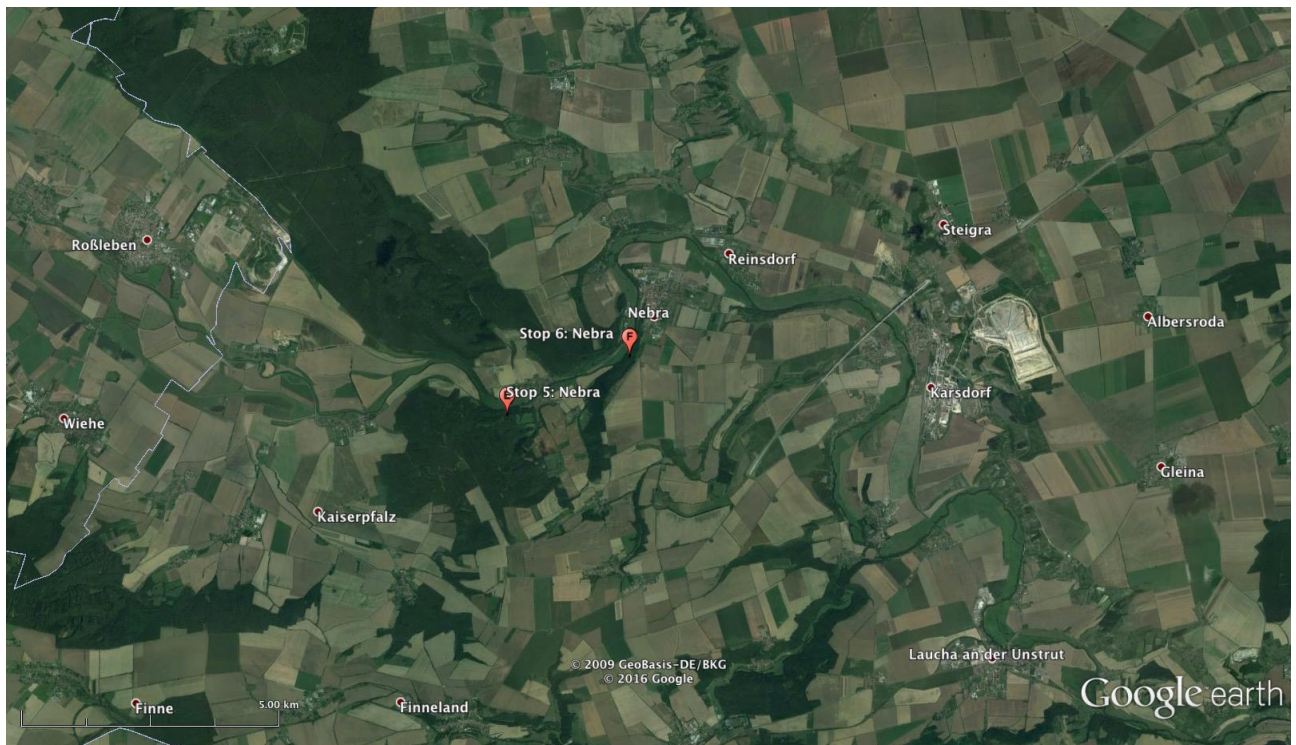


Figure 43. Detail from visited outcrops during fieldwork. (Nebra, Sachsen-Anhalt, Germany) (Google Earth, 2016)

Stop 1.1

9:30, 3/12/2015

Hardegsen

Homogenous shale layer overlying cross-bedded coarse sandstones(400-600 μm). Shale layers in the cross-bedding are up to several cm thick.



One thick homogenous shale layer of ca. 10cm with sharp transitions with cross-bedded sandstones. Thicker homogeneous sandbanks of ca. 1 to 2 metres alternated with braided streams with clearly visible cross-bedding. Relative very small clay layers(up to max several mm) are present in the cross-bedding.

Stop 1.2

10:00, 3/12/2015

Hardegsen

Shale Layers are very homogenous over the total distance of the outcrop. Around the clay layers, locally very coarse sediments, 2000 μm . More than 30m over the total length of the outcrop.

General flow direction: W/SW. Channels: E/W. See picture.



Stop 1.3

10:15, 3/12/2015

Hardegsen

Very thick(2-3 m) sand beds, alternated with thinner(10-30 cm) braided streams with white fine grained sediments. In the white cross beds, locally reddish layers are presents. These layers are very likely to be from diagenetic origin. Very small black layers with high mica content. mica layers are up to 1.5 cm thick. Grain size in the sand layers is ca. 100 μm .

Stop 1.4

10:22 3/12/2015



Hardegsen

Very thick homogeneous beds(up to 2.5 m). Smaller clay layers(25 a 30 cm), homogenous over the total length of the outcrop.

Stop 2.1

11:19, 3/12/2015

Lower Bunter

Sandstone beds of 20-3 cm, smaller banks are usually white. The total outcrop consists for more than 50% out of clay and silt layers. The layers are very homogenous over the total length of the outcrop and there is no visible cross-bedding. Outcrop is Ca. 100 metres in length, 10 metres thick.



Stop 2.2

11:25, 3/12/2015

Volpriehausen/Lower Bunter

Lower Bunter: More than 50 % reddish clay, with sand beds up to 10 cm. Sharp as well as smooth transitions between the beds.

Volpriehausen: Sandbeds are up to 50 cm. The formations consists for 90% out of sand. Locally more fine grained(silt) is present. De layers are homogenous in the length direction. The sand grains vary mostly up to 150 μm , and are badly sorted. There are some banks with grain sizes up to 300 μm .



Stop 2.2.1

Volpriehausen

Very thin clay layers are present and are very homogenous over the total length of the outcrop. High diversity in grain sizes, no visible cross-bedding but for one layer. Some layers show more poor sorting than others. One sand bank of 20 cm with clearly visible cross-bedding. This layer is only locally present and does not continue in the total length direction(ca. 5m). Banks of 10 cm are present with grain sizes of 1000 μm .

Stop 2.2.2

Volpriehausen

Shale layers occur regularly, but are never thicker than one centimeter. The layers continue in lateral direction over the entire outcrop

Stop 2.2.3

11:43, 3/12/2015

Few layer of ca. 50 cm with visible cross-bedding are present. The layers of 50 cm are alternated with thinner layers of 50 to several centimetres.

Stop 2.3

11:47, 3/12/2015

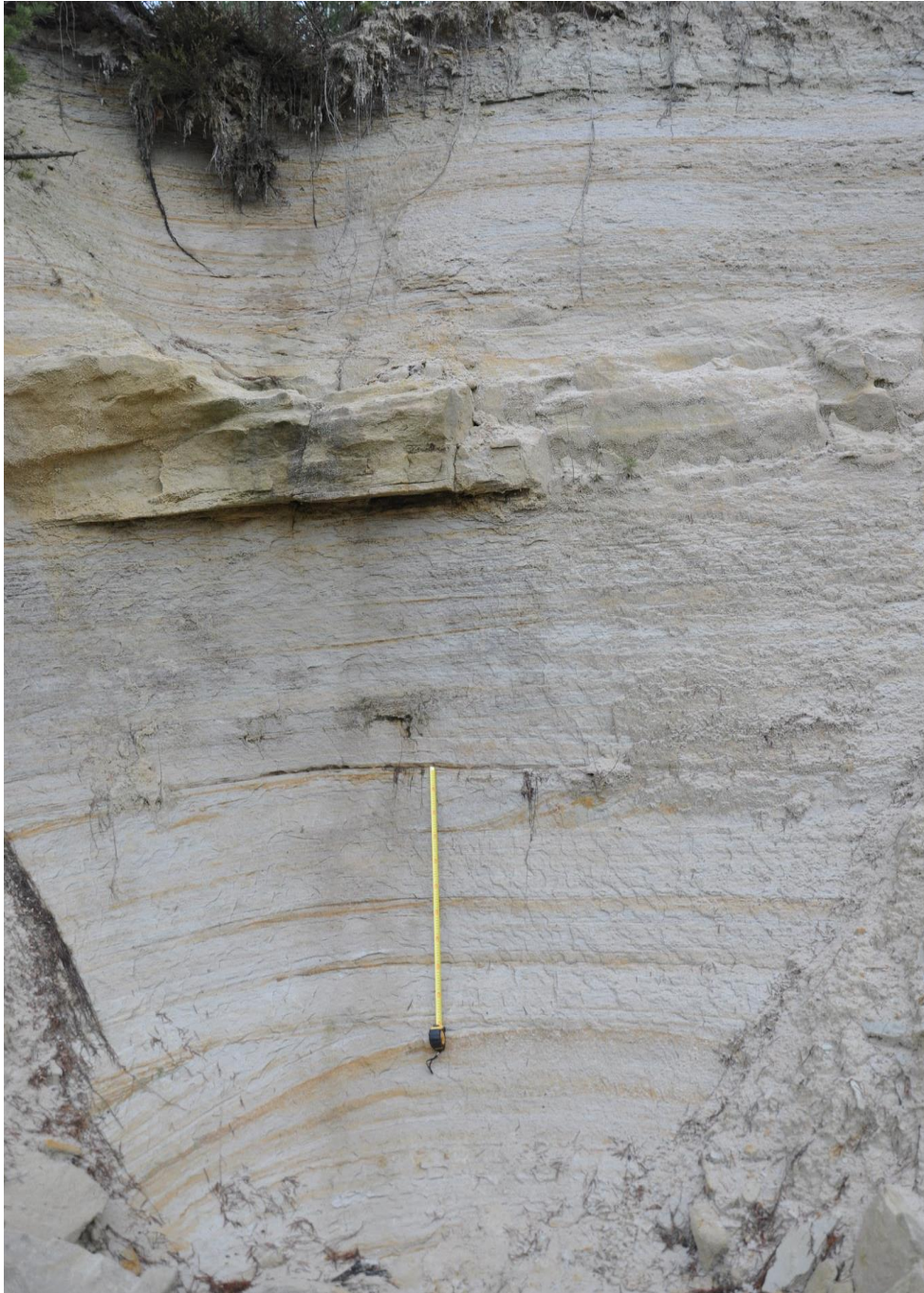
Sandbanks continue homogenous in the length direction. There is no visible cross-bedding present in the sand banks. The outcrop contains Ca. 99% sandstone. Several clay layers are present, but are never thicker than one cm. They continue in the length direction over the entire outcrop(50 m).

Stop 3.1

13:30, 3/12/2015

Colvorde formation

Sand Pit Remschutz. Several layers of loosely cemented coarse sandstone, with in half of the layers clearly visible cross-bedding. The layers are up to ca. 50 cm thick. White to light yellow sand with small oxidized layers. One solid bank of 50 cm is present with an oker/yellow color.



Stop 3.2

13:50, 3/12/2015

Colvorde Formation

Higher in the sandpit, the banks become more solid than below. This could either be caused by different cementation or later excavation, causing less erosion of the cement than the lower part of the pit. The sand banks become thinner in the upper part of the pit, and continue homogenous in the length direction. In the upper part of the pit, no visible cross-bedding is present. Several clay layers of maximal 5 mm are present in the upper part of the pit. The grain size widely varies between the sandbanks, but is never coarser than 600 μm . The grain size distribution gets generally worse when the banks are thicker.



Stop 3.3

3/12/2015



Very thick (up to 3 m) cross-beds are present in the bottom of the pit. The formation is very loosely cemented and very little clay is present. The sand is moderately sorted up to 100- 300 μm .

Stop 4.1

9:30, 4/12/2016



Upper Detfurth/ Bottom Hardegsen.

Stop 5.1

11:50, 4/12/2015

Bernburg and Volpriehausen



The presence of shale layers in the Bernburg formation is heavily dependent on cross-bedding. Volpriehausen redbeds are visible, just below a thick (0.5 meter) laterally consistent shale layer. The redbeds have grainsizes just below $200 \mu\text{m}$, with peaks of $300\text{-}400 \mu\text{m}$. The redbeds are poorly sorted. Shale layer of 50 cm thick is present. Layers are homogenous over at least 50 m in the length direction. Although through extensional faulting not totally visible. Some faulting probably took place during deposition as can be seen from the pictures.

The sand layers are up to 2 m thick and are homogenous over the length direction. Very large color differences occur, but no evidence of large difference in grain sizes are found



Stop 6.1

13:14, 4/12/2015

Hardegsen (upper 2) and Solling sandstone.



Very thick homogeneous sandstones, with very little clay layers. layers are up to several m thick and are well sorted. Samples of 1 layer gave 420 mcm. Clayey layers are up to 50 cm thick and consists out of alternations of clay, silt and sand layers. These layers are homogenous over at least 100 m in the length direction. Sand beds are smaller than clay layers in the alternation.



Huge mud pebbles are found in the redbeds everywhere. If exposed, they usually erode much faster than the sandstone itself, causing huge holes to form in the sandstone.

Stop 6.2

13:30, 4/12/2015



Stop 6.3

13:33, 4/12/2015



Stop 6.4

Huge cross-beds, up to 3 m. overlaying alternations of sand and clay. The holes that are present in the huge cross-beds are eroded mud pebbles. Pebbles that are still present have been visualized at stop 6.1.



Appendix F – Inversion of reservoir quality F and L quadrants, summary.

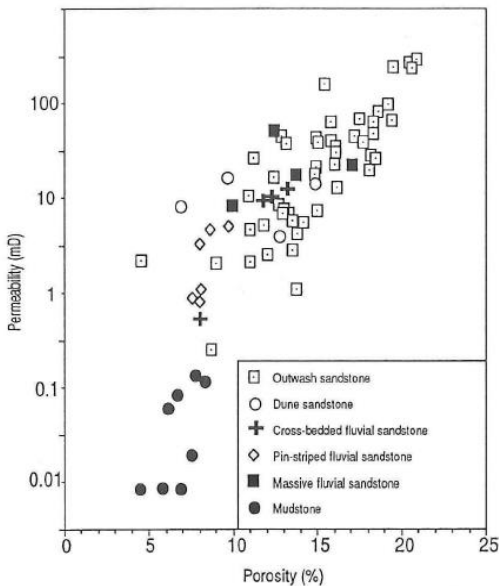


Figure 46. Porosity permeability plot of different Buntsandstein deposits. (Purvis & Okkerman, 1996)

Although the original reservoir quality of the Buntsandstein deposits could be very well linked to the depositional origin, cementation of the different reservoir intervals turned out to be remarkable for in-situ permeability and porosity (Purvis & Okkerman, 1996). The main cement content of the Buntsandstein formation in the Netherlands is: Dolomite, Anhydrite and Halite. All three cements are very likely to be from early depositional origin, since minus-cement percentages of the samples are very high. Dolomite is often enclosed by anhydrite (minus-cement up to 48.3%) and Halite (minus-cement up to 33.9%). An explanation for the very early cementation is the absence of gypsum. There is very little gypsum cement observed in the samples, although this would be expected in a (semi)-arid environment. The most likely reason for this absence is the dissolution of gypsum during burial and acting as a potential source for anhydrite cement during later

diagenesis (Purvis & Okkerman, 1996). Another explanation is the precipitation of anhydrite as well as halite derived from the underlying Zechstein. Purvis & Okkerman (1996) suggest that transformation of Zechstein gypsum would lead to overpressured brines, that entered the Buntsandstein through

181

Table 1. Major lithofacies in Triassic Main Buntsandstein reservoir intervals.

Lithofacies	Main features	Origin
Cross-bedded sandstone	Planar cross-bedded, well to very well sorted, medium- to fine-grained sandstones, with dips of up to 30°. Grains are well rounded and frosted	Small (2–3 m) aeolian dunes
Irregular horizontally laminated sandstone	Fine-grained, poorly to well sorted sandstones, showing poorly defined horizontal and irregular, undulatory lamination. Thin clay drapes are locally developed	Sandsheets formed by a combination of aeolian and fluvial sheetflood processes
Pin-striped sandstone	Well sorted and well stratified fine-grained sandstones with low angle cross-bedding. Erosive bases are overlain by asymptotic laminations, passing up into low angle cross-bedding	Fluvial deposits of unconfined sheet flow and/or minor channelised flow
Cross-laminated sandstone	Trough cross-laminated, fine-grained sandstones with erosive bases. Typically overlain by irregular horizontally laminated sandstones	Deposits of confined, channelised flow. Possibly related to fluvial bars
Non-stratified sandstone	Fine-grained, structureless, moderately to well sorted sandstones	Fluvial sandstones, homogeneous as a result of absence of grain size variation, or post-depositional homogenisation
Mudstone	Laminated, red-brown claystone with minor admixed or interlayered siltstone and fine-grained sandstone. Structures include siltstone dykes, asymmetrical ripples and local mudstone conglomerates	Shallow lake or ponds with frequent fluxes of fluvial sands and silts

Figure 45. Major lithofacies in the Buntsandstein reservoir intervals. (Ames & Farfan, 1996)

hydrofractures in the mudstones. Off course, these brines would be more likely to follow higher porous and permeable sandstones precipitating anhydrite (Purvis & Okkerman, 1996). For Halite, there could also be another explanation than the underlying Zechstein. Since it is also very likely to be from early burial origin (high minus-cement), there is a possibility that the halite was introduced during the deposition of the Buntsandstein.

Following the conclusions of Purvis & Okkerman (1996), cementation by anhydrite and halite cement has generally lowered the reservoir properties of the parts with the best depositional porosity and permeability. We will try to link these conclusions to our own core descriptions in order to make a general statement for the onshore West Netherlands Basin Buntsandstein.